Impact of spatio-temporal variability of the Mascarene High on weather and climate over southern Africa

Nkosinathi Goodman Xulu (15012556)

The dissertation is submitted in fulfillment of the requirement for the degree of Master of Environmental Sciences in the field of Climatology

Department of Geography and Geo-Information Sciences

School of Environmental Sciences

University of Venda

Supervisor: Dr. N.S. Nethengwe

Co-supervisor: Dr. H. Chikoore

Co-supervisor: Dr. M.M. Bopape (CSIR)

February 2017

ABSTRACT

Subtropical anticyclones locate and modulate weather and climate over subtropical belts for both the Northern and Southern Hemispheres. This study investigates the spatio-temporal variability of the Mascarene High over the South Indian Ocean on (anomalous) weather and climate over southern Africa at intraseasonal, seasonal, interannual, multidecadal and event time-scales. The Mascarene High is located 25-35°S, 40-110°E, playing a vital role in day-to-day weather and climate patterns conditions over southern Africa. Spatio-temporal characteristics of the Mascarene High investigated in this study span the period 1985-2014 and 2071-2100, using NCEP-NCAR reanalysis datasets for present-day climate observations and the Conformal-Cubic Atmospheric Model (CCAM) for future projections. The Mascarene High is analysed using mean sea level pressure (MSLP) extracted from ECMWF ERA-interim monthly reanalysis data. The Mascarene High is also subjected to Principal Components Analysis, depicting eastern displacements of the weather system to be dominant for weather and climate fluctuations over southern Africa. The Mascarene High migrates south (north) during austral summer (winter) and is centred over the eastern Indian Ocean in summer in connection with the Indian Ocean Subtropical Dipole. Event scale analysis is also employed for investigating Mascarene High blocking and induced anomalous weather. Mascarene High blocking leads to anomalous rainfall events over southern Africa associated with tropical cyclones, cut-off lows and cloud bands. There is also a vital geographical variability of the Mascarene High development, distribution and movement in the South Indian Ocean at the different time-scales. Projections of the Mascarene High indicate a shift in mean location as a result of future expansion and intensification. This projected expansion and intensification is expected to shift tropical cyclone trajectories equatorward, with the baroclinic structure of cold fronts expected to shift poleward affecting changes in the weather and climate of southern Africa. This finding is important as it projects changes in weather and climate conditions over southern Africa in a changing climate due to increased greenhouse gas emissions.

Keywords: Subtropical anticyclones, Mascarene High, South Indian Ocean, Spatio-temporal variability, Southern Hemisphere.

ACKNOWLEDGEMENTS

This Master's dissertation was supervised by Dr. N.S. Nethengwe, co-supervised by Dr. H. Chikoore, both from the University of Venda and Dr. M.M. Bopape from the Council for Scientific and Industrial Research (CSIR). I would like to express my deep and sincere gratitude to them for their continuous support. They have contributed numerously to my understanding of different topics within this study and provided the necessary skills and knowledge for me to complete this dissertation.

I would also like to express much appreciation to the National Research Foundation (NRF) Research and Innovation, Applied Centre for Climate and Earth Systems Science (ACCESS) and the University of Venda for funding this research project. A special thanks to the CSIR in Pretoria for providing Conformal-Cubic Atmospheric Model (CCAM) datasets, resources and analysis techniques during my time spent there for research visits. Dr. Yushi Morioka from the Japan Agency for Marine-Earth Science and Technology (JAMSTEC) is also acknowledged. Many thanks to colleagues and staff of the Department of Geography and Geo-information Sciences, University of Venda.

DEDICATION

My utmost appreciation is directed to the enormous support given by my family, especially my father; Mr. Moses G. Xulu and lastly, I would also like to dedicate this work to my late son; Amkelo Xulu and my two lovely daughters; Chibote and Lwandisa.

DECLARATION

I acknowledge that I have read and understood the University's policies and rules applicable to postgraduate research, and I certify that I have, to the best of my knowledge and belief, complied with their requirements.

I declare that this dissertation, save for the supervisory guidance received, is the product of my own work and effort. I have, to the best of my knowledge and belief, acknowledged all sources of information in line with normal academic conventions.

I further certify that the work done is original, and that the material to be submitted for examination has not been submitted, either in whole or in part, for a degree at this or any other university.

I have subjected this document to the University‘s similarity checking procedures and I consider it to be free of any form of plagiarism.

Signature _____

Date _____

CONTENTS

LIST OF FIGURES

LIST OF TABLES

LIST OF ACRONYMS

ACCESS	Applied Centre for Climate and Earth System Sciences
AR	Assessment Report
CCAM	Conformal-Cubic Atmospheric Model
CGCM	Climate General Circulation Models
CSIR	Council for Scientific and Industrial Research
CSIRO.	Commonwealth Scientific and Industrial Research Organization
CPC	Climate Prediction Centre
CMAP	Climate prediction Centre Merged Analysis of Rainfall
COLA	Centre for Ocean-Land-Atmosphere Studies
DEM	Digital Elevation Model
GEOS-5	Goddard Earth Observing System Data Assimilation System Version 5
GrADS	Grid Analysis and Display System
ECMWF	European Centre for Medium-Range Weather Forecasts
ENSO	El Niño Southern Oscillation
EOF	Empirical Orthogonal Function
ERA	European Reanalysis
GPCP	Global Precipitation Climatology Project
GHGs	Greenhouse Gases
GHGN	Northern Geopotential Gradient
GHGS	Southern Geopotential Height Gradient
GIS	Geographic Information System

GLOBE	Global Land One-km Base Elevation
GPCC	Global Precipitation Climatology Centre
GPCP	Global Precipitation Climatology Project
hPa	Hectopascal
IPCC	Intergovernmental Panel on Climate Change
IndOOS	Indian Ocean Observing System
IOD	Indian Ocean Dipole
IRI	International Research Institute
ITCZ	Inter-Tropical Convergence Zone
JAMSTEC	Japan Agency for Marine-Earth Science and Technology
KNMI	Koninklijk Nederlands Meteorologisch Instituut (Royal Netherlands Meteorological Institute)
MERRA	Modern Era Retrospective-analysis for Research and Applications
MSLP	Mean Sea Level Pressure
NASA	National Aeronautics and Space Administration
NCEP-NCAR	National Centres for Environmental Prediction-National Centre for Atmospheric Research
NDVI	Normalized Difference Vegetation Index
NGDC	National Geophysical Data Centre
NH	Northern Hemisphere
NRF	National Research Foundation
NWP	Numerical Weather Prediction
NOAA	National Oceanic and Atmospheric Administration

OISST	Optimum Interpolation Sea Surface Temperature
OLR	Outgoing Longwave Radiation
PCA	Principal Components Analysis
PDSI	Palmer Drought Severity Index
QBO	Quasi-Biennial Oscillation
RCM	Regional Climate Model
RCPs	Representative Concentration Pathways
SH	Southern Hemisphere
SAM	Southern Annular Mode
SICZ	South Indian Convergence Zone
SPI	Standardized Precipitation Index
SST	Sea Surface Temperature
SOI	Southern Oscillation Index
SWIO	Southwest Indian Ocean
TC	Tropical cyclone
TTT	Tropical temperate troughs
WCRP	World Climate Research Programme

CHAPTER 1: INTRODUCTION AND BACKGROUND

1.1 Introduction

Semi-permanent subtropical anticyclones are synoptic scale weather systems surrounding an area of high pressure, consisting of circulation which is clockwise in the Northern Hemisphere (NH) and counter-clockwise in the Southern Hemisphere (SH). Subtropical anticyclones reflect subsidence occurring in the descending limb of the Hadley Cell (Tyson and Preston-Whyte, 2000) and owe their existence to monsoonal heating that occurs during the austral summer season over land and they also require air-sea interaction (Seager *et al.* 2003).

Observations show that light and variable winds are found near the centre of a subtropical anticyclone, having clear skies due to subsidence (Sinclair, 1996; Tyson and Preston-Whyte, 2000), unlike cyclones, which consist of strong winds near the centre and are comparably smaller (Sinclair, 1996). Subtropical anticyclone centres are generally located in the eastern portions of the Pacific, Atlantic and Indian Ocean basins over the SH. In these regions large scale subsidence is balanced with strong large scale low-level divergence (Richter and Mechoso, 2008), playing an important role on global weather and climate (Xue *et al.* 2003).

Subtropical anticyclones influence weather and climate over the subtropics during their development, distribution and movement (Davis *et al.* 1996). The persistent easterly trade winds of the tropics blow out of the subtropical anticyclones and can transport moisture from the tropical oceans onto the continents (Tyson and Preston-Whyte, 2000). Weather systems such as tropical cyclones have motion largely determined by these trade winds. Subtropical anticyclones are a large scale circulation, concentrated around 25˚N-45˚N and 25˚S-45˚S bands and account for much of the short-term weather variations in extra-tropical regions (Sinclair, 1996).

In the South Indian Ocean is the South Indian Ocean High or the Mascarene High which plays a major role on the weather and climate of southern Africa. This study investigates and projects the mean climate and anomalous weather patterns over southern Africa under the influence of the Mascarene High. The location and intensity of the Mascarene High may change due to warmer air temperatures in the future.

The average temperature of the globe is increasing because of the increase in concentration of the anthropogenic greenhouse gases (IPCC, 2014). Observations have shown that the mean temperature over southern Africa is also increasing (Kruger and Shongwe, 2004), and the

increase is occurring at twice the global rate (Engelbrecht *et al.* 2015). The precipitation trend and projections are less robust compared to those of temperature, however, lower precipitation is expected in general. The study will also investigate the projected changes in the Mascarene high due to increased anthropogenic greenhouse gases and associated changes in winds.

1.2 Problem statement

The distribution, strength and movement of the Mascarene High modulate weather patterns over southern Africa throughout the year. Research done on subtropical anticyclones in the SH has led to some understanding on the behavior of these weather systems. However, the occurrence of anomalous weather patterns over southern Africa during Mascarene High blocking events need to be thoroughly examined. Projections of how the Mascarene High is likely to change in a future climate is also vital to our understanding of the evolution of rainfall patterns over southern Africa.

One major factor in the behaviour of the Mascarene High is the occasional blocking of the usual flow of transient disturbances into a region causing persistence and slow movement of these disturbances (Sinclair, 1996). Blocking events can give rise to anomalous regional weather patterns for extended periods, causing extreme weather conditions. Over the years, the study of the influence of global warming on the structure of subtropical anticyclones has improved in the literature. Changes in the climatology of subtropical anticyclones due to global warming may play a major role in long-term temperature and rainfall changes (Rohli, 1995).

This research project focuses on the spatio-temporal variations of the Mascarene High and weather patterns over southern Africa at seasonal to interannual, multidecadal and event time-scale cycles of subtropical anticyclones over the Indian Ocean.

1.3 Research aim and specific objectives

The aim of the study is to analyse the impact of spatio-temporal variability of the Mascarene High on weather and climate patterns over southern Africa for the period 1985-2014 and to analyse projections for the period 2071-2100.

Specific objectives of the research project are:

- To map mean spatial characteristics and seasonal shifts of the Mascarene High;

- To determine how ocean-atmosphere interactions influence variability of the Mascarene High in the context of the El Niño Southern Oscillation (ENSO) and anomalies in the Indian Ocean;
- To identify and analyse the effect of blocking due to the Mascarene High on weather over southern Africa;
- To model future changes in intensity and spatial characteristics of the Mascarene High in a changing climate, and their effects on rainfall and temperature.

1.4 Research questions

- How do seasonal shifts of the Mascarene High affect the circulation over southern Africa?
- How do the oceans modulate Mascarene High variability?
- To what extent does Mascarene High blocking influence anomalous weather over southern Africa?
- How is the future Mascarene High projected to change, and how will it affect the weather and climate patterns over southern Africa?

1.5 Study area description

The Mascarene High is located over the South Indian Ocean between the tropical belts and temperate belts. This work focuses on a region extending from 25-35°S and 40-110°E (after Manatsa *et al.* 2014) in the South Indian Ocean to investigate the Mascarene High (Figure 1.1). The southern African subcontinent lies well above 1000 m and is characterised by a moderately elevated plateau (Figure 1.2). The elevated interior, the low-altitude coastal plain and mountain systems are the three basic landforms of southern Africa.

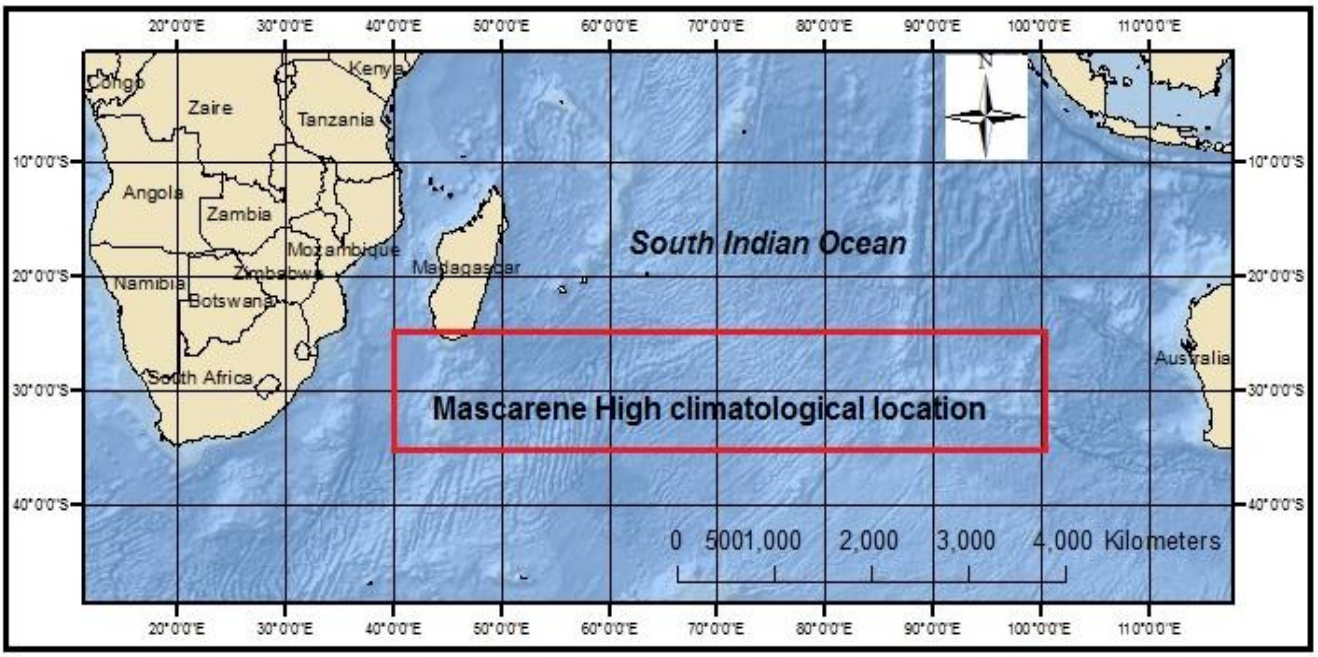

Figure 1.1: South Indian Ocean and surrounding mainland.

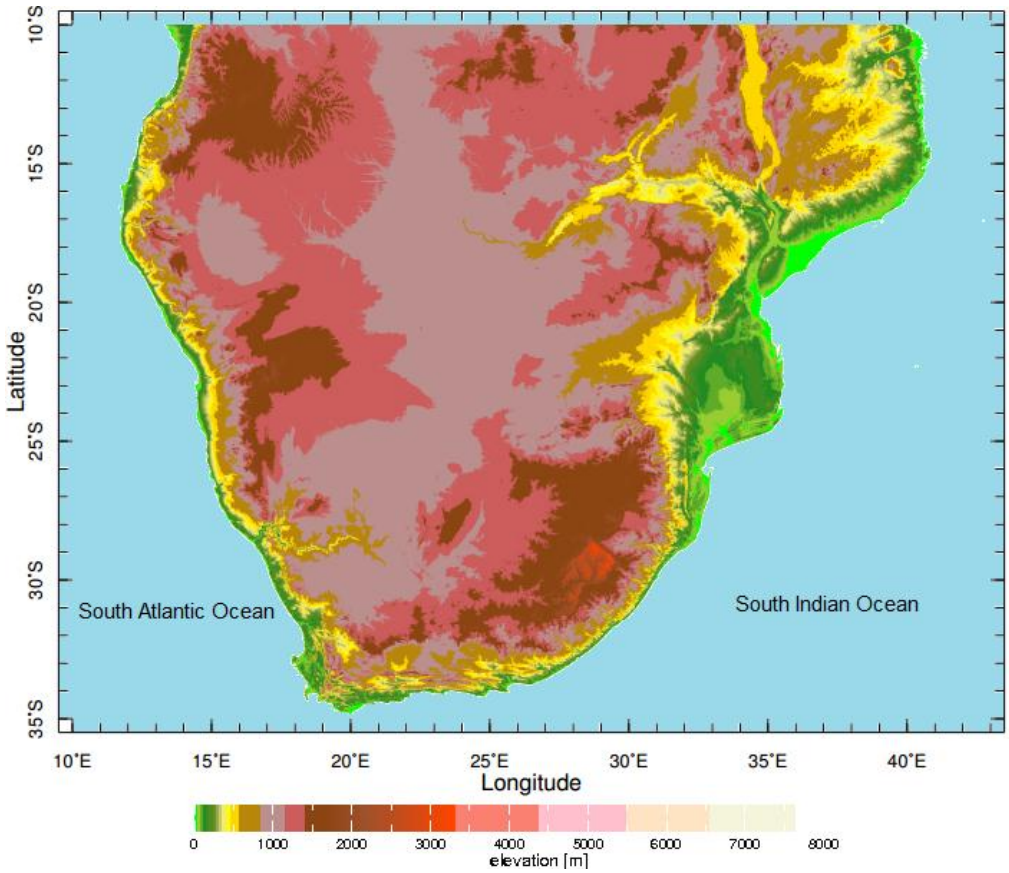

Figure 1.2: Southern Africa elevation (shaded in m).

1.6 Justification of the study

Subtropical anticyclones are known as large scale systems with centres characterised by weak pressure gradients and no frontal activity (Sinclair, 1996). They are also accompanied by air subsidence, compression and adiabatic warming of the local atmosphere (Tyson and Preston-Whyte, 2000). Consequently, they are generally referred to as fine weather systems.

Persistent subtropical anticyclones are found to cover the subtropical oceans for both the SH and NH (Richter and Mechoso, 2008). Throughout the globe, subtropical oceans consist of a low-level circulation that is steered by subtropical anticyclones, which are found throughout the year, while occupying around 40% of the earth's surface (Rodwell and Hoskins, 2001) and are associated with weather patterns that occur in those regions. Subtropical anticyclones are known to form and intensify over regions where atmospheric mean and underlying geographic environmental features are favorable for their growth (Whittaker and Horn, 1983). The mean structure and underlying geographic environmental features that are linked to subtropical anticyclones require further investigations. Blocking and future evolution of the Mascarene High also motivate for further investigations of the weather system.

Investigation for some ocean-atmosphere processes is motivated by the availability of reanalysis data fields and satellite estimates. Lastly, studying the behaviour of the Mascarene High and its effect on anomalous weather patterns over southern Africa is important because of the impact these weather patterns can have on energy use, agriculture and other socio-economic activities (Rohli, 1995).

1.7 Definition of key terms

- Subtropical anticyclones: Circulations of trade winds at a large scale surrounding high atmospheric pressure in the subtropical belts. They have clockwise circulation in the NH and counter-clockwise circulation in the SH (Sanders, 1953).
- Mascarene High: also known as the South Indian anticyclone, is an anticyclonic circulation of trade winds surrounding central high pressure (Tyson and Preston-Whyte, 2000) in the South Indian Ocean. This weather system is named after a group of islands that are located over the east of Madagascar. These are Mauritius, Réunion and Rodrigues.
- Southwest Indian Ocean: Third world's largest ocean, covering nearly 20% of the Earth's surface water over the Indian Ocean. The part bounded by southern Africa and

Australia, bounded by the Southern Ocean in the mid-latitudes referred to as the SWIO (Meteo-France, 2015).

- Mean sea level pressure (MSLP): Measurement of pressure that is attuned to sea level, not being the actual local atmospheric pressure. The normal range of fluctuations in atmospheric pressure is taken into account and decreases with height (ECMWF, 2015).

1.8 Dissertation structure

The study consists of seven chapters. Chapter 1 has provided the introduction, background, problem statement, aim, specific objectives and justification of the research. The description of the study area is also done in this section.

Chapter 2 provides an in-depth review of literature of previous studies done for subtropical anticyclones. Data and methods of analysis employed in the study are described in Chapter 3.

Chapter 4 focuses on analysing spatial characteristics and ocean-atmosphere interactions of the Mascarene High in the South Indian Ocean. The focus was based on methods and data that allowed for mapping seasonal mean location and shifts of the Mascarene High. Chapter 5 represents the analysis of Mascarene High blocking and how it induces anomalous weather at an event scale.

Chapter 6 focuses on simulating future characteristics in intensity and structure of the Mascarene High in a changing climate due to an increase in anthropogenic greenhouse gases. Lastly, Chapter 7 presents dissertation conclusions, key findings of the study and recommendations for future work.

CHAPTER 2: LITERATURE REVIEW

2.1 Introduction

A comprehensive review of the literature on subtropical anticyclones from a global perspective is presented in this chapter. This section evaluates existing knowledge and establishes possible gaps to generate research questions for the study. Another important aspect of this chapter is to identify methods and techniques previously used when studying subtropical anticyclones. This chapter is organized in thematic areas and begins with understanding the general circulation of the atmosphere.

2.2 General circulation of the atmosphere

Solar heating is a major driving force for circulation in the ocean and atmosphere (Tyson and Preston-Whyte, 2000). The earth's surface consists of unevenly distributed solar heating, being greatest near the equator and least at the poles (Tyson and Preston-Whyte, 2000) resulting in warmer equatorial regions and cooler poles. Energy is therefore transported poleward through atmospheric and ocean circulations resulting in a weakening of the equator-pole temperature gradient. Circulation of global heat and moisture are a result of the Hadley, Ferrel and Polar cells (Preston-Whyte and Tyson, 2000). Global air circulation has one primary circulation cell which is known as the Hadley Cell and is complemented by two secondary circulation cells, referred to as the Ferrel cell and Polar cell (Figure 2.1). Over the subtropics, subtropical anticyclones have been historically linked to the descending limb of the Hadley cell. For both hemispheres, subsidence is greatest on the eastern sides of subtropical anticyclones and tends be stronger in summer when the Hadley Cell is weaker (Li *et al.* 2012). The circulation around subtropical anticyclones is clockwise in the NH and counterclockwise in the SH.

Subtropical anticyclones are also linked to concepts of angular momentum conservation, thermal wind balance and radiative– convective equilibrium and these explain the structure of the annual-mean and zonal-mean Hadley circulation (Rodwell and Hoskins, 2001). Rotating turbulences at a large scale are dominated by columnar vortices that are associated with the axis of rotation (Sreenivasan and Davidson, 2008). Subtropical anticyclones are low-level synoptic scale weather systems and are important weather systems over the subtropics (Chen *et al.* 2001). Subtropical belts consist of cool and surface divergent air that sinks from the upper levels where air converges and originating from the tropical and temperate belts (Tyson and Preston-Whyte, 2000).

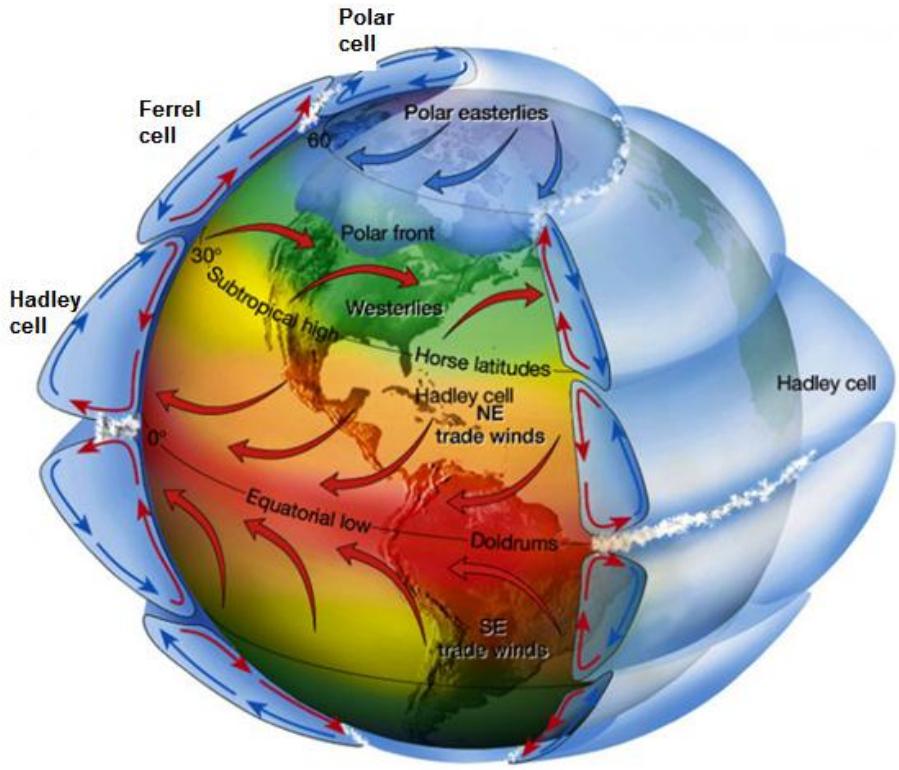

Figure 2.1: Thematic diagram of global wind circulation showing the Hadley Cell, Ferrel Cell and Polar Cell (source: Lutgens *et al.* 2007).

2.3 Characteristics of subtropical anticyclones

In the subtropical belts, anticyclonic perturbations are found to occur on a daily scale within the mean flow in the Southern Hemisphere (SH). The seasonal displacements of subtropical anticyclones is about 4-7° in latitude and usually farthest equatorward, where high-pressure cell concentrations are greatest (Tyson and Preston-Whyte, 2000). The most significant feature of subtropical anticyclones in the SH is the extent to which a tendency is shown for the strongest cells to form well south of a subtropical ridge (Tyson and Preston-Whyte, 2000).

2.3.1 Regions of subtropical anticyclones

The distribution of global subtropical anticyclones is shown in Figure 2.2. A semi-permanent subtropical anticyclone in the North Atlantic basin in the Northern Hemisphere (NH) is known as the Azores High or Bermuda High or North Atlantic High (Davis *et al.* 1996), and it has a major influence on weather and climate over Western Europe, North America and northwestern Africa.

The Siberian High is found in the NH over Siberia. In the SH, over the Pacific Ocean resides a South Pacific High, which is an important and major feature of the austral winter climatology while the North Pacific High or Hawaii High is found over the NH Pacific Ocean (Richter and Mechoso, 2008). The St. Helena High or South Atlantic High is situated over the Atlantic Ocean whilst the Mascarene High is situated over the Indian Ocean.

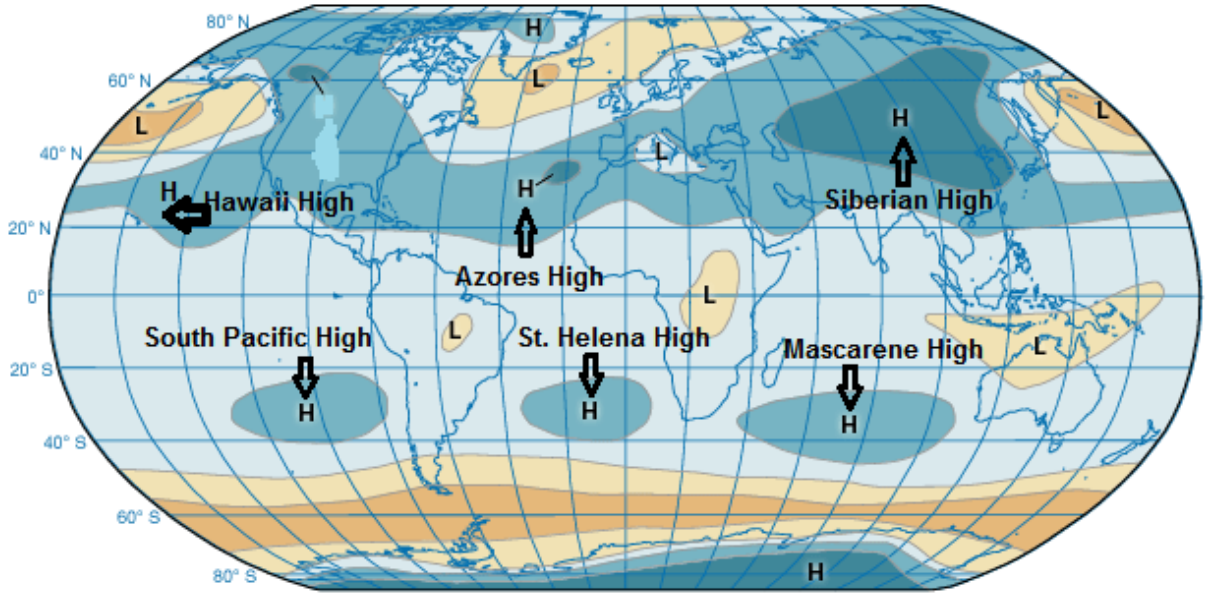

Figure 2.2: Global wind circulation (after: Encyclopedia Britannica, Inc.).

Prevalence of closed anticyclone centres is known to be maximized over the subtropical oceans throughout all seasons (Bell and Bosart, 1989), having different locations for different seasons. It has been determined that there is a substantial monthly, seasonal and interannual variability for closed high centres, a variability that is also found for closed cyclone centres (Bell and Bosart, 1982). Subtropical anticyclones are identified when daily surface air pressure is greater or equal to 1020 hPa (Davis *et al.* 1996), and are known to exhibit a vertical westward phase tilt and a horizontal southwest–northeast phase tilt (Davis *et al.* 1996). Origin of summer circulations is generally well understood over the NH, where numerous studies on subtropical anticyclones have been done (Chen *et al.* 2001). SH summertime climatology for subtropical anticyclones is understood in the same framework as in the NH subtropical anticyclones (Misiyaka and Nakamura, 2010), making the prediction of these systems easier.

In the eastern portion of subtropical ocean basins reside centres of subtropical anticyclones on an annual basis propagating from west to east. In essence, subtropical anticyclones tend to form and intensify in eastern regions of ocean basins (Misiyaka and Nakamura, 2010), with weakening and dissipation found on west of oceans (Sinclair, 1996). Regions such as New Zealand, Africa, South America and southeast of Australia are prone to rapid subtropical anticyclogenesis (Greenhut, 1977).

Generally, west to east movement of global subtropical anticyclones is due to the earth's rotation. This generates moisture transport and vertical motion over subtropical belts for both hemispheres. Variations of the mean location of subtropical anticyclones are observed to bring variations in weather conditions (Li *et al.* 2012). Subtropical anticyclones movements also have a major role in determining the amount of severity of cold waves over affected regions (Rogers and Rohli, 1991).

The SH is dominated mostly by oceans and subtropical surface pressure over oceans maximizes when mid-latitudes westerlies are at their strongest at the end of winter (Seager *et al.* 2003). In the South Indian Ocean, the general shift of the Mascarene High has been linked to the position of the sea surface temperatures (SSTs) influenced by shifts in the Indian Ocean Dipole (IOD) (Manatsa and Behera, 2014).

2.3.2 Trade winds, midlatitude westerlies and equatorial monsoons

Subtropical anticyclones link tropical trade winds regime with the midlatitude westerly belt at the near-surface, having significant influence in the formation of the world's subtropical deserts and Mediterranean climate zones (Li *et al.* 2012). Trade winds are easterly winds found equatorward of the subtropical highs while westerlies characterise the mid-latitude and are the main cause for daily weather patterns over temperate zones, for both hemispheres. Subtropopausal west winds tend to find little space above subtropical anticyclones and are partially pushed downwards. Parts of the winds descend in the horse latitudes and some flow further to the poles. The rotation of the earth diverts these winds to the right (NH) or left (SH), becoming westerly winds in both hemispheres (Tyson and Preston-Whyte, 2000).

Migration of the ITCZ brings the prevalence of monsoon weather systems (Greenhut, 1977). Monsoons and subtropical anticyclones are known to play a major role in the global circulation of the atmosphere and oceans (Rodwell and Hoskins, 2001). Monsoons are defined as 180° seasonal reversal of trade winds accompanied by corresponding changes in rainfall amounts

(Figure 2.3). It may be noted that monsoon rainfall throughout the world sustains 1-half of the human population. Monsoons form when trade winds which blows out of subtropical highs cross the equator and become westerlies under opposite influence of the Coriolis force.

East of subtropical anticyclones over the NH, there exist a steady response to monsoonal convective heating (Rodwell and Hoskins, 2001; Chen *et al.* 2001) and shallow heating to cooling couplets over the west coasts of the subtropical continents (Liu and Wu, 2004). A study by Rodwell and Hoskins (2001), found that the combined effects of monsoonal heating and topography to the east are important for the generation of a surface subtropical anticyclone and subsidence aloft with the strengthening by local cooling over the eastern oceans (Misiyaka and Nakamura, 2010).

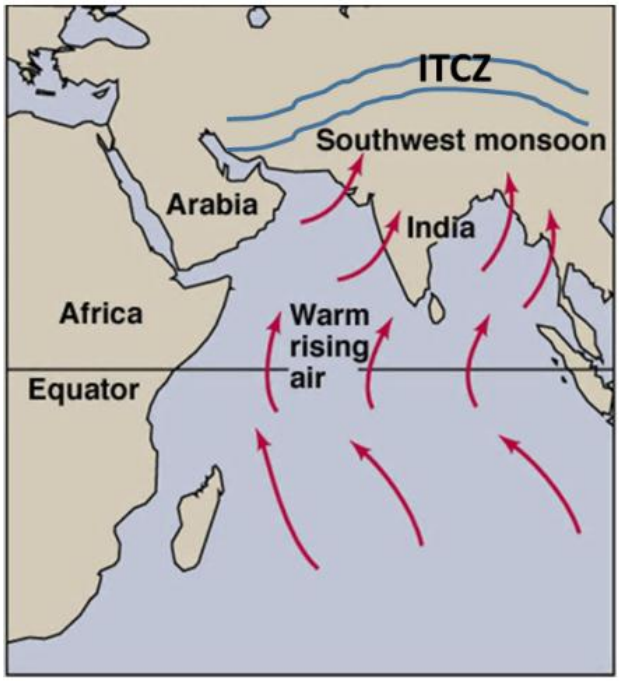

Figure 2.3: Indian monsoon (source: http://global.britannica.com/science/West-African-monsoon).

2.3.3 Isallobaric winds

When a subtropical anticyclone moves from west to east, it creates high and low pressure changes resulting in ageostrophic winds, called isallobaric winds. They develop moving from an isallobaric high towards an isallobaric low. Isallobaric winds also known as Brunt–Douglas isallobaric winds, are wind velocity that occur when the Coriolis force is in balance with a local

accelerating geostrophic wind (Tyson and Preston-Whyte, 2000). Isallobaric winds are real and primarily result from a spatial gradient in pressure and blow perpendicular to isallobars (lines of constant surface pressure change). When pressure changes, the initial response of wind is to be directed to the region of low pressure, thus the balance for this movement results from the Coriolis force. These winds are part of ageostrophic winds contributed by non-stationarity and are instantaneous response to change in surface pressure.

2.3.4 Continental and ridging subtropical anticyclones

In winter, a continental anticyclone is located over southern Africa such that subsidence, settled fine and dry weather prevail over, much of the subcontinent. A Kalahari High (Figure 2.4) is semi-permanent and is situated over the interior and forms part of a subtropical ridge system. It is termed the Kalahari High because it lies over the Kalahari Desert. An important continental high over the NH is the Siberian High. It is the most pronounced feature with surface circulation dominated by huge atmospheric centre of action centred over Asia and controls circulation over the continent (Gong and Ho, 2002).

Berg winds are likely to occur along southern and southeastern coasts of southern Africa due to the presence of the Kalahari high (Tyson and Preston Whyte, 2000). In some cases, when the centre of the subtropical anticyclone is located such that airflow is directly onshore, occurrences of localized unsettled conditions may result (Figure 2.4). When the subtropical anticyclone is centred to the south or southwest of the subcontinent, the ridging of the system over land may cause widespread unsettled weather and rainfall, particularly in coastal areas (Tyson and Preston Whyte, 2000). Ridging anticyclones contribute about half (46%) of the annual rainfall of the Cape South coast of South Africa (Engelbrecht *et al.* 2015). The air circulation transport that may be due to continental anticyclones has been found to follow an annual cycle over southern Africa, having a peak during the austral winter where easterly flow predominate these weather systems over southern Africa (Tyson *et al.* 1996).

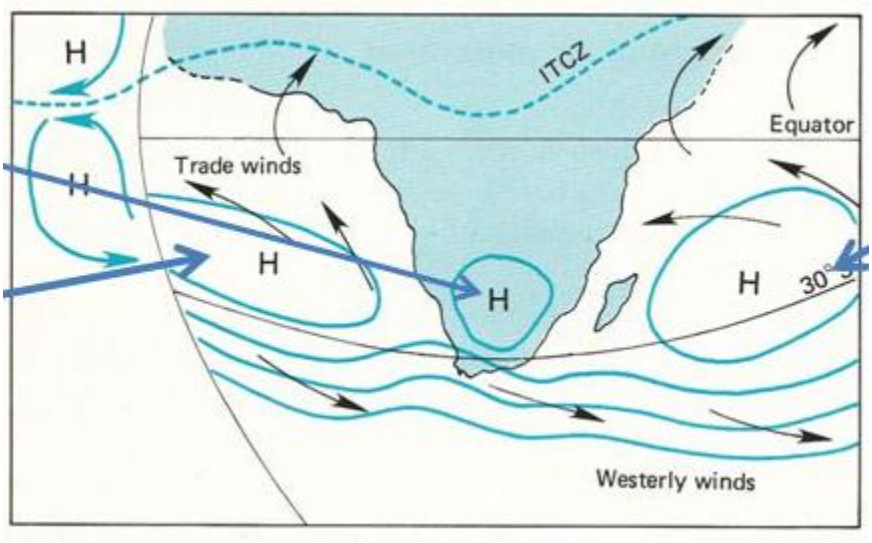

Figure 2. 4: Southern African circulation associated with continental anticyclones (source: Tyson and Preston-Whyte, 2000).

2.3.5 Blocking anticyclones

Blocking action of subtropical anticyclones is generally known as the state of circulation, having normal zonal flow disturbed by strong and persistent meridional-type flow. Blocking of subtropical anticyclones is a circulation anomaly and a local occurrence (Tsou and Smith, 1998) which is a slowing down of the west-east movement of highs, resulting in blocking of disturbances in the westerlies behind the system. These high pressure regions usually consist of pressure and temperature significantly above normal in the troposphere, with pressure in the stratosphere being above normal and temperature below normal (Elliott and Smith, 1949). According to Trenberth and Mo (1985), blocking subtropical anticyclones occur when the westerly flow becomes detached and this results in a long-lived blocking subtropical anticyclone at the surface.

Blocking anticyclone movements are relatively slow from day to day during prevalence, this may be associated with occurrences of anomalous weather conditions (Sanders, 1953). Blocking anticyclones may persist over an area for a number of days and when it breaks its pressure falls off slowly each day. Blocking duration in the NH tends to be longer than blocking in the SH (Trenberth and Mo, 1985). Variations in distribution, characteristics and intensity of the St. Helena High and the Mascarene High plays an important role in rainfall distribution over southern Africa. The slow process can be easily identified. Blocking anticyclones are known to cause the development of long and atmospheric waves which are stable from commencement until they dissipate (Tsou and Smith, 1998).

On average, blocking anticyclones frequently form at latitudes that are higher than those where the subtropical anticyclones normally develop or move such that it is often associated with cut-off lows and cloud bands in the lower latitudes (Tyson and Preston-Whyte, 2000). Blocking regularly associated with a split of the upper westerly jet consisting of two branches. Blocking anticyclones are also associated with semi-stationary waves that are semi-permanent due to large scale planetary subsidence of air which is on the poleward side of the Hadley cell circulation (Tyson and Preston-Whyte, 2000). Low-level blocking episodes are identified by central MSLP that exceeds the time averaged MSLP by more than 20 hPa (Sinclair, 1996). Persistent positive MSLP anomalies can account for the existence of the variable weather patterns over the subtropical regions, through the blocking of other systems (Sinclair, 1996).

2.4 The Mascarene High

2.4.1 Moisture flux, meridional pressure gradient and the Angola Low

Southern Africa is largely semi-arid and experiences a variety of climatic regimes (Tyson and Preston-Whyte, 2000). The subcontinent receives the majority of its rainfall during austral summer. The warm southwest Indian Ocean (SWIO) is a source of moisture for the subcontinent (Ohishi *et al*. 2015).

The Angola Low is a heat low over Angola that regulates moisture convergence over southern Africa. A deep Angola and an intense Mascarene High over the Indian Ocean create a north-south steep pressure gradient allowing for transport of moisture onto the subcontinent (Figure 2.5). The Angola low over southern Africa is identifiable with loops of half-hourly geostationary satellite images, by locating low-level cyclonic and anti-cyclonic upper tropospheric circulation depicted by the cloud motion (Van Heerden and Taaljard, 1998).

In the atmosphere, tropical-temperate interactions play a major role in the general atmospheric circulation. Southern Africa and the SWIO have been identified as important location for tropical–temperate interactions (Washington and Todd, 1999). It has been shown that troughs linking tropical convection over the southern Africa subcontinent, having transients in the zonal westerlies are identifiable as cloud bands on visible and infrared satellite imagery. This weather system is an important austral summertime rainfall-producing system over this region of southern Africa (Harangozo and Harrison, 1983; Smith, 1985 and Diab *et al.* 1991). The weather system is an important feature in the SH subtropical belts. They can extend for 3 000 to 8 000 km, it connects a cold front at their southeastern end to the Inter-Tropical Convergence Zone (ITCZ) at their

northwestern end (Tyson and Preston-Whyte, 2000). On average, an easterly wave is present over the equatorial end of the cloud bands. They play an important role in the interaction between the ITCZ and the mid-latitude frontal belt.

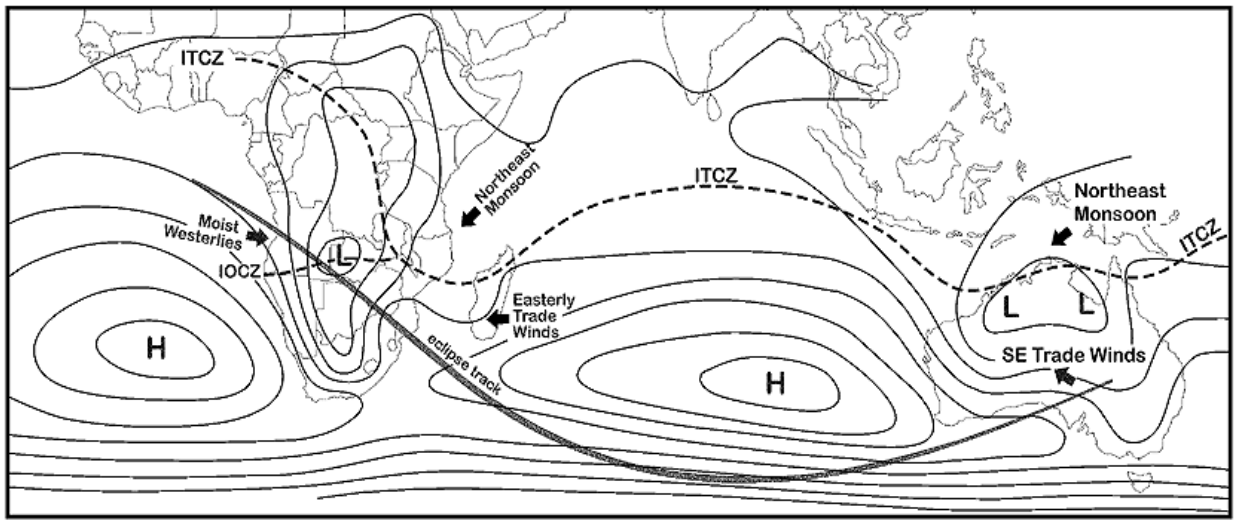

Figure 2.5: Pressure systems influencing southern Africa (source: NASA, 2002).

2.4.2 Steering of tropical revolving systems

Tropical revolving systems (tropical storms, depressions or cyclones) are notoriously destructive because they occur with strong winds, heavy rainfall and abnormally high tides that they generate. For instance, tropical cyclones may cause massive inundation in low-lying areas that are near the coast. Typically, tropical cyclones (TCs) are much smaller than their extra-tropical counterparts; having a diameter of about 650 km. Trajectories of tropical cyclones are mainly influenced by the flow of easterly trade winds that generate from subtropical anticyclones, resulting in their general east to west movement (Jury *et al.* 1993).

Chikoore *et al.* (2015) investigated the 2011/12 season (Jan-Mar) for tropical cyclone occurrences over the Mozambique Channel and found that the Mascarene High can induce an easterly steering flow over the Mozambique Channel that guides weather systems onto the plateau of southern Africa. The loss of human lives due to TC landfalls is usually reduced by the well organized and executed TC alertness and pre-warning mechanisms (Parker, 1999; Roux *et al.* 2004).

2.4.3 Cut-off lows

Another weather system affected by a blocking Mascarene High, is an intense form of westerly trough known as a cut-off Low (Tyson and Preston Whyte, 2000). Cut-off lows are deep low pressure systems, strongest in the middle troposphere, which form at 500 hPa steering levels (Taljaard, 1985). This is when the upper air system separates from the principal westerly flow of the mid-latitudes and it is generally said to be “cut-off” from its westerly flow, forming a cut-off low (Figure 2.6). However, it needs to be noted that the definition of the cut-off low weather systems vary to some extent through literature. Here, it is defined as a low pressure system that separates from a planetary circulation that spins off autonomously as it is no longer linked to the westerly wave (Tyson and Preston-Whyte, 2000).

This weather system is identifiable because it loses all its momentum and can locate over a region for a number of days or propagate slowly before dispersing. They are linked with instability in the mid-troposphere and deep convection and can also bring anomalous weather patterns over a region. They are one of the main drivers of damaging floods and consist of semi-annual variation (Molekwa, 2013). Having peaks between March to May and September to November, with their lowest frequencies between December and February they are mostly associated with blocking subtropical anticyclones (Singleton and Reason, 2007).

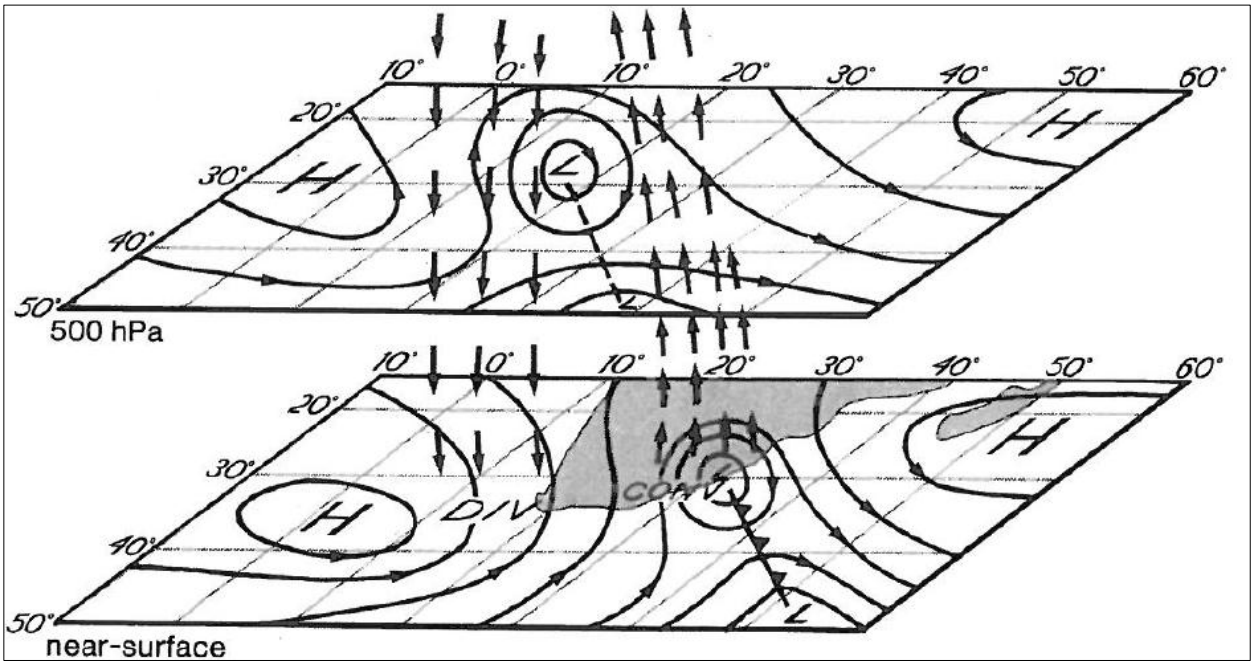

Figure 2.6: 500 hPa and the near surface circulation with the vertical flow associated with a typical cut-off low (source: Preston-Whyte and Tyson, 1988).

2.4.4 The mid-tropospheric Botswana High

The Botswana High is a high pressure cell existing in the mid-troposphere usually situated over central Namibia and parts of Botswana during late austral summer. It is a reflection of the Mascarene High in the upper air as surface highs tilt to the northwest with height. The Botswana High has been found to impact rainfall over parts of the subcontinent, with a stronger than usual Botswana High usually associated with below average rainfall over parts of Zimbabwe (Ratna *et al.* 2013).

For agricultural purposes, it is known that southern African countries that experience the highest levels of yield variation per unit harvested are generally those that lie on the boundary of the ITCZ (Tyson and Preston-Whyte, 2000). High rainfall periods are characterised by a persistence of the ITCZ while drought is linked with dominance of the Botswana High over the subcontinent. Rainfall variability over southern Africa depends mainly on the location and strength of the ITCZ and also the passage of upper westerly waves of the midlatitude (Unganai and Mason 2002). The influence of westerly waves can sometimes be affected by the presence of a strong Botswana High or a persistent Mascarene High blocking extending from the Indian Ocean.

2.5 Ocean-atmosphere interactions

2.5.1 Subtropical anticyclones and surface ocean currents

Ocean currents over the adjacent oceans of southern Africa enhance west to east gradients of rainfall amounts over the subcontinent (Landman and Tennant, 2000). Mean rainfall gradually increases from southwest to northeast. Varying from below 50 mm annual rainfall in the west to above 900 mm in the east (Bartman *et al.* 2003). The cold Benguela current on the west of southern Africa is linked to the occurrence of upwelling and aridity (Jury *et al.* 1996). By contrast, the warm Agulhas current has a significant influence on the regional climate of southern Africa (Jury *et al.* 1993), especially east of the subcontinent. During austral summer, this enhances the development of the South Indian convergence zone (Cook, 2000) influencing annual rainfall over southern Africa.

The Agulhas Current (Figure 2.7) is a western boundary current in the south Indian Ocean (Lutjeharms *et al.* 2012) which plays a vital role in modulating weather and climate over southern Africa. In the greater Agulhas current, warm SSTs are associated with higher than normal summer rainfall as it leads moisture and unstable marine air masses advected from the SWIO onto the

land (Singleton and Reason 2006). The Agulhas current enhances evaporation and transportation of low-level warm moisture toward the southern part of southern Africa and this is a major source of moisture over the southern tip of southern Africa (Singleton and Reason 2006).

The Mozambique current (Figure 2.7) lies within the Mozambique Channel, flowing southward (Zinke *et al.* 2004). It is connected to the Agulhas current and tends to be warm. It increases the evaporation rate over the Indian Ocean which enhances rainfall over the southeast (Reason and Lutjeharms 2000). Previously, it was believed that the Mozambique current is continuous (Lutjeharms *et al.* 2001), but a study by Lutjeharms *et al.* (2012) demonstrated that the circulation of the current is dominated by three large anticyclonic eddies, drifting poleward. According to Lutjeharms *et al.* (2012), a continuous current which is not necessarily an inherent part of the Mozambique eddies may exist along the full Mozambican shelf beak.

The Benguela current (Figure 2.7) is located over the south eastern part of the Atlantic Ocean basin adjacent to southern Africa. This ocean current is fed by the South Atlantic current with minor but significant input of the Indian Ocean thermocline (Gordon *et al.* 1992). During the retroflection of the Agulhas current, the Indian Ocean water is drawn to the Benguela current (Lutjeharms and Cooper 1995). According to Hogan (2013), this ocean current is about 200 to 300 km wide but broadens when flowing northwest along the coast of Namibia and South Africa. The Benguela current, because of its cold nature, produces mild climate over the subtropical western parts of southern Africa (Kimura 2005). Air temperature from the seashore to the land over the subcontinent increases and westerly advection of fog over the Benguela current causes fog over Namib Desert. Over the ocean, subsiding air warms by compressing and, coupling with cool low layers that overly cold ocean currents over west coasts of continents. This creates a temperature inversion (warm air over cold), known as the trade-wind inversion. It functions as a barrier to vertical convection, responsible for aridity and high fog frequency along west coasts of the subtropical continents (Tyson and Preston-Whyte, 2000). These surface ocean currents discussed above are wind driven currents under stress due to subtropical highs

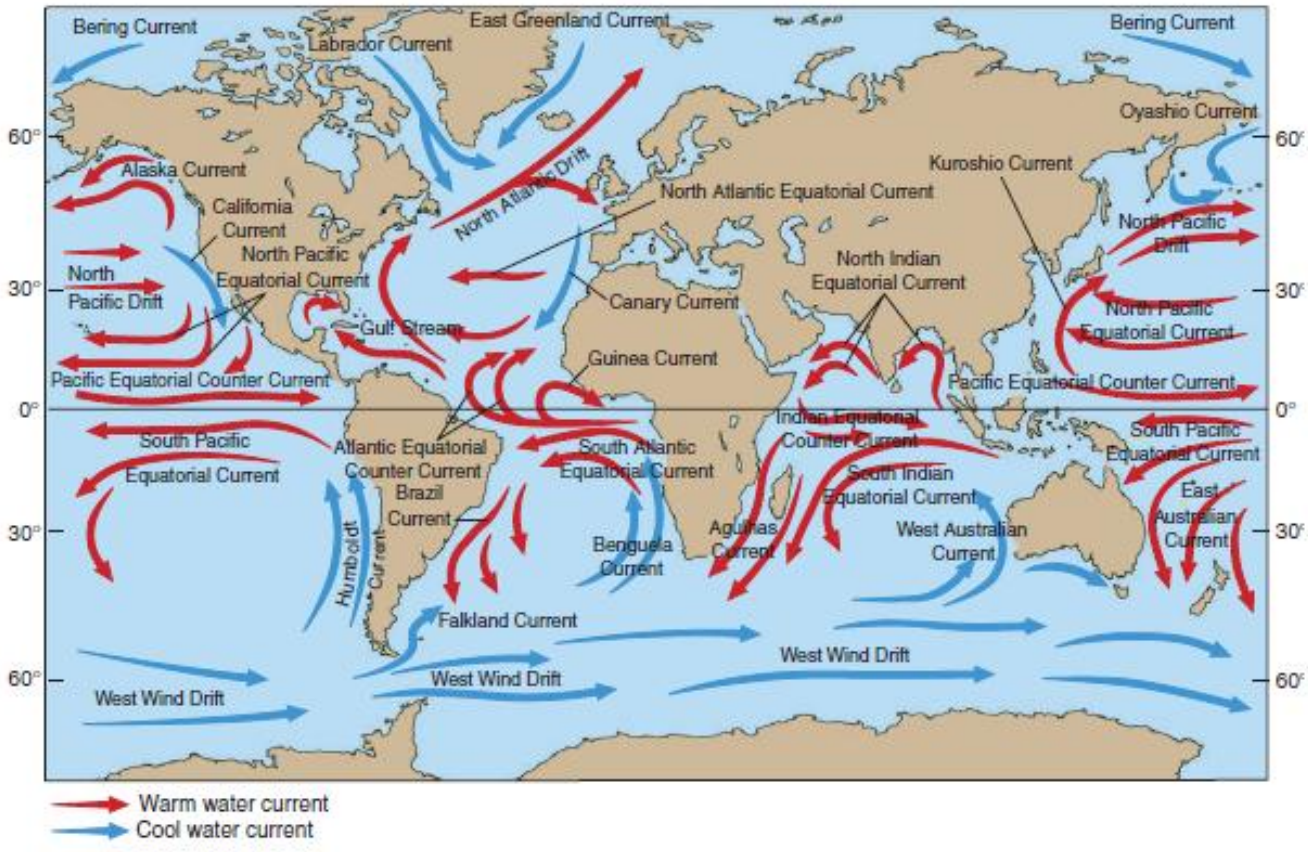

Figure 2.7: Global ocean currents (source: http://www.cengage.com)

2.5.2 El Niño Southern Oscillation

The El Niño Southern Oscillation (ENSO) is one of the main factors governing the variability of rainfall over southern Africa. It can alter the circulation and dynamics of the atmosphere, for example, resulting in changes in the Walker and Hadley cell circulation (Nicholson, 2000). The ENSO signal can be communicated in two ways over the southern African rainfall fields. One way depends entirely of the atmosphere. This is an atmospheric mechanism, related to the generation of the Rossby wave, resulting in Walker circulation adjustments (Cook, 2000). The second one involves ocean-atmosphere interactions.

Droughts occur over southern Africa mostly during ENSO negative phase, coinciding with El Niño years (Rouault and Richard, 2005). When rainfall over southern Africa was correlated SSTs over the equatorial Pacific ocean, it was found that the majority of rainfall events were modulated by ENSO with some resulting in extreme rainfall events (Nicholson and Kim, 1997). In most cases, rainfall over the eastern parts of southern Africa decreases during El Niño (Nicholson and Kim, 1997; Phillips *et al.* 1998). In addition to warm ENSO phase, droughts over the area may also be

influenced by various local and global factors such as the negative Indian Ocean Dipole (IOD) and frequent cyclogenesis over the South West Indian Ocean (SWIO; Masih *et al.* 2014). ENSO phases are identifiable using 4 regions of SSTs in the Pacific Ocean. These regions are namely; Nino 4, Nino 3.4, Nino 3 and Nino 1+2.

2.5.3 Indian Ocean Dipole

An important mechanism that plays a vital role in the formation of IOD is the Bjerknes feedback (Bjerknes, 1969), induced by the equatorial easterly wind mechanism of IOD occurrences (Feng *et al.* 2014). Secondly, there is a wind evaporation-SST feedback that exists over the southeast tropical Indian Ocean. This occurrence is considered as another air-sea coupled process, enhancing the growth of IOD (Hilary *et al.* 2005). Thirdly, it has been shown that the Rossby and Kelvin wave track has an oceanic dynamic process during IOD events (e.g., Webster *et al.* 1999; Rao *et al.* 2002; Xie *et al.* 2002; Feng and Meyers, 2003). A study done by Fischer *et al.* (2005) and Zhao *et al.* (2009) indicated that the Mascarene High triggers the internal variability of the IOD.

2.5.4 Subtropical Indian Ocean Dipole

Related to the recent studies of coupled atmospheric-ocean interactions, similar to the IOD and ENSO is the Subtropical Indian Ocean Dipole (SIOD) phenomenon which is influenced by atmospheric forcing and boundary layer circulation (Behera and Yamagata, 2001). SIOD exists because SSTs in the subtropical Indian Ocean consists of interannual events that are dominant during austral summer (Behera and Yamagata, 2001). The interannual dipole is defined by positive and negative phases.

An understanding of the role and occurrence of the SIOD over the subtropical Indian Ocean has increased in recent decades. Behera and Yamagata (2001) found that the subtropical Indian Ocean SST anomalies are characterised by a basin-wide dipole pattern consisting of opposite modes in different austral summers, with these patterns usually referred to as the SIOD modes. The poles of occurrence for the SIOD are found within Australia and south of Madagascar (Manatsa *et al.* 2014). SIOD phases are identified by the location of warm (cold) SST anomalies in the southwestern (southeastern) subtropical Indian Ocean. The positive phases are characterised by warm SSTs anomalies in the southwestern part and cooler SSTs anomalies in the southeastern part of the subtropical Indian Ocean. Whereas, negative phases are characterised by cooler SSTs anomalies in the southwestern part and warm SSTs anomalies in

the southeastern part of the subtropical Indian Ocean due to the strengthening of the Mascarene High winds in the east of the subtropical Indian Ocean (Manatsa *et al.* 2014).

Rainfall over southern Africa has been shown to be sensitive to the location of Indian Ocean SST anomalies (Huang and Shukla, 2006). Many studies have been done to investigate the links between SIOD to weather and climate over southern Africa (Reason, 2001). SIOD positive phases have been studied to be associated with above normal rainfall over numerous south-central African regions (Behera and Yamagata, 2001). SIOD has also been shown to have major influences over central-southern African floods and droughts (Behera and Yamagata, 2001) which previously could not be explained by the IOD and ENSO (Sovara, 2014). Wetter conditions in eastern and central South Africa have been linked to warm SSTs located in the southwestern Indian Ocean during austral summer (Mason, 1995). It has also been found that TC trajectories in the SWIO are influenced by the SIOD and ENSO (Ash and Matyas, 2012). In the Indian Ocean, strongest interannual variability of SSTs is evident in the southern subtropical-extratropical region (20-50°S; Huang and Shukla, 2006). The enhanced SST fluctuation in the subtropical-extratropical open ocean is a common feature of the Southern Oceans (Huang and Shukla 2006).

2.6 Climate change and subtropical anticyclones

The climate system is changing because of the increase in concentration of anthropogenic greenhouse gases. Projections of the climate system on global and regional scales are mainly based on dynamic model applications which use the laws of physics applied to the earth system with a set of complex partial differential equations (Engelbrecht *et al*. 2011). A variety of models are used to make projections, these include earth system models, coupled ocean-atmosphere models as well as atmosphere only models (Richter and Mechoso, 2008). Statistical and dynamical downscaling techniques are used to provide high resolution detail over an area of interest.

Although projections of dynamic climate models are increasingly being used to inform climate-change adaptation studies, they are sometimes criticized as not being verifiable (Engelbrecht *et al.* 2009). The argument is that it will only be possible to verify the reliability of the projections several decades into the future (Engelbrecht *et al.* 2011). The models are generally verified using present day climate, and an assumption is made that if they simulate present day climate well, their future projections are usable.

Models are projecting the expansion of tropical regions in the future due to global warming (IPCC, 2013; Quan *et al.* 2014). This expansion is expected to cause poleward migration of the Mascarene High and the cold fronts. There is a growing body of the literature suggesting long-term changes are occurring in the boundaries of the Hadley cells. Studies of the expanding tropics and changes in the large scale systems in a changing climate are still developing in the body of knowledge. Changes in the circulation system will result in a change in the weather and climate over southern Africa which include shifts in the subtropical dry zones and significant changes in midlatitude rainfall. These changes may result in vital societal and ecological consequences.

2.7 Summary

This chapter presented a review on studies relevant to the study of the Mascarene High and weather over southern Africa. Most importantly is the development, movement and characteristics of subtropical anticyclones and their influence over subtropical region. Hence, subtropical anticyclones exist over a non-continuous subtropical belts, punctuated by landmasses. The weather and climate over southern African together with ocean-atmosphere interactions that affect this region was also reviewed. The importance of the ocean-atmosphere interactions of Mascerene High on weather and climate over southern Africa was also presented. From the review it can be said that Mascarene High:-

- Drives moisture fluxes onto the southern African region via the trade winds.
- The strength of the trade winds will depend upon the north-south pressure gradient from the Mascarene High to the Angola Low on the interior.
- The mid-tropospheric Botswana High is a reflection of the Mascarene High as surface highs tilt northwest with height.
- The large scale flow from the Mascarene High steers tropical revolving systems in the SWIO westward.
- On occasion, the Mascarene High blocks the passage of disturbances in the westerlies which results in anomalous weather over the subcontinent.
- The seasonal shift eastwards of the Mascarene High is modulated by the Subtropical Indian Ocean Dipole.

CHAPTER 3: DATA DESCRIPTION AND METHODOLOGY

3.1 Introduction

Indian Ocean circulation and transport of heat are quite unique in many aspects, compared to the Pacific and Atlantic Oceans. This led to the development of a sustained ocean observing system over the Indian Ocean, in order to provide ocean observations needed for climate research. The Indian Ocean Observing System (IndOOS) manages data through uses of surface mooring, surface drifters, Expendable Bathythermographs (XBT) lines, biogeochemical observations and Argo floats. These techniques usually complement data collected and monitored through satellite techniques, and have contributed to improved monitoring of the Indian Ocean over the years.

Several datasets employed in this study are obtained from global and regional climate centres which consist of hubs that allow online interactive manipulation and representation of the datasets. Various secondary datasets used in this work are classified under their climatic domain as atmospheric and oceanic. Observations and model projections in this work mainly span from 1985-2014 and 2071-2100 which are basically present day and future 30 year periods. The National Centres for Environmental Prediction-National Centre for Atmospheric Research (NCEP-NCAR) reanalysis I data is used for the present-day climatology period from 1985-2014. Seasons investigated in this study are defined as total of 3 months, with austral summer from December to February and austral winter from June to August. The main aim of this chapter is to present and detail the datasets and methods of analysis employed in this study.

3.2 Description and Sources of Data

3.2.1 Circulation variables

a) Mean sea level pressure

In this work, mean sea level pressure (MSLP) is the primary variable that is analysed. MSLP data over the South Indian Ocean is used to identify spatio-temporal patterns, distribution and intensity of the Mascarene High. MSLP data is obtained from European Centre for Medium-Range Weather Forecasts (ECMWF) European Reanalysis (ERA)-interim reanalysis data via Koninklijk Nederlands Meteorologisch Instituut (KNMI) Climate Explorer. ERA-Interim MSLP is calculated using an atmospheric model and reanalysis system which is an ECMWF's Integrated Forecast System, introduced operationally in September 2006 (Richard *et al.* 2006). The atmospheric model is coupled to an ocean-wave model resolving 30 wave frequencies and 24 wave directions

at nodes reduced to 1°x1° grid (Hoskins *et al.* 1989). MSLP datasets are then compared using NCEP-NCAR reanalysis and National Aeronautics and Space Administration-Modern Era Retrospective-analysis for Research and Applications-Modern Era Retrospective-analysis for Research and Applications (NASA-MERRA) datasets (Suarez, 2008) for the period 1985-2014. NASA-MERRA reanalysis is for the satellite era that employs a major version of Goddard Earth Observing System Data Assimilation System Version 5 (GEOS-5). Comparison of the different MSLP datasets (Figure 3.1) shows agreement and consistency in their annual cycles.

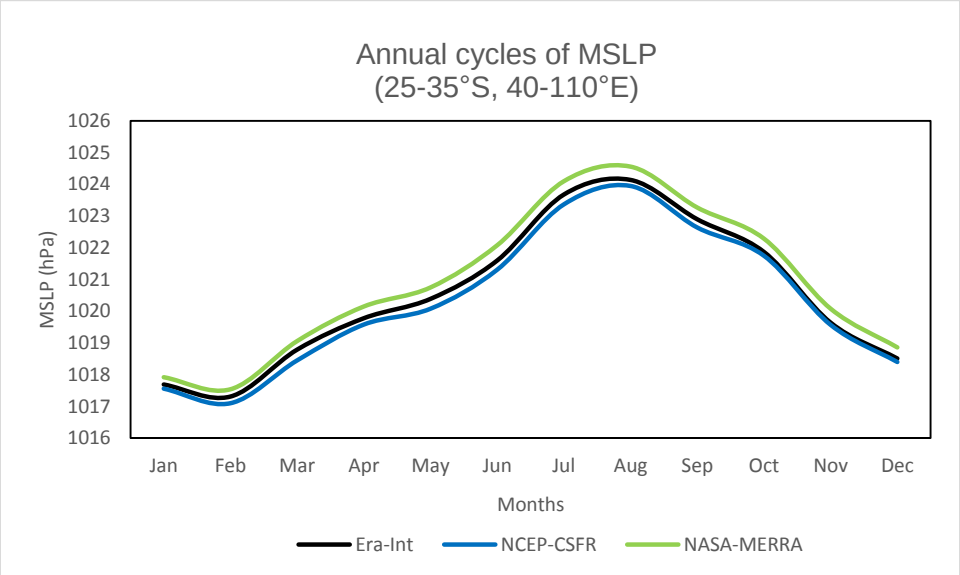

Figure 3.1: NCEP-CFSR, NASA-MERRA and ERA-interim MSLP (hPa) annual cycles (1985-2014).

b) Geopotential height

Geopotential height is defined as a representation of the height of pressure surface in the free atmosphere. Given by the hypsometric equation, derived from the hydrostatic equation and the ideal gas law:

$$h = z_2 - z_1 = \frac{R_d \bar{T}_v}{g} \ln\left(\frac{p_1}{p_2}\right), \qquad \text{(Equation 3.1)}$$

Where, z_1 and z_2 are geometric heights at pressure levels p_1 and p_2, respectively. R_d is the gas constant for dry air, $\bar{T}_v$ is the mean virtual temperature of the layer and g is gravity.

Low height regions are associated with a cold column of air between the surface and (e.g. 850 hPa) and regions of high height are associated with warm columns of air. Geopotential height at 850 hPa datasets is extracted and visualised using NCEP–NCAR reanalysis I online interactive portals (Kalnay *et al.* 1996).

c) Horizontal winds

Horizontal wind vectors (and anomalies) are extracted and visualised from NCEP-NCAR reanalysis I. This provided insights on the mean anticyclonic circulation of wind over the South Indian Ocean. The wind vectors are a representation of the horizontal flow of trade winds and westerlies influenced by the circulation and displacements of the Mascarene High. In the study, wind is used to investigate circulation over the South Indian Ocean and southern Africa influenced by the Mascarene High.

Zonal wind (*u*) is a large scale atmospheric flow consisting of west to east components (latitudinal). South Indian Ocean *u* is plotted to provide a description of wind circulation characteristics influenced by the Mascarene High. Zonal wind circulation is mapped for analysing zonal wind flow in the South Indian Ocean due to large scale circulation of the Mascarene High. Thus, *u* represents westerly wind and -*u* represents an easterly wind.

NCEP-NCAR reanalysis I datasets for *u* is used as a proxy for east-west winds flow. *u* is influenced by the Mascarene High and it usually transports moisture from the warm South Indian Ocean towards the interior plateau of southern Africa. Tropical cyclone (TC) motion in the South Indian Ocean (SWIO) is predominantly due to advection of planetary vorticity by the large scale flow (trade winds).

Meridional wind (*v*) is a large scale atmospheric flow consisting of a south to north components (longitudinal). It is the flow of wind along the longitude. *v* over the South Indian Ocean is plotted to provide a description of longitudinal influenced circulation of the Mascarene High. Thus, *v* represents southerly flow and -*v* represents northerly flow.

d) Vertical velocity

Vertical velocity is a useful parameter for determining air uplift or subsidence. Vertical velocity (ω) may be defined as,

$$\omega = \frac{Dp}{Dt}. \quad \text{(Equation 3.2)}$$

Where Dp is the change in pressure and Dt is the change in time. Since pressure decreases monotonically with height in the earth's atmosphere, ω is negative for uplift and positive for subsidence. The data is obtained from NCEP-NCAR reanalysis I (Rayner *et al.* 2003) and visualised via the online interactive NCEP-NCAR model. In the study, vertical velocity is used to investigate events of Mascarene High blocking and uplift (subsidence) circulations over southern Africa.

e) Vorticity and divergence

Vorticity is a measure of the spin of an air mass, such as a low or high pressure weather systems. Closed-vortex perturbations in atmospheric circulations are common and at any one time many such vortices can be observed in the SH. They tend to move across southern Africa and the South Indian Ocean, from the west and may be long lived. This circulation is produced by both shear and curvature effects (Tyson and Preston-Whyte, 2000).

Thus, curvature vorticity is defined by

$$\text{Curvature vorticity} = \frac{V}{r} \qquad \text{(Equation 3.3)}$$

Where, V is the angular velocity and r is the radius of curvature.

Shear vorticity is generally specified by

$$\text{Shear vorticity} = \frac{dv}{dx} - \frac{du}{dy} \qquad \text{(Equation 3.4)}$$

Where, $\frac{dv}{dx}$ is the change in meridional velocity over change in the x directions and $\frac{du}{dy}$ is the change in zonal velocity over change in the y directions.

Total relative vorticity is the sum of curvature and shear vortices, and is given by

$$\zeta = \frac{V}{r} + \frac{dV}{dn} \qquad \text{(Equation 3.5)}$$

In terms of u and v velocity variables, thus relative vorticity can be expressed as

$$\zeta = \frac{dv}{dx} - \frac{du}{dy} \qquad \text{(Equation 3.6)}$$

This is the rate of change of v (meridional) component of the wind and in the x (east-west) direction and u (zonal) component in the y (north-south) direction. Vorticity is only changed if there is tangential force acting on its surface.

Plotting of vorticity is done at sigma levels, defined as,

$$\sigma = \frac{P}{P_S} \qquad \text{(Equation 3.7)}$$

Where, σ is sigma, *P* is pressure level and *Ps* is surface pressure.

Divergence is referred to as air accumulation or drawing apart and this refers specifically to horizontal inflow (convergence) or outflow of air. Divergence of wind is influenced by speed and direction (Tyson and Preston-Whyte, 2000). Divergence is positive when the area is increasing and divergence is negative when the area is decreasing. Negative divergence is referred to as convergence. Convergence can be a result of winds directed towards a similar point. While, divergence of wind may result from winds moving away from a point and also due to increase in speed. Positive values (+) indicate divergence and negative (-) values indicate convergence. In the study, divergence (convergence) are observed at 850 hPa and 200 hPa atmospheric levels.

$$div = \frac{du}{dx} + \frac{dv}{dy} + \frac{dw}{dz} \qquad \text{(Equation 3.8)}$$

3.2.2 Rainfall

Rainfall datasets employed in the study are from the Global Precipitation Climatology Project (GPCP) Version 2.2 (Huffman *et al.* 2009). GPCP datasets uses rain gauge observation at the surface, merged with polar orbiting and geostationary climate and meteorology satellites observations (Huffman *et al.* 2009). GPCP datasets are available since 1979 to present, in global grids of 2.5° x 2.5° resolutions at monthly timescales and this motivates for the use in the study.

3.2.3 Air temperature

Maximum and minimum air temperatures used in the study are extracted and visualised using the NCEP reanalysis I model. NCEP reanalysis I is a version of the NCEP Reanalysis I model and consists of data which is more accurate, with fixed errors of the past model datasets resulting from physical processes (Kanamitsu *et al.* 2002). The model consists of datasets of global grids with varying resolutions (Kanamitsu *et al.* 2002). Temperature is mainly used for CCAM projections and presented patterns caused by changes in future anthropogenic greenhouse gases.

3.2.4 Outgoing Long-wave Radiation

Outgoing Long-wave Radiation (OLR) is defined as the radiation from the earth and its atmosphere that is emitted in the form of infrared radiation towards space. It is the radiation emitted by the earth's surface and its atmosphere in the infrared wavelengths and sensed by satellites. OLR is estimated by polar orbiting meteorological satellites at the top of the atmosphere (~200 hPa). The presence of deep convective clouds reduces the amount of OLR escaping to space such that regions of low OLR in the tropics are regions of deep convection and high rainfall (Levey and Jury 1996). Several studies have used OLR as a proxy for convection and rainfall in southern Africa (e.g. Mulenga 1998; Reason and Kiebel 2004; Chikoore and Jury 2010).

In this work, OLR is used as a proxy for convection during anomalous weather events. National Oceanic and Atmospheric Administration (NOAA) OLR datasets are measured at the top of the atmosphere via NOAA polar-orbiting satellites. OLR is obtained from NCEP-NCAR reanalysis I datasets (Rayner *et al.* 2003), using 2.5° x 2.5° resolution longitude/latitude grid over southern Africa for the period 1985-2014. . In the study, OLR is used to investigate events of Mascarene High blocking circulations over southern Africa.

3.2.5 Sea Surface Temperatures

Sea Surface Temperatures (SSTs) is water temperature over the ocean's surface. The actual meaning of surface may vary, depending on measurement method employed between average of 1 mm and 20 m below the sea surface. Air masses in the earth's atmosphere are highly modified by SSTs within a short distance. Warm SSTs are known to allow convection and tropical cyclogenesis over the earth's oceans.

HadISST (Rayner *et al.* 2003) data are obtained using NCEP-NCAR reanalysis II portal, for the period 1985-2014. SST analysis done in the study are via Climate Explorer, from HadISST1 of the Met Office Hadley Centre's sea ice and SST datasets. This is a monthly global 1°x1° grid SST and sea ice concentration dataset spanning from 1870 to present. HadISST (Rayner *et al.* 2003) is an SST dataset institution that presents a globally complete monthly record from January 1870 to present. The climatology in this study is defined as the mean SST for the period 1985-2014.

In addition, SIOD investigation is done for the regions 27-37°S, 55-65°E and 18-28°S, 90-100°E following a study done Behera and Yamagata (2001). Calculation of SIOD is decrscribed below:

- Calculate monthly SST anomaly after subtracting monthly climatology and linear trend (for the period 1985-2014).
- Take area-average of the above SST anomaly in the gridded boxes defined by 2001, then calculate monthly SIOD index.
- Calculate austral summer (Dec-Feb) mean SIOD index for each year and define the event year with the index above one standard deviation

3.2.6 Southern Oscillation Index

Southern Oscillation Index (SOI) is a measure of the El Niño Southern Oscillation (ENSO) and is computed using monthly MSLP anomalies between Tahiti (T) and Darwin (D). SOI [T-D] is an optimal index that combines the Southern Oscillation into one series. SOI noise [T+D] series is a measure of small scale and/or transient phenomena that are not part of the large scale Southern Oscillation. SOI values are similar to those calculated by the Climate Prediction Centre (CPC) in that they have been derived using normalization factors derived from monthly values. Thus, SOI is given by:

$$\mathrm{SOI} = 10\,\frac{(\mathrm{Pdiff} - \mathrm{Pdiffav})}{\mathrm{SD\ (Pdiff)}} \qquad \text{(Equation 3.10)}$$

Where;

Pdiff = (average Tahiti MSLP for the month) - (average Darwin MSLP for the month),

Pdiffav = long term average of Pdiff for the month in question, and

SD (Pdiff) = long term standard deviation of Pdiff for the month in question.

The development and intensity of both La Niña and El Niño events are given by the SOI (Figure 3.2). The SOI is used for identifying ENSO phases in the study and how the phenomenon relates to the Mascarene High. SOI is one measure of the large scale fluctuations in air pressure occurring between the western and eastern tropical Pacific (i.e., the state of the Southern Oscillation) during El Niño and La Niña episodes. It needs to be noted that SOI is an index of ENSO. Tahiti is located 17.5°S, 149.6°W and Darwin 12.4°S, 130.4°E. Neutral conditions are between +1 and -1, below -1 indicates El Niño conditions and above +1 indicate La Niña conditions. La Niña conditions account for most frequent occurrence of TCs over the SWIO.

Typically, smoothed time series of the SOI corresponds well with changes in ocean temperatures across the eastern tropical Pacific (Tyson and Preston-Whyte, 2000). The negative phase of the

SOI represents below-normal air pressure at Tahiti and above-normal air pressure at Darwin. Prolonged periods of negative (positive) SOI values coincide with abnormally warm (cold) ocean waters across the eastern tropical Pacific typical of El Niño (La Niña) episodes. Monthly data for the SOI from NOAA CPC is used in this study and is obtained via KNMI Climate Explorer. Monthly southern oscillation indices are used in each year from 1985-2014.

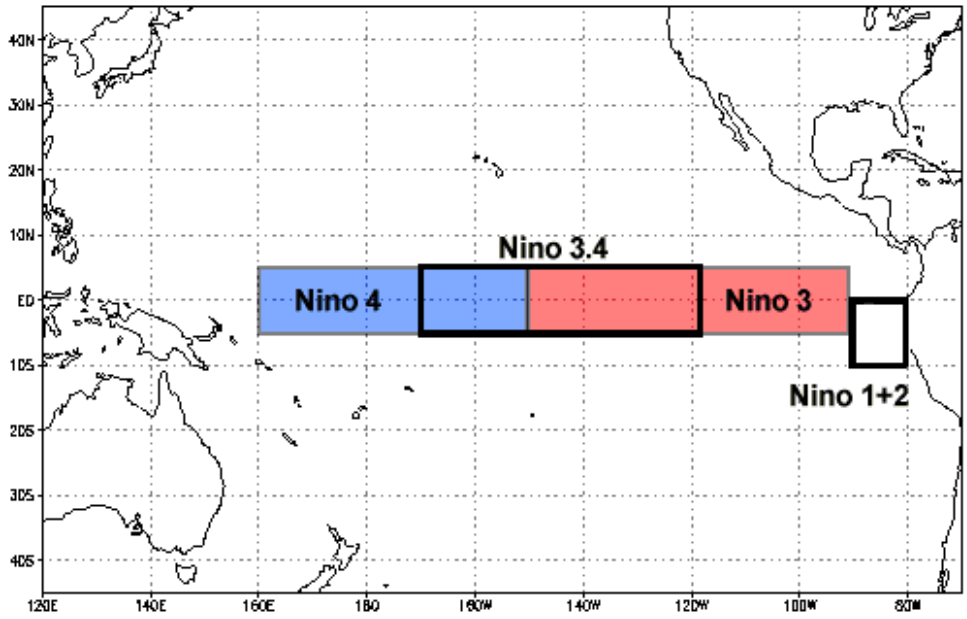

Figure 3.2: Equatorial Pacific Ocean Niño regions (source: NOAA's national climatic data centre 2013).

3.3 Research Methods

The study identifies the Mascarene High MSLP for its features and also geopotential height at 850 and 500 hPa to identify blocking (after Sinclair, 1996). Changes leading to dynamical modes of variability of the Mascarene High and how it varies seasonally are also examined. The relationship of the Mascarene High blocking with other weather systems such as cold fronts, TCs, cut-off lows and cloud bands is also investigated at event time-scales.

3.3.1 Principal Components Analysis

Principal Components Analysis technique (PCA) or Empirical Orthogonal Function (EOF) analysis technique is applied to study spatial modes and patterns of variability together with how they change in time (space-time variance). In statistics, the description of the PCA analysis technique is categorized as a multivariate statistical technique (Shea, 2015). This analysis technique is

useful in identifying spatio-temporal cycles and patterns (Davis *et al.* 1996) of ocean-atmosphere variables.

PCA is useful for identifying common fluctuations which depend on the data for the phenomenon of interest. PCA has been used widely in the geophysical sciences including meteorology and oceanography (Bollen *et al.* 2009). It allows for calculation and orthogonal linear combinations for variables accounting for maximum possible amount of variance within the data (Mulenga, 1998). PCA has been considered to be quite useful for climate data reduction and factor analysis (Preisendorfer, 1988 and Jackson, 1991) .The technique has a number of advantages and are labeled below:

- Description of important patterns of data variability
- Compressed datasets
- Data is filtered using significant components
- Orthogonality property of the components is useful for predictor variables
- Exploratory analysis of data allows dominant data description for inter-relationships

One specific objective of the study is to map mean spatial characteristics and seasonal shifts of the Mascarene High. This is done by investigating the MSLP over the South Indian Ocean and an analysis on whether it varies seasonally. In this study, it is useful for investigating spatio-temporal variability patterns.

3.3.2 Trend Analysis

Analysis of trends and other statistical significance are vital in climate research. Trends may be linear or non-linear and detects rate of change patterns over a time period. Linear MSLP trends for the period 1985-2014 are determined using trend analysis. In this study this technique investigates MSLP variability and cycles in the South Indian Ocean. MSLP datasets employed are obtained from ECMWF ERA-interim via KMNI archives for analysis.

3.3.3 Correlation Analysis

Correlation analysis is the prediction of the behavior of one or more variables and is based on fluctuations of one or more related variables. South Indian Ocean MSLP may be linked to the global ENSO, IOD and SIOD phenomena. Thus, this study investigates the relationship by applying the correlation analysis technique using cross-correlation. MSLP, ENSO, IOD and SIOD data is correlated for seasonal means, standard deviations and seasonal anomalies. Cross-

correlation is performed to determine the relationships between MSLP and ENSO at seasonal and intraseasonal time scales applying different leads and lags. South Indian Ocean HadISST (Rayner *et al.* 2003) datasets are correlated with MSLP. Correlation analysis is done to determine the relationship between MSLP, Indian and Pacific Ocean SST's.

3.3.4 Anomalies

An anomaly is a deviation from what is standard or normal. The anomaly technique is for investigating anomalous circulations resulting from Mascarene High blocking. Wind fields are mapped to determine variations in trade winds circulations. NCEP-NCAR reanalysis I portal is a continually updating gridded dataset representing the state of the earth's atmosphere, incorporating observations, having NWP model output dating back to 1948. This is a joint product from NCEP-NCAR. 1985-2014 is the normal period for the study. Wind vector, zonal wind and geopotential height anomalies obtained from NCEP-NCAR reanalysis I (Kalnay *et al.* 1996) and are analysed.

3.3.5 Composite Analysis

Composite analysis is used in climatological studies to show common occurrences and characteristics for selected years or seasons investigated. The technique is similar to correlation analysis as it shows better trends as compared to trends shown by individual cases (Chikoore, 2005). It is a technique used for studying structures of synoptic disturbances by displaying common features for a group of cases, which are not easily identified by individual cases as it depicts relationships within meteorological variables (Keshavamurty and Rao, 1992).

In this study, composite analysis is used to investigate South Indian Ocean MSLP, South Indian Ocean, Pacific Ocean SST's and southern Africa rainfall, OLR, wind and omega in relation to the Mascarene High distribution and movement. Intra-seasonal and event time-scales composites for selected MSLP anomalous distribution events with large amplitude changes in the South Indian Ocean are also analysed. These events are important in the study by indicating anomalous weather patterns over southern Africa caused by Mascarene High blocking. Circulation variables for selected events are also investigated.

3.3.6 Event Scale Analysis

Event scale analysis is used for Mascarene High blocking events and anomalous weather patterns over southern Africa. Event scale analysis is used for gaining an in-depth knowledge about Mascarene High blocking. Event scale analysis focuses on identifying Mascarene High

blocking (anomalies) at events scales and investigates how these blocking affect the occurrence of TCs, cut-off lows and cloud bands weather systems over southern Africa.

3.3.7 Blocking Index

Blocking subtropical anticyclones are referred to as an intense high pressure systems which can form further south than usual and tend to remain near stationary for extended daily periods of time (Sinclair, 1996). These subtropical anticyclones somehow "block" the west to east progression of weather systems (Sinclair, 1996).

Mascarene High blocking prevails when the usual passage of transient disturbances through a region during circulation in the subtropical belts is temporarily obstructed by a long-lived circulation feature (Sinclair, 1996). Blocking indices are calculated based on NCEP-NCAR reanalysis I (Kalnay *et al.* 1996) daily operational analyses for positive MSLP anomalies. This follows a method used by Sinclair (1996) where ECMWF daily reanalysis data is used. Seasonal event time-scale anomalies of MSLP and geopotential height (500 hPa) for the period 1985-2014 are mapped using daily composite NCEP-NCAR reanalysis I.

This study uses a blocking index defined by Tibaldi and Molteni (1990), which is modified from Lejenas and Okland (1983). The index is suited for real-time atmospheric monitoring, isolating regions of easterly flow at 500 hPa associated with high-latitude blocks. For each longitude, the southern 500 hPa geopotential height gradient (GHGS) and northern geopotential gradient (GHGN) are computed by:-

$$\text{GHGS} = \left[\frac{Z(\Phi_O) - Z(\Phi_{\S})}{\Phi_O - \Phi_{\S}}\right]$$

$$\text{GHGN} = \left[\frac{Z(\Phi_n) - Z(\Phi_o)}{\Phi_n - \Phi_{\S}}\right]$$

Where, Φ_n = 80°S + §, Φ_O = 60°S + §, $\Phi_{\S}$ = 40°S + §, § = 5°, 0°, 5°

A given longitude is said to be blocked at a given time if the following conditions are satisfied for at least one value of §:

GHGS > 0 or GHGN <-10 m/deg latitude

A 5 day running mean can be applied to the 500 hPa height field prior to calculating GHGS and GHGN to isolate potential blocking episodes of sufficient duration.

3.3.8 Hovmöller diagram

This is a diagram that shows isopleths of atmospheric variation, such as pressure or thickness, usually averaged over a band of latitude. Displaying time versus longitude on the axis, demonstrating the progression of large scale atmospheric features over a long period of time. The study employed these diagram for MSLP (surface and mid-levels) to identify Mascarene High blocking events.

3.3.9 NCEP-NCAR reanalysis

NCEP-NCAR reanalysis is a joint product consisting of datasets that are continually updated in grids that represent the state of the earth's atmospheric variables (Kalnay *et al.* 1996). It is a research and development application, incorporating observations and Numerical Weather Prediction (NWP) model outputs that date back to 1948 (Kalnay *et al.* 1996).

Atmospheric reanalysis data provides necessary ocean-atmosphere variables at spatio-temporal domains. Reanalysis data is widely used in climate research, as the data spans for periods greater than 60 years (Manatsa *et al.* 2014). Meteorological reanalysis is a meteorological data assimilation technique used by model through assimilating historical observational data which can span for an extended period through applying consistent assimilation (Sinclair, 1996).

NCEP-NCAR reanalysis (Kalnay *et al.* 1996) is used to map spatial distribution of MSLP, wind vector, zonal wind, vorticity at 0.995 sigma, geopotential height at 500 hPa, SSTs dominant modes of variability and velocity potential. The portal is also used to map omega at 500 hPa, to show vertical motion of air over the South Indian Ocean and southern Africa. The maps produced by NCEP-NCAR (Kalnay *et al.* 1996) model represent weather and climate parameters within different latitudes and represents data for sparse observations. The region identified for the Mascarene High is defined by the box 25-35°S and 40-110°E (Figure 1.1).

3.4 International Research Institute Climate Data Library

The International Research Institute (IRI) data library contains a variety of land, ocean-atmospheric variables from vast datasets sources. Elevation over southern Africa (Figure 1.2) is generated via IRI data Library archives. Some plots were generated using IRI maproom on http://iridl.ldeo.columbia.edu. The data is extracted from NOAA NGDC (National Geophysical

Data Centre), Gridded 1 km, consisting of quality control by the global Digital Elevation Model (DEM) data from the Global Land One-km Base Elevation Project (Hasting *et al.* 1999).

3.5 Conformal-Cubic Atmospheric Model

Atmospheric simulations for present day and future climate are done using the Conformal-Cubic Atmospheric Model (CCAM) for the period 1961-2100, however only data for 1985-2014 and 2071-2100 is used for this study. CCAM was developed by the Commonwealth Scientific and Industrial Research Organization (CSIRO) and is a hydrostatic atmospheric model with 2 time-level semi-implicit time differencing (Quan *et al.* 2014). The model applies semi-Lagrangian advection associated with bicubic horizontal interpolation and total-variation-diminishing vertical advection (Quan *et al.* 2014; Engelbrecht *et al.* 2009). It also comprises of enhanced and no lateral boundary condition requirements because it runs in stretched grid mode over the whole globe when it is not employing quasi-uniform resolution globally (Katzfey et al. 2011).

CCAM has been shown to provide present day simulations that are satisfactory for variables such as annual rainfall and temperature distributions over southern Africa (Engelbrecht, 2005; Engelbrecht *et al.* 2009). Engelbrecht *et al* (2009) discussed projected changes in intensity and displacements of the Mascarene High in a changing climate using CCAM under the previous A2 scenarios. CCAM has been used extensively in South Africa (e.g. Engelbrecht *et al.* 2002; Engelbrecht, 2005; Olwoch *et al*. 2008; Engelbrecht *et al.* 2009; Potgieter, 2009) and it is the model that the Council for Scientific and Industrial Research (CSIR) employs for projections on a daily, seasonal and multidecadal timescales. CCAM is forced in the surface with Sea Surface Temperatures and Sea ice concentrations from six different coupled models. These coupled models are ACCESS, CCSM4, CNRM, GFDL, NOR and UKMO, resulting in six different ensemble members for different greenhouse gas concentration paths. In this study CCAM is forced with two paths of greenhouse gas concentrations as described in the next subsection.

3.5.1 Representative Concentration Pathways

Representative Concentration Pathways (RCPs) are four greenhouses gas concentrations (not emissions) paths adopted in the 5th 2014 Intergovernmental Panel on Climate Change Assessment Report 5 (IPCC-AR5) and precisely used in research and climate modeling. RCPs describe four possible climate projections and they can be considered possible depending on how much greenhouse gases will be emitted in future (Figure 3.3). The four climate futures are RCP 2.6, RCP 4.5, RCP 6, and RCP 8.5. RCPs consists of a possible range of scenarios for radiative

forcing projections towards the year 2100 (Van Vuuren *et al.* 2011). RCPs predict possible future changes in the earth's climate. Four important reasons for RCPs development include:

- Covering a wider range of greenhouse gas (GHG) concentrations.
- Need for a wider set of parameters.
- Scenarios covering mitigation & adaptation issues.
- Use more recent insight into trends in scenario drivers.

This current study employs RCP 4.5 and 8.5 scenarios to force the CCAM to simulate for the period 2071-2100. RCP 8.5 is based on high emissions and is consistent with a future that has minimal policy changes reducing emissions. It was developed by the International Institute for Applied System Analysis in Austria and is characterised by increasing concentration of greenhouse gas emissions over time (Engelbrecht *et al.* 2011). RCP 4.5 is developed by the Pacific Northwest National Laboratory in the United States of America, whereby, radiative forcing is stabilised and consistent with a future with reductions in emissions.

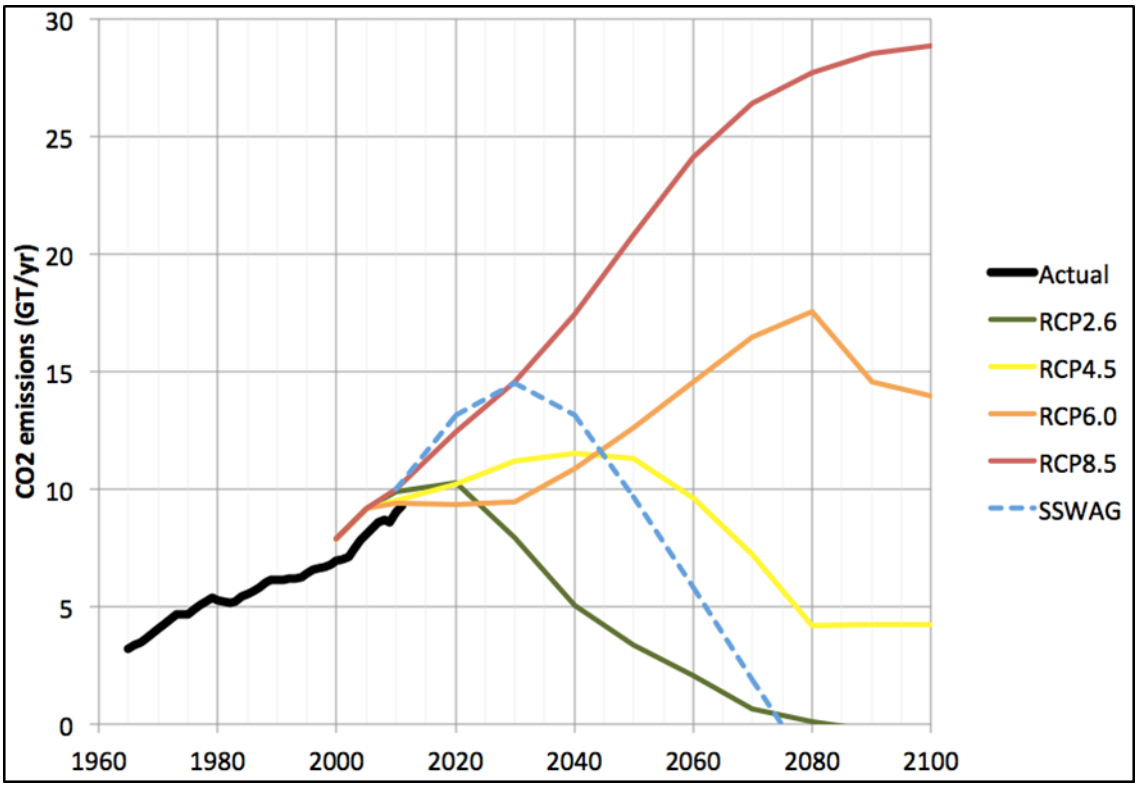

Figure 3.3: Fossil fuel carbon dioxide emissions to 2100 (Source: IPCC 5th Report, 2013).

3.6 Grid Analysis and Display System Version 2.0.2.oga.2

Grid Analysis and Display System (GrADS) was developed by the Centre for Ocean-Land-Atmosphere Studies (COLA). GrADS is a visualisation tool or software that allows for displaying and manipulating earth science data. It can be used on binary, GRIB, NetCDF and HDF-SDS formats. Most of the ocean-atmosphere parameters plotted in the study are visualised using GrADS. The visualisation tool is used to map ocean-atmosphere parameters over southern Africa and the South Indian Ocean. Monthly mean and 30 year means modelled using CCAM and other variables derived from the NCEP/NCAR reanalysis I, are also displayed using GrADS.

3.7 Summary

This chapter described datasets and methods employed to achieve the specific objectives. The main datasets described is MSLP over the South Indian Ocean. Variables that are linked to the development, distribution and movement of the Mascarene High in the South Indian Ocean are also detailed, including their sources.

NCEP–NCAR reanalysis (Kalnay *et al.* 1996) was employed for observational datasets. KNMI monthly reanalysis correlation of MSLP in the South Indian Ocean with ENSO is also described in this chapter. Composite analysis of the regional circulation discussed in relation to large scale impacts of the Mascarene High. GrADS is useful for interactive manipulation and visualisation of the datasets. In the next chapter, results of the study are presented and discussed with reference to objectives set in Chapter 1.

CHAPTER 4: SPATIAL PATTERNS AND TEMPORAL CHARACTERISTICS OF THE MASCARENE HIGH AND INTERACTIONS WITH THE OCEANS

4.1 Introduction

The Southern Hemisphere (SH) consists of three dominant synoptic scale subtropical anticyclones and they are the South Pacific High (Pacific Ocean), St. Helena High (Atlantic Ocean) and Mascarene High (Indian Ocean; Figure 4.1). In this chapter, investigations of mean spatial characteristics and shifts of the Mascarene High are presented. Maps presented show occurrence, distribution and movement of the Mascarene High in the South Indian Ocean based on 30 years National Centres for Environmental Prediction-National Centre for Atmospheric Research (NCEP-NCAR) reanalysis datasets. Fluctuations in spatial characteristics and intensity of the Mascarene High that are analysed, determine the behaviour of atmospheric circulations and rainfall contribution over southern Africa. Lower and upper tropospheric fields are also investigated, focusing on describing ocean-atmosphere interactions and circulations.

Analyses presented in this chapter include spatial characteristics, seasonal and annual cycles, intensity and interannual variability of the Mascarene High. Ocean-atmospheric interactions in relation to the Mascarene High are also presented.

4.2 Spatial patterns of the Mascarene High

4.2.1 Mean spatial characteristics and seasonal shifts

Latitudinal and longitudinal boundaries of the Mascarene High are based on monthly north-south and west-east MSLP locations and displacements. In this study, Mascarene High boundaries are defined as 25-35°S; 40-110°E (Figure 4.2) in agreement with earlier studies by Xue *et al.* (2003) and Manatsa *et al.* (2014). The boundaries are defined by mapping north-south and west-east limits of the maximum Mascarene High isobar, which is ≤1023 hPa (Figure 4.2).

There's variability in seasonal location of the Mascarene High (Figure 4.3) which is linked to the Inter-Tropical Convergence Zone (ITCZ) and South Indian Convergence Zone (SICZ), persisting in early austral summer over southeast of southern Africa (Cook 1998). Migration of the SICZ is influenced by meridional and zonal wind convergence flow, eddy activities and moisture advection associated with the Mascarene High circulation. The SICZ which is a land-based convergence zone and the ITCZ, migrate equatorward (poleward) during austral winter (summer). This migration largely contributes to the equatorward (poleward) location of the Mascarene High during

austral winter (summer). Thus, it is vital to consider ITCZ and SICZ seasonal migration and location influences on seasonal Mascarene High displacements. During summer (winter), the Mascarene High is displaced southeast (northwest) (Figure 4.3a and b).

Highest latitudinal location is found to be 28°S during austral winter whilst the lowest latitudinal location 37°S is observed during austral summer (Figure 4.4). In addition to seasonal displacements, mean monthly migration of the Mascarene High is shown in Figure 4.5. Highest longitudinal displacement is 87°E, found in late austral summer. Lowest displacements is 60°E, found in early austral winter. It is important to note that there Mascarene High consist of variability in location and displacement at different time-scales.

At 850 hPa, the mean location of the Mascarene High is displaced to the northwest relative to its location at the surface (Figure 4.5). Due to the high plateau over southern Africa, the 850 hPa surface is closer to the land. Whilst, seasonal location of the Mascarene High varies and dominance is found in austral summer when the weather system migrates westward (Figure 4.6).

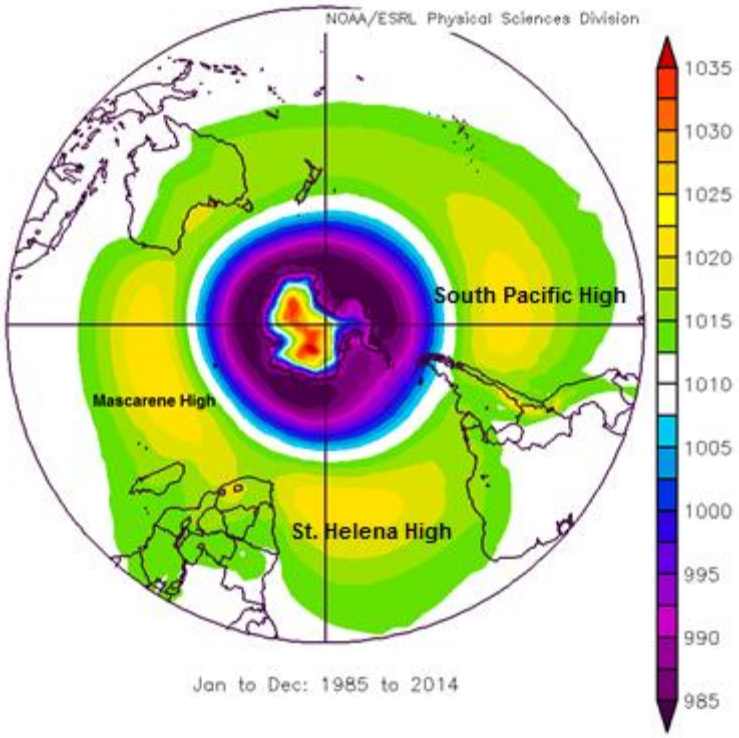

Figure 4.1: Mean annual MSLP (hPa) over the SH (1985-2014).

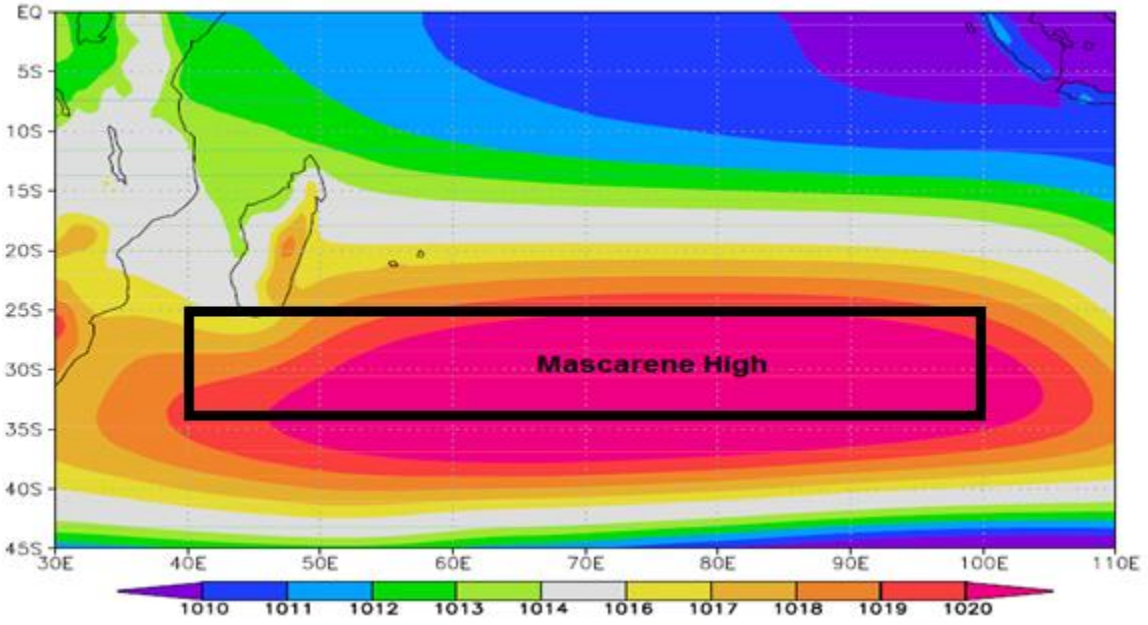

Figure 4.2: Annual mean position of the Mascarene High over the South Indian Ocean (1985-2014).

a)

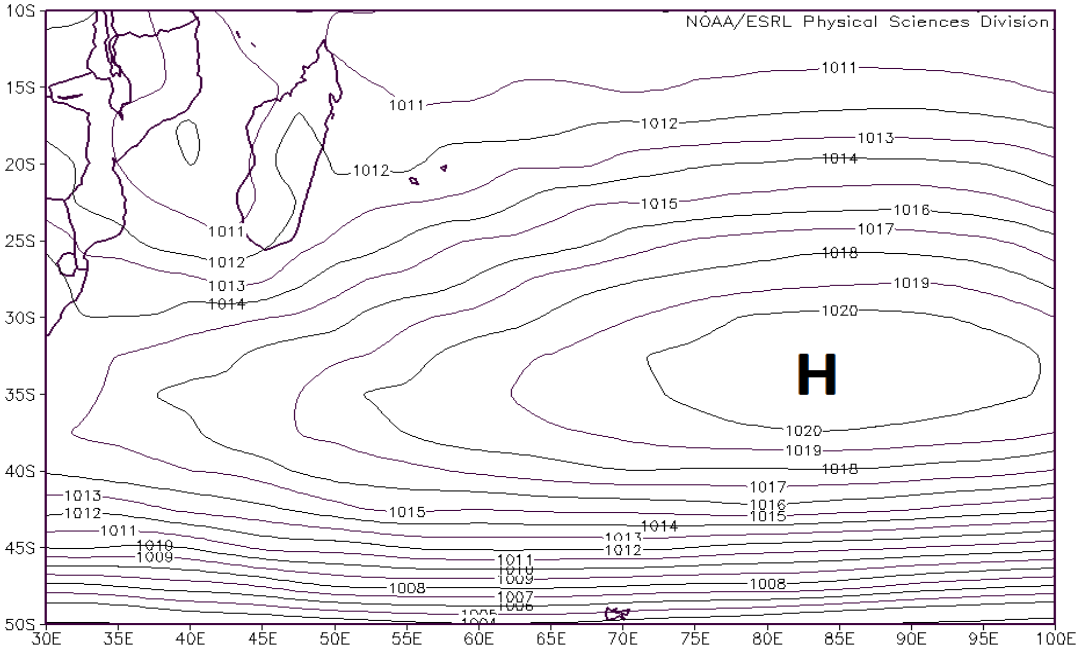

b)

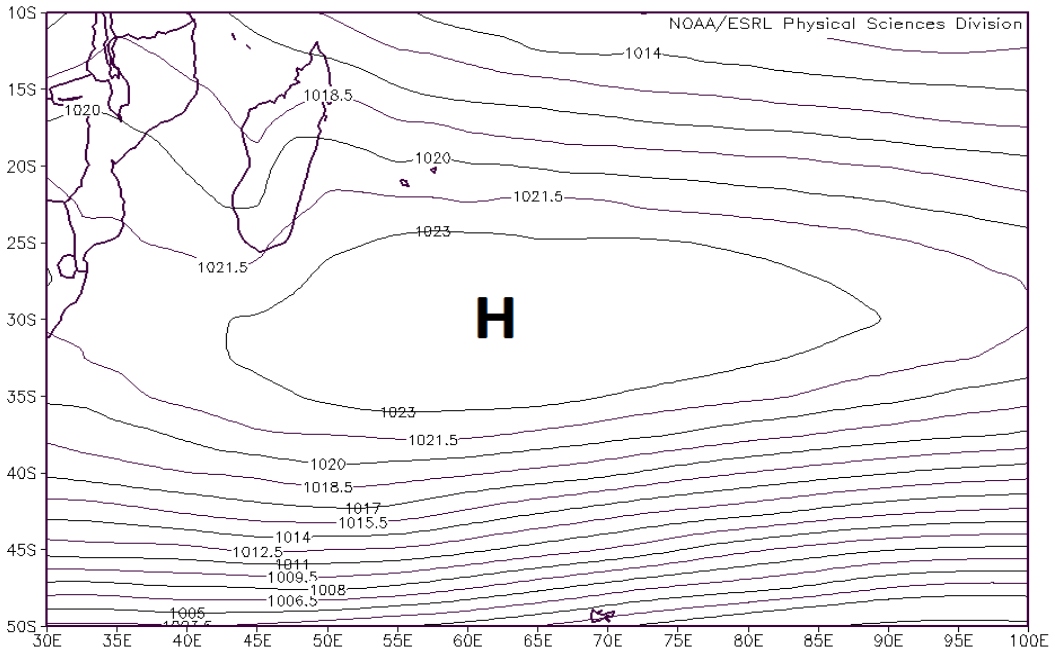

Figure 4.3: Mean spatial characteristics and intensity of the Mascarene High over the South Indian Ocean a) summer and b) winter (1985-2014).

a) b)

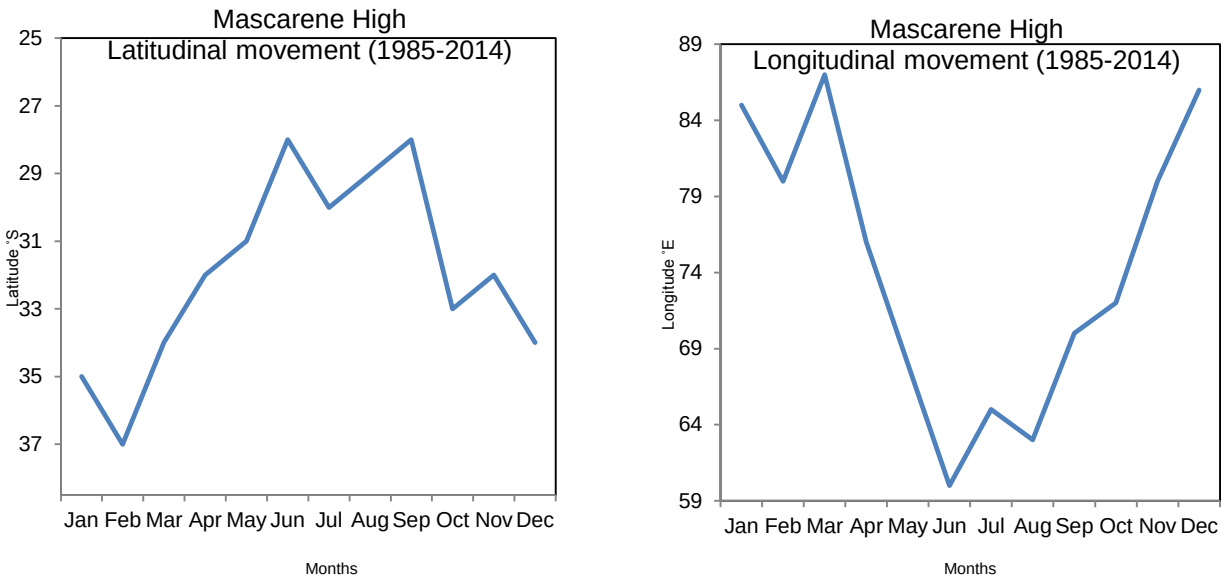

Figure 4.4: Mean annual a) Latitudinal and b) locations of the Mascarene High (1985-2014).

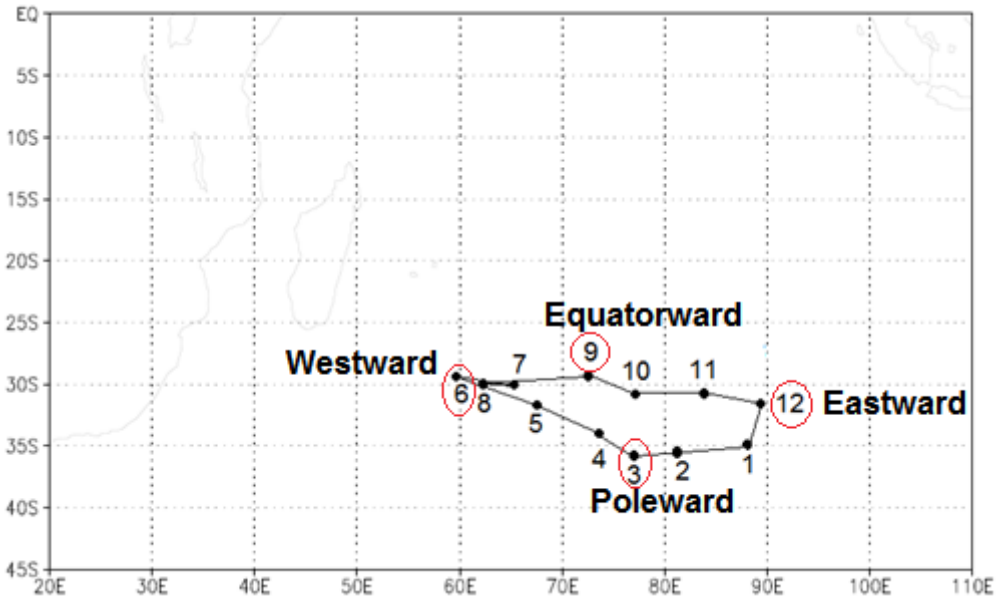

Figure 4.5: Mascarene High monthly mean position over the South Indian Ocean (1985-2014).

a)

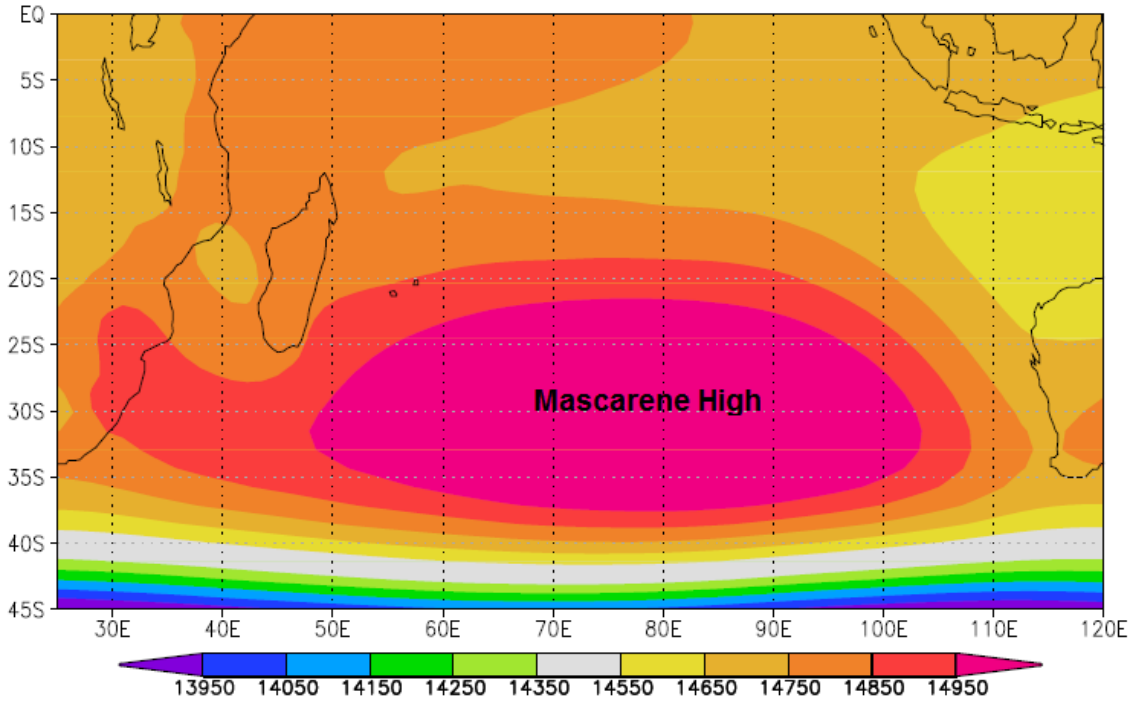

b)

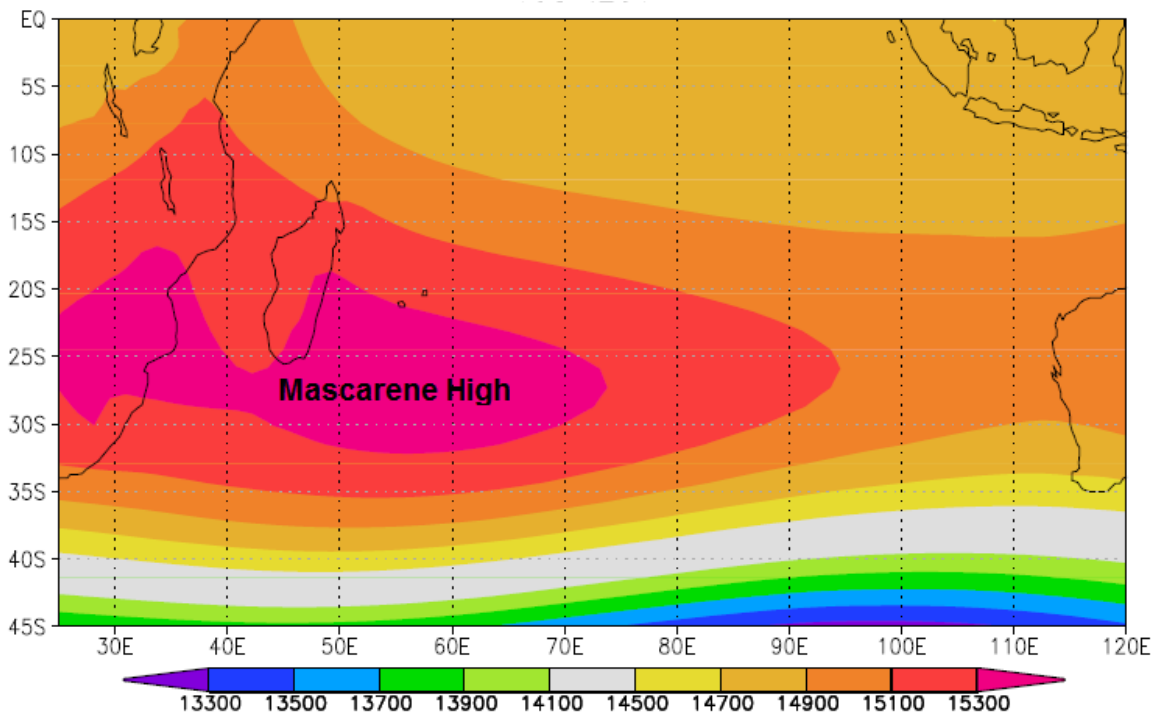

Figure 4.6: Mean geopotential height at 850 hPa over the South Indian Ocean (1985-2014).

4.2.2 PCA for MSLP over the South Indian Ocean

PCA of MSLP over the Indian Ocean, indicates two distinct regions of variability over the South Indian Ocean (Table 4.1 and 4.2). Dominant modes of MSLP (PC1 and PC2) are orientated in the southwest during austral summer (Figure 4.7). The first mode of variability explains 43.96% of the total variance (Figure 4.7). The second seasonal PCA mode explains 23.58% of the total variance, consisting of a poleward orientated Mascarene High location (Figure 4.7). However, austral winter MSLP PCA's show different modes of spatial dominance and variability. PC1 is oriented further south of the South Indian Ocean (Figure 4.8), explaining 59.25% of the total variance. PC2 explains 13.97% of the total variance and shows dominance to be southwest of the South Indian Ocean (Figure 4.8). Spatial loadings of the results maximize in an elongated region with mean location 25˚-35˚S and 40˚-110˚E which is the spanning of the loading zone of the Mascarene High.

a)

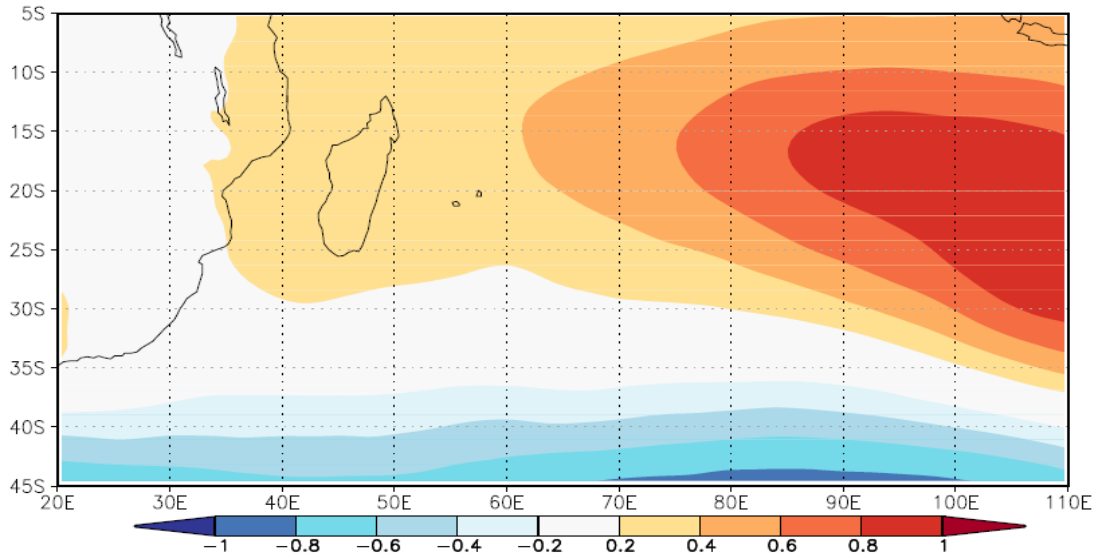

b)

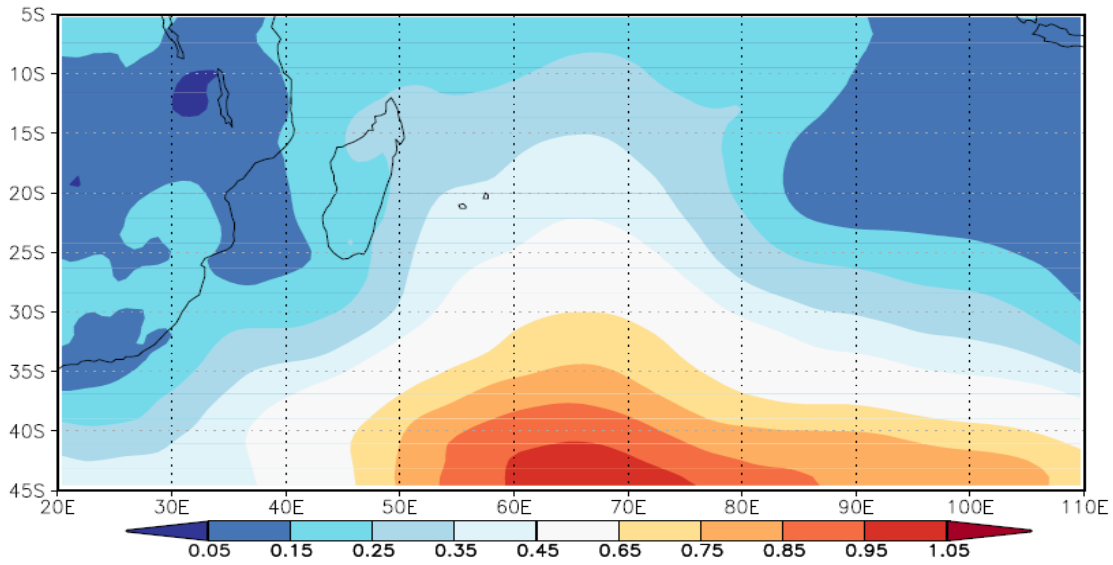

Figure 4.7: Austral summer MSLP (hPa) a) PC1 and b) PC2 over the South Indian Ocean (1985-2014).

a)

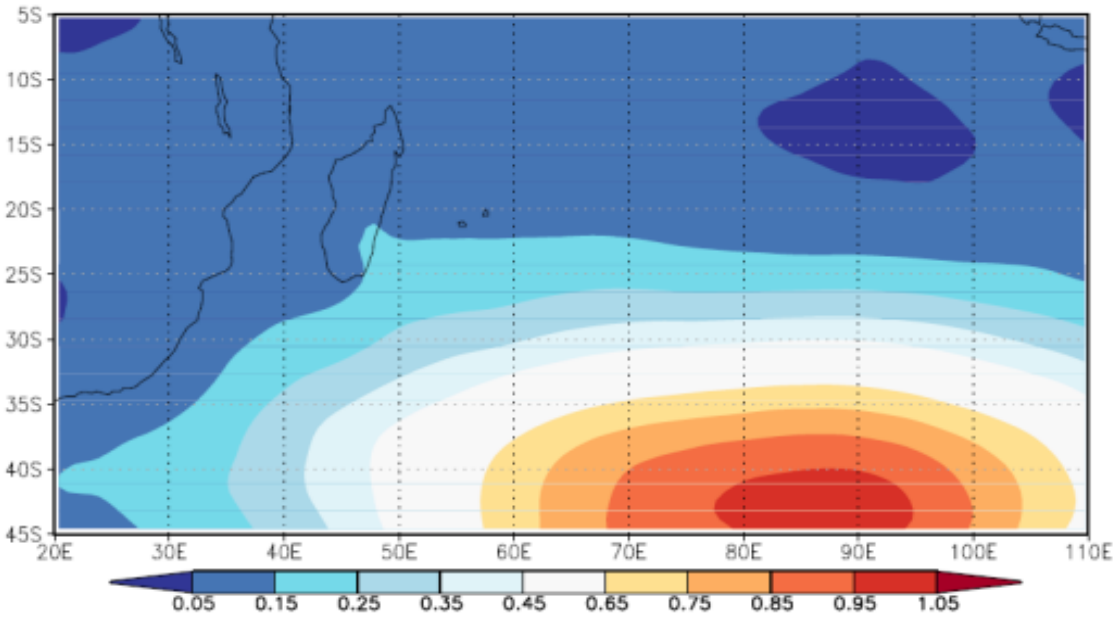

b)

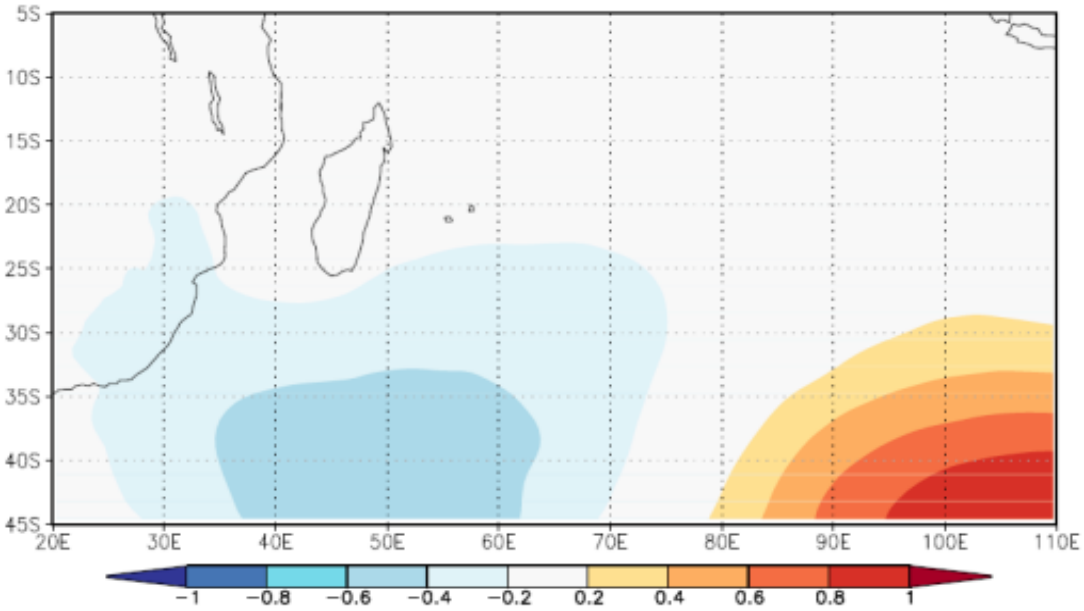

Figure 4.8: Austral winter MSLP (hPa) a) PC1 and b) PC2 over the South Indian Ocean (1985-2014).

Table 4.1: Austral summer PCA variance and cumulative percentage over the South Indian Ocean.

PCA no.	Explained variance (%)	Cumulative (%)
PC1	43.96%	43.96%
PC2	23.58%	67.54%

Table 4.2: Austral winter PCA variance and cumulative percentage over the South Indian Ocean.

PCA no.	Explained variance (%)	Cumulative (%)
PC1	59.25%	59.25%
PC2	13.97%	73.22%

4.3 Temporal variability of the Mascarene High pressure cell.

4.3.1 Annual cycle

The earth's climate annual cycles are a result of insolation and other surface fluxes due to global summer and winter variations (Jury and Mpeta, 2005). The annual cycle of the Mascarene High MSLP shows strong seasonality with peak values found during austral winter and minimum during austral summer (Figure 4.9). This monthly variability is also influenced by the difference in seasonal location of the Mascarene High (Figure 4.9), discussed in section 4.2.1. It maximizes to about 1027 hPa during mid-August. Lower intensity of the Mascarene High is in late summer, having minimum of 1017 hPa (Figure 4.4). During austral winter, location of the Mascarene High is poleward and intensification tends to be dominant.

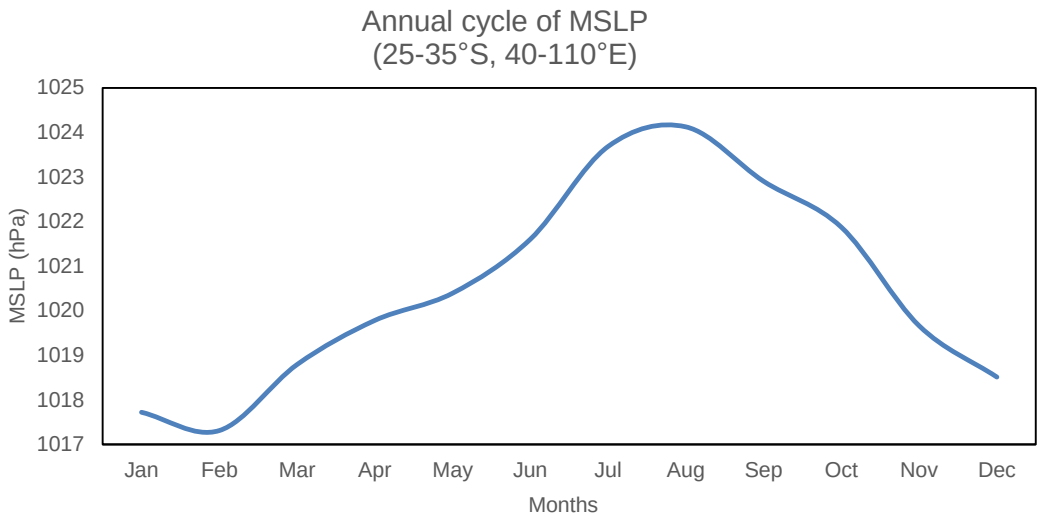

Figure 4.9: Annual cycle of MSLP (hPa) in the Mascerene High over the South Indian Ocean.

4.3.2 Interannual variability and trends

Interannual variability of MSLP in the Mascerene High (Figure 4.10), indicates a repetitive interannual trend (1985-2014). Year to year variability of the Mascarene High is dominated by the seasonal cycle with an insignificant trend (Figure 4.10). The long term mean anomaly also shows significant variability about the mean (Figure 4.11).

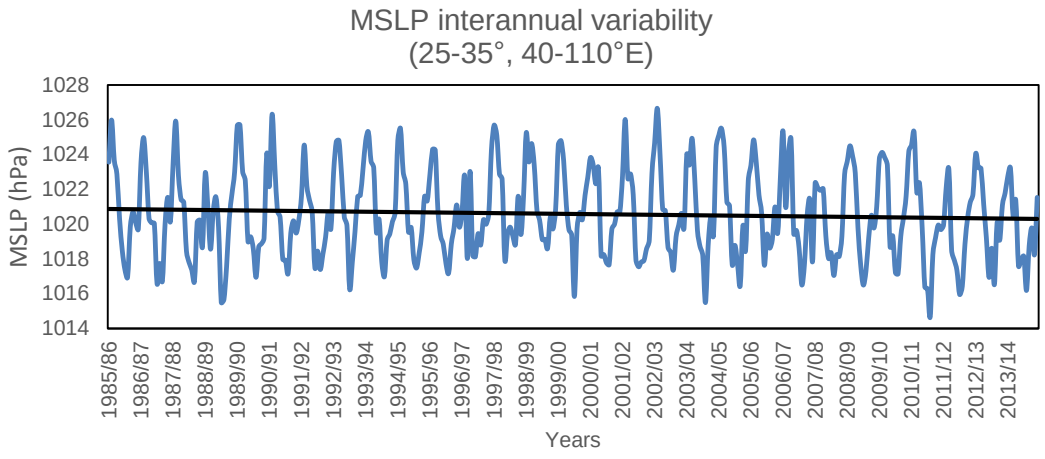

Figure 4.10: Interannual variability of MSLP (hPa) over the Mascerene High (1985-2014).

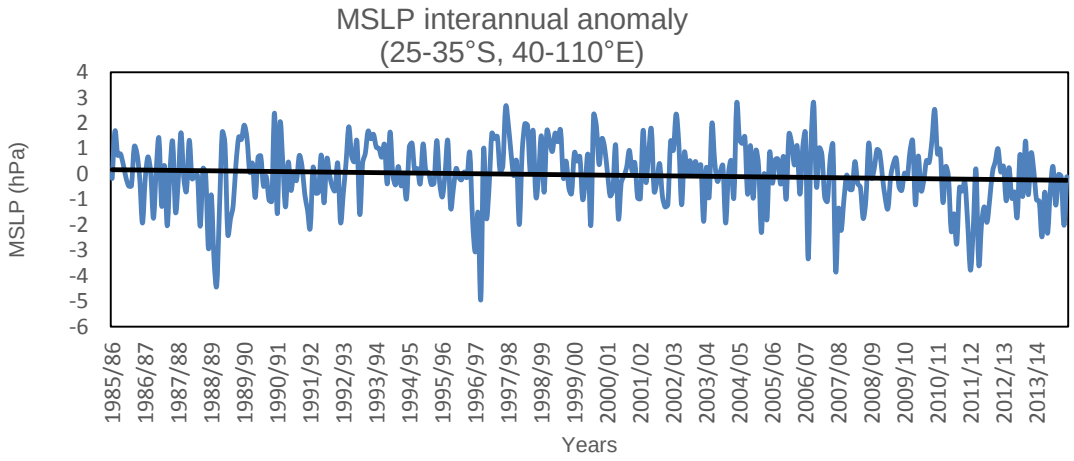

Figure 4.11: Interannual variability of MSLP (hPa) anomaly over the Mascerene High (1985-2014).

4.4 Mean circulation

South Indian Ocean seasonal mean circulation is predominantly anticyclonic, influenced by the Mascarene High (Figure 4.12). With strong alongshore equatorward winds observed in the eastern flank of the Mascarene High (Figure 4.12). It is also evident that the centre of the Mascarene High is characterised by light and variable winds (Figure 4.12). Seasonal mean for Omega at 0.995 sigma values also indicates that the centre of the Mascarene High is dominated by subsidence motion (Figure 4.13a and b) over the South Indian Ocean. During austral summer (winter), wind vector circulation locates equatorward (poleward), with seasonal circulations greatest during austral winter than austral summer. The mean circulation of the Mascarene High contributes largely to weather and climate over southern Africa, relative to mean wind circulation over the South Indian Ocean.

Seasonal surface mean vorticity balance present over southern Africa and the South Indian Ocean (Figure 4.14) result from cyclonic planetary vorticity advection due to winds alongshore (Tyson and Preston-Whyte, 2000). Anticyclonic and cyclonic vorticity centres located above poleward and equatorward regions induce anticyclonic vorticity tendencies to their immediate east by mean zonal advection and by anomalous planetary-vorticity advection, respectively. These tendencies are often balanced with the offsetting effect due to local subsidence.

a)

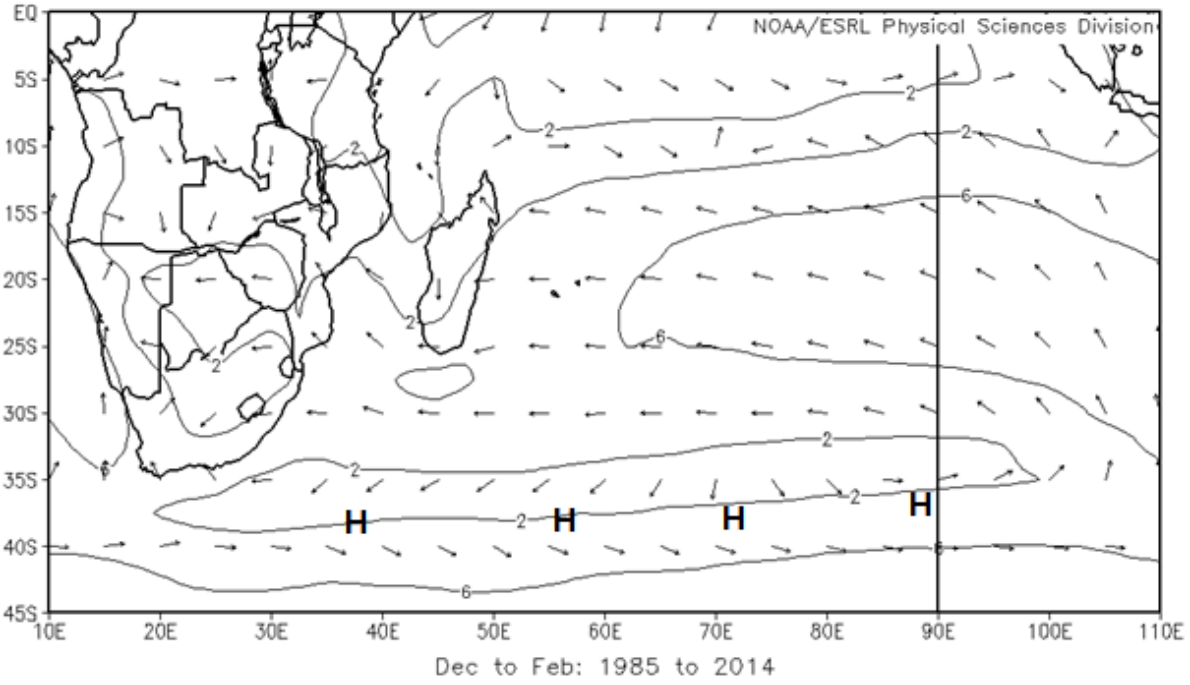

b)

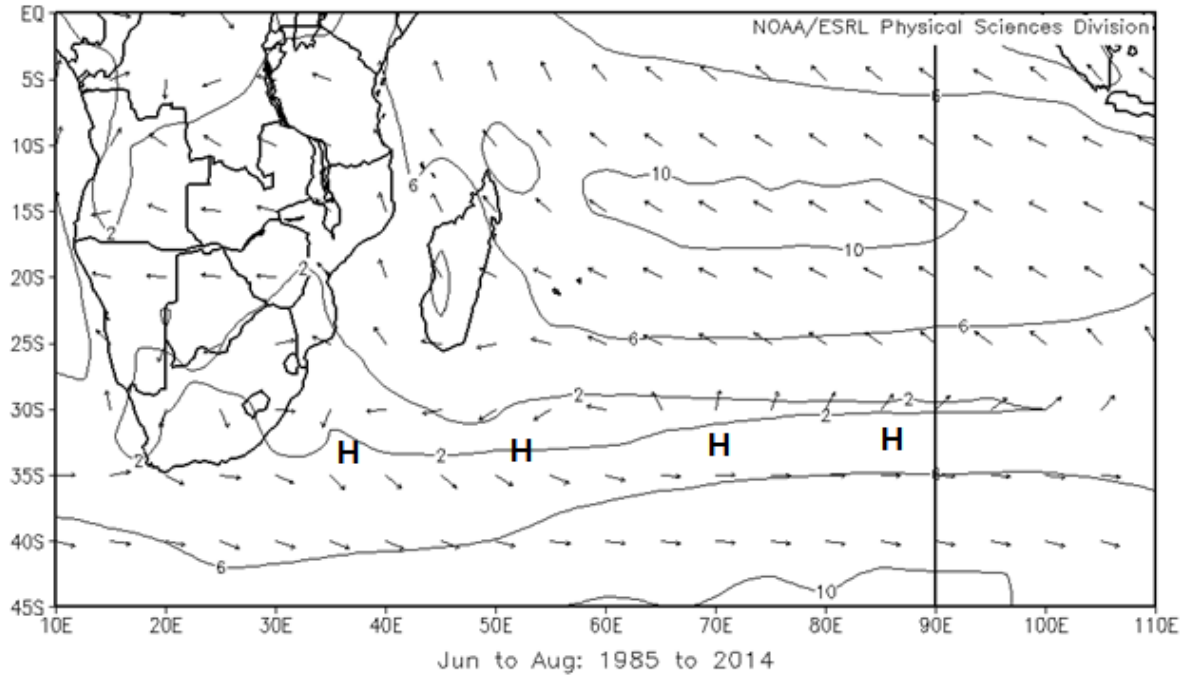

Figure 4.12: Seasonal wind vector for austral a) summer and b) winter for the period 1985-2014.

a)

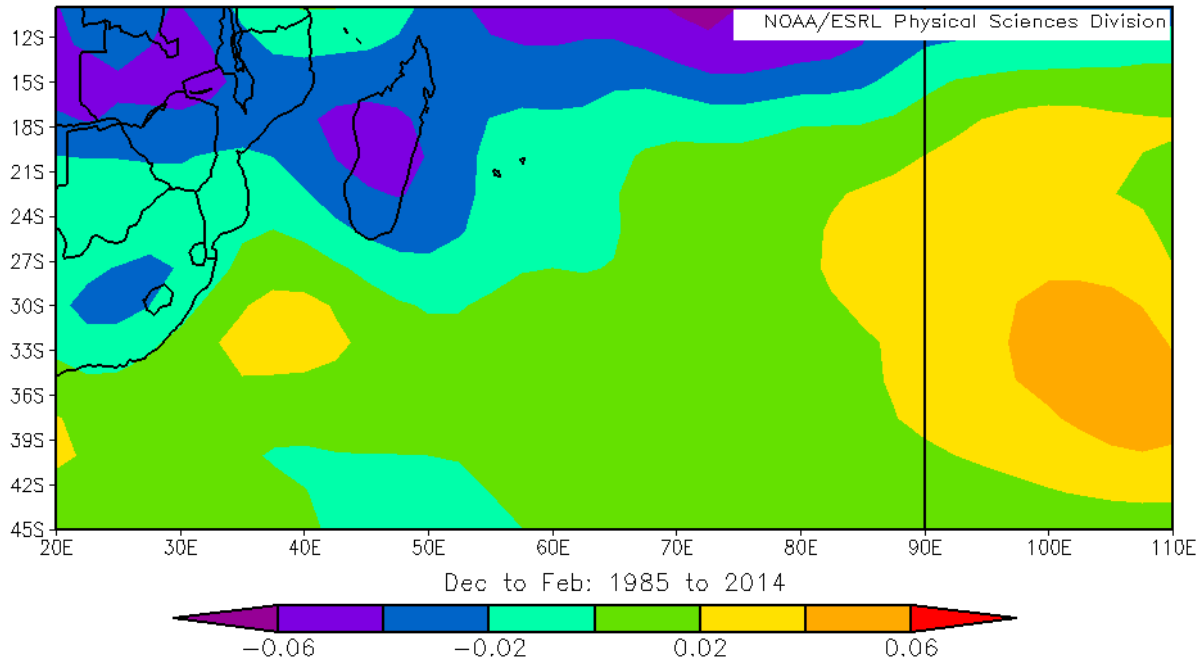

b)

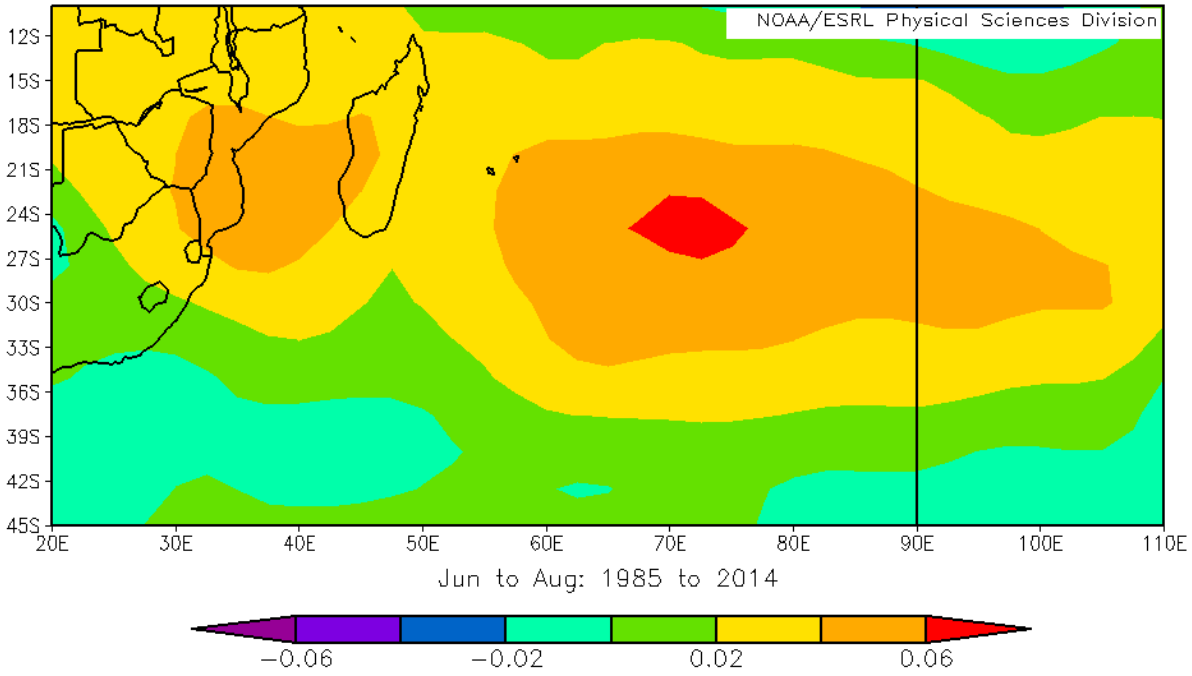

Figure 4.13: Mean omega at 500 hPa for austral a) summer and b) winter over the South Indian Ocean and southern Africa (1985-2014).

a)

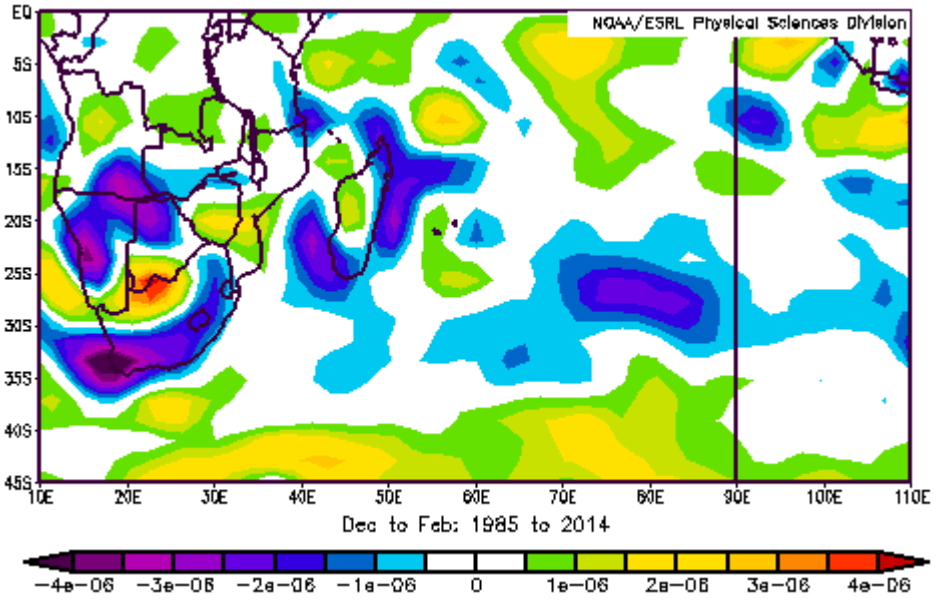

b)

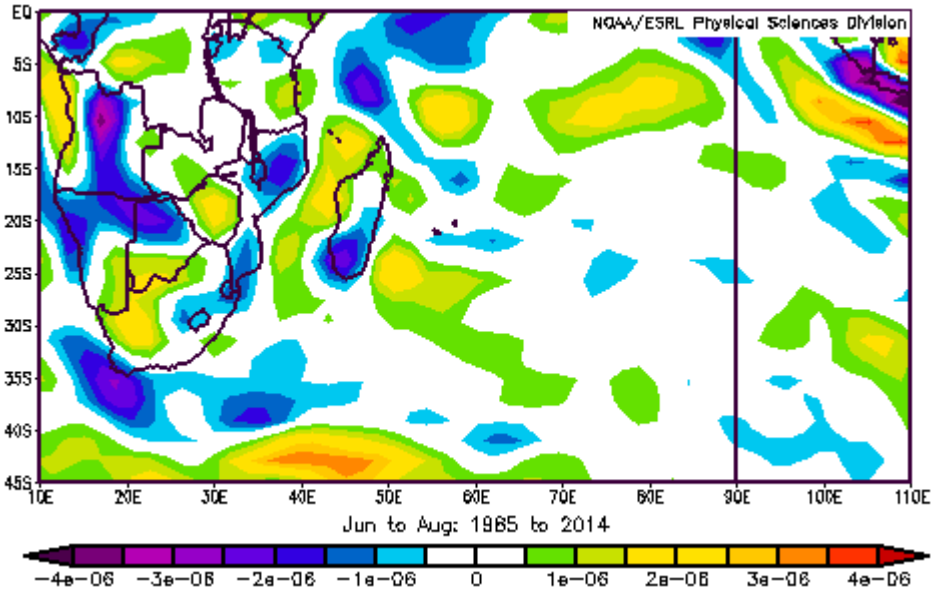

Figure 4.14: Mean vorticity for austral a) summer and b) winter over the South Indian Ocean and southern Africa (1985-2014).

4.5 Mascarene High and Angola Low interactions

During austral summer, there is presence of a shallow heat low deepening in January and February over the Bie plateau region of Angola. The Angola low regulates moisture convergence over southern Africa. It is identified by the presence of a vortex located over Angola in the low-level circulation and water-vapour flux field (Figure 4.15). It is maintained by moisture, radiative forcing, and higher temperature at the surface influencing surface evaporation and low pressure at 850 hPa (Mulenga, 1998). These findings support the importance of heating (sensible and latent heat) over Angola and cooling of the adjacent ocean for wet summer events investigated in chapter 5.

The relationship between the shallow Angola Low and the Mascarene High is significant during austral summer as a continental high becomes dominant in winter (Figure 4.15). This relationship largely influences a strong pressure gradient between the South Indian Ocean and the subcontinent. The pressure gradient determines the strength of winds bringing moisture from the warm Indian Ocean to the subcontinent.

In addition, the South Indian Ocean is dominated by a large presence of wind divergence (Figure 4.16), with the southeast coast dominated by convergence due the mountain range that slows down wind. This is influenced by surface wind moving towards the eastern part of southern Africa. The western part of the subcontinent is usually dominated by a cyclonic circulation resulting from the Angola Low (Figure 4.15). Cyclonic circulation extends to the central plateau of South Africa which in turn weakens the wind strength. With the Limpopo valley characterised by convergence which may be due to wind moving towards the southeast coast.

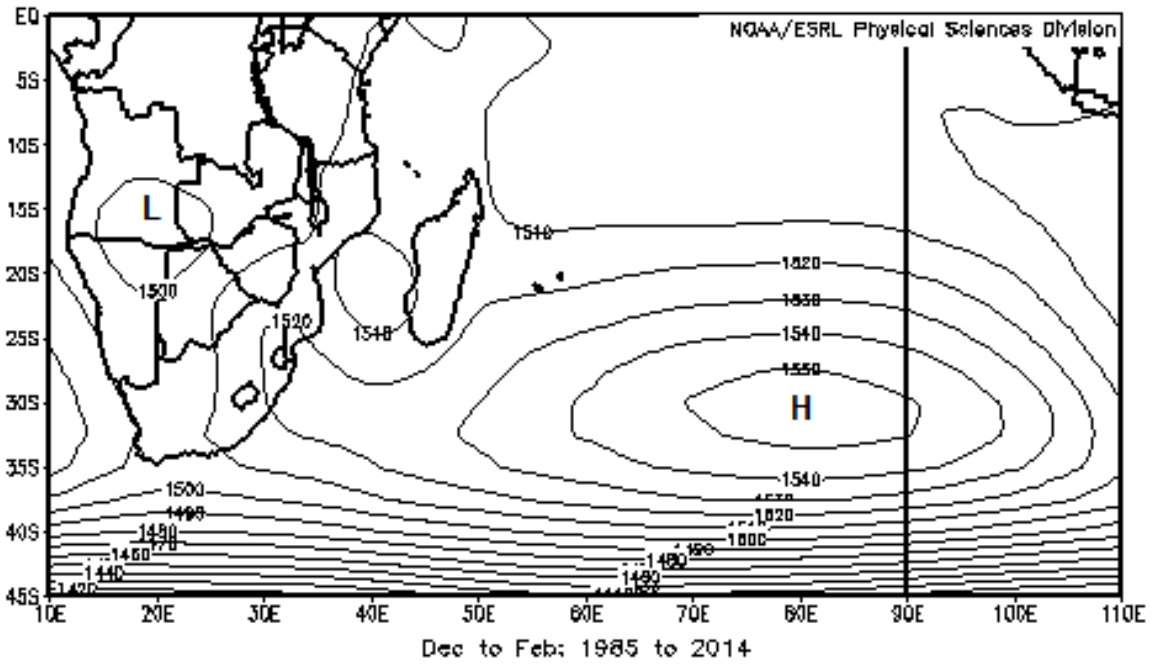

Figure 4.15: Austral summer geopotential height (850 hPa) over the South Indian Ocean and southern Africa (1985-2014). .

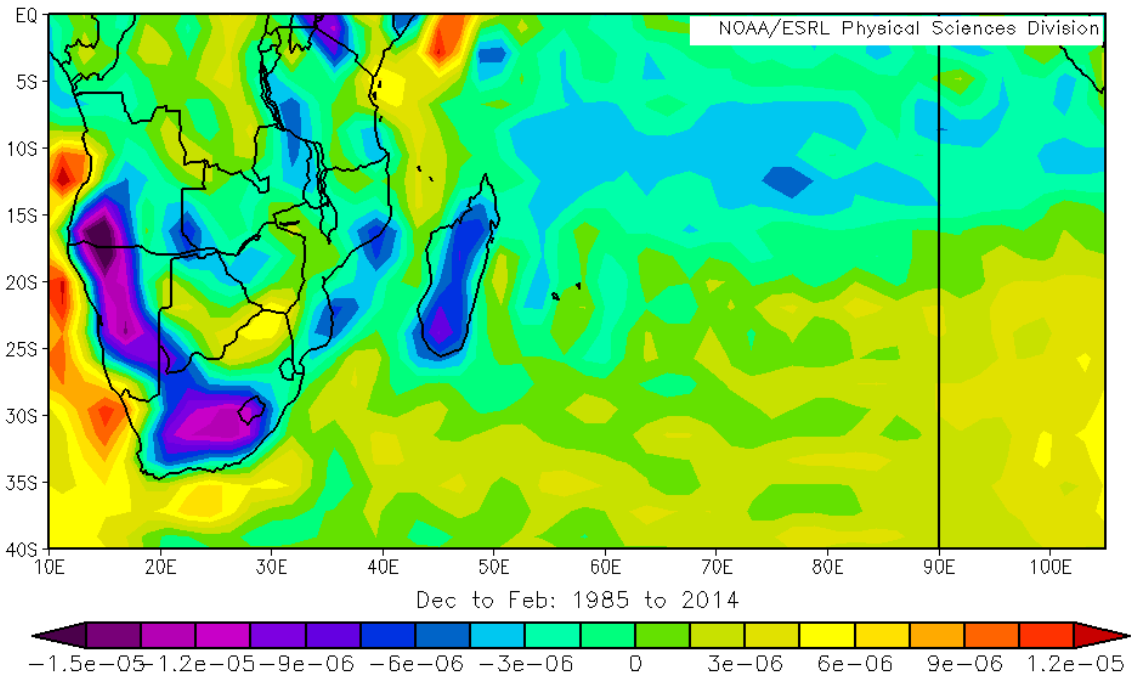

Figure 4.16: Austral summer 0.995 Sigma divergence composite mean over the South Indian Ocean and southern Africa (1985-2014).

4.6 Ocean-atmosphere interactions

The equatorial Pacific, Indian and Atlantic Oceans play a vital role in southern Africa weather and climate (Mulenga, 1998). Most importantly, ocean-atmosphere-land interactions over southern Africa and the South Indian Ocean are vital for weather and climate over this region. El Niño Southern Oscillation (ENSO) phases influence southern African weather and climate and this can be predictive using seasonal forecast techniques (Bjerknes 1969). This section investigates the relationships between the Mascarene High, Indian Ocean Dipole (IOD), Subtropical Indian Ocean Dipole (SIOD) and ENSO. Relative contributions of both the Indian Ocean and Pacific Ocean SSTs to rainfall variability over southern Africa are important. Variability of southern Africa rainfall has been found to be statistically related to the oceans (e.g. Goddard and Graham, 1999). The relationship between SSTs and rainfall results from a response to atmospheric forcing (Nicholson and Entekhabi, 1987).

Seasonal PCA's, statistically derived for SSTs over the South Indian Ocean region indicate a distinct dominant region of variability. Dominant modes show SSTs to be oriented over the central and southeast regions of the South Indian Ocean. The first mode of variability for austral summer, explains 28.54% of the total variance (Figure 4.17a). Seasonal modes for austral winter explains 26.41% of the total variance (Figure 4.17b). Findings for seasonal SSTs dominance follows that of the Mascarene High displacements identified by austral summer (PC1) and winter (PC1) mapped in Figure 4.6 and 4.7, respectively. Hence, it can be concluded that the location of the Mascarene High follows displacements of warm SSTs in the South Indian Ocean.

a)

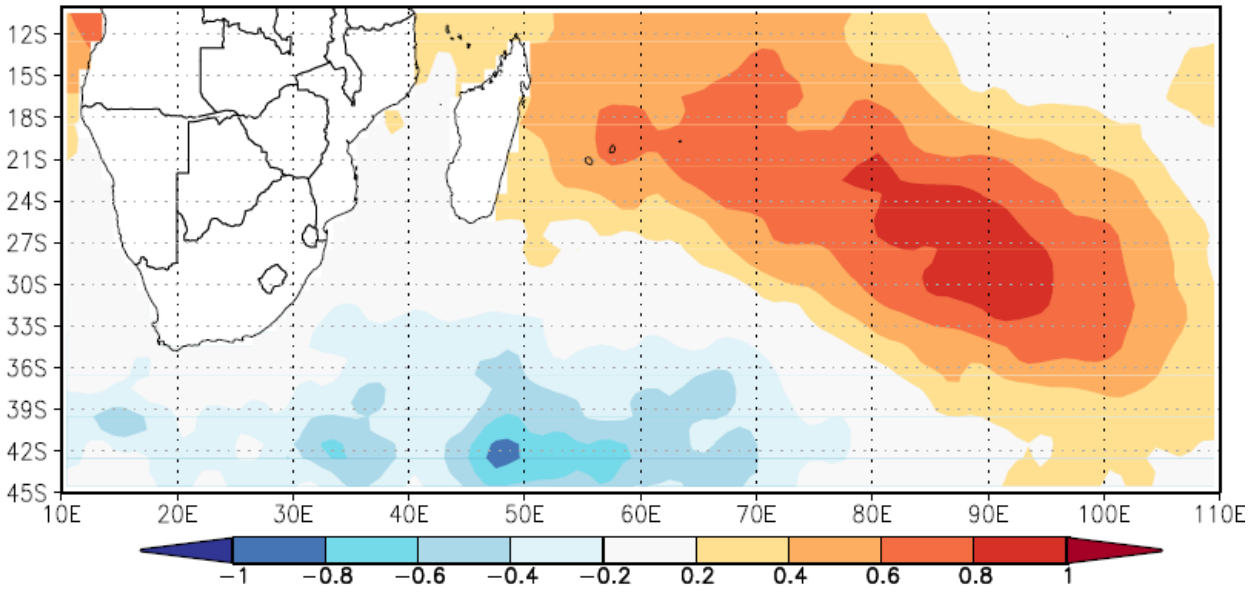

b)

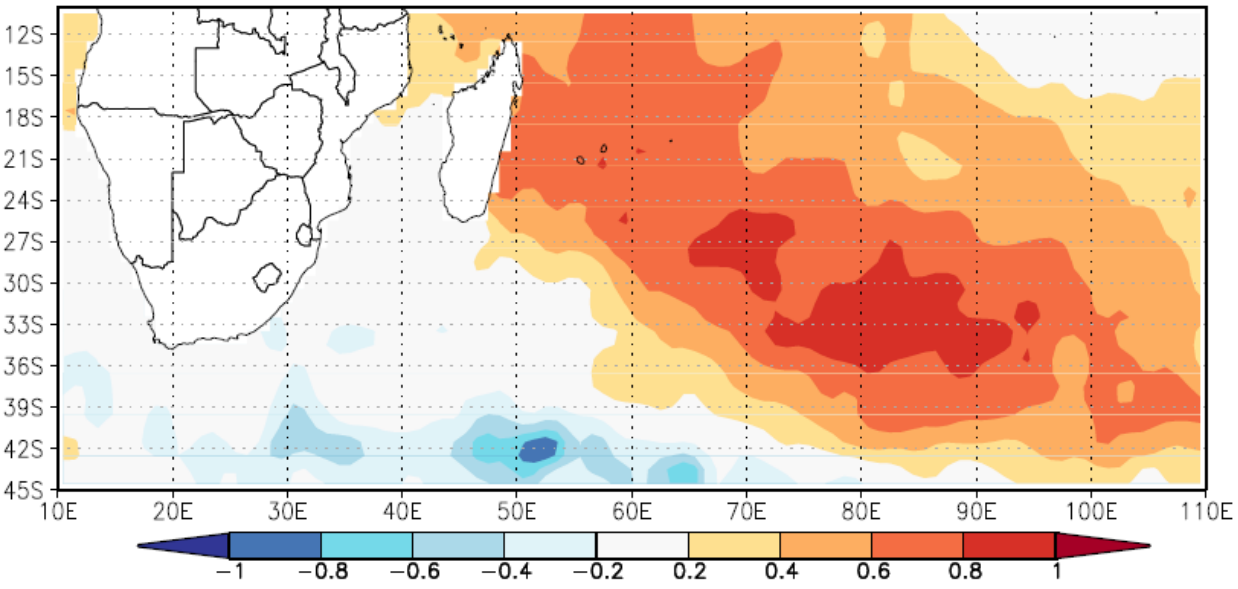

Figure 4.17: Austral summer SSTs a) PC1 and austral winter b) PC2 for the period 1985-2014 over the South Indian Ocean (1985-2014).

4.6.1 ENSO

There's a relationship between Niño 3.4 and zonal wind at the surface and mid-levels over the South Indian Ocean (Figure 4.20a and b). At the surface the relationship is dominant entirely over the equatorial Indian Ocean, SWIO and some parts of southern Africa (Figure 4.20a and b). In the mid-levels the relationship extends over Madagascar and east Africa, spreading to the entire subcontinent. These findings suggest that a warmer equatorial Pacific influences anomalous westerly winds over the equatorial Indian Ocean. Westerly winds then drive moisture and in some cases trajectories of tropical cyclones (TCs) away from the subcontinent.

ENSO seasons (Table 4.3) consists of inverse relationship with the Mascarene High (Figure 4.18) and during El Niño the Mascarene High has anomalous anticyclonic circulation at the surface and upper levels (Figure 4.21). El Niño phases, consist of a negative relationship when correlated with rainfall over southern Africa (Figure 4.19). On average, this relationship causes El Niño to be associated with dry conditions (droughts) or low amount of seasonal rainfall over the subcontinent (Figure 4.19). Drying over southern Africa results from atmospheric responses to ENSO warming over the eastern Pacific. Variability of SSTs over the tropical Pacific Ocean exerts a major influence on rainfall over southern Africa, the ocean-atmospheric response over the Indian Ocean also play a major role. During austral summer, there is a significant (90% significance) relationship between geopotential height at 850 hPa and Niño 3.4 (Figure 4.21). The relationship is dominant over vast parts of the South Indian Ocean and southern Africa. Lastly, El Niño occurrences appear to be directly linked to a rise in the amount of MSLP over the Indian Ocean.

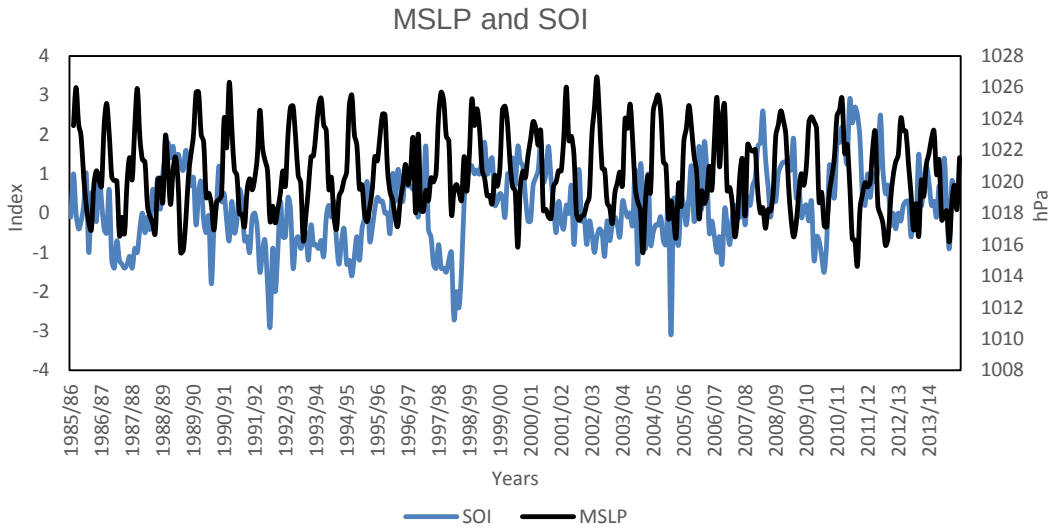

Figure 4.18: SOI and MSLP (hPa) correlation in the Mascarene High over the South Indian Ocean (1985-2014).

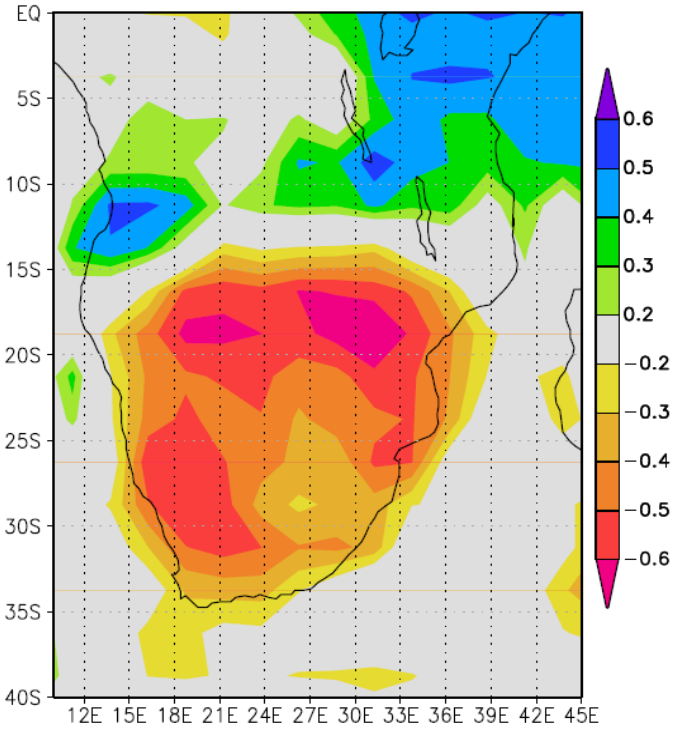

Figure 4.19: Correlation of Niño 3.4 with austral summer rainfall (mm/day) over southern Africa (90% significance).

a)

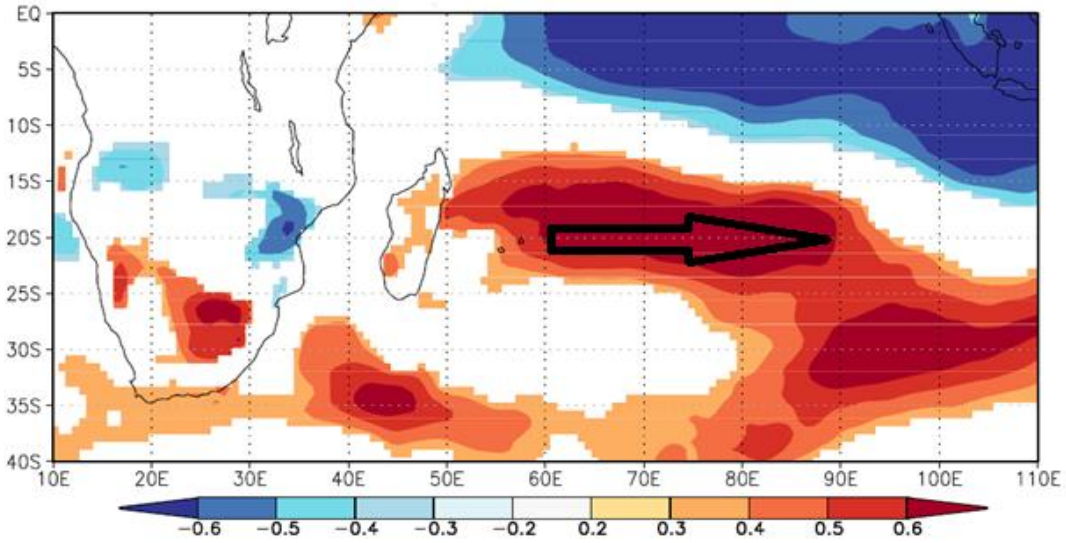

b)

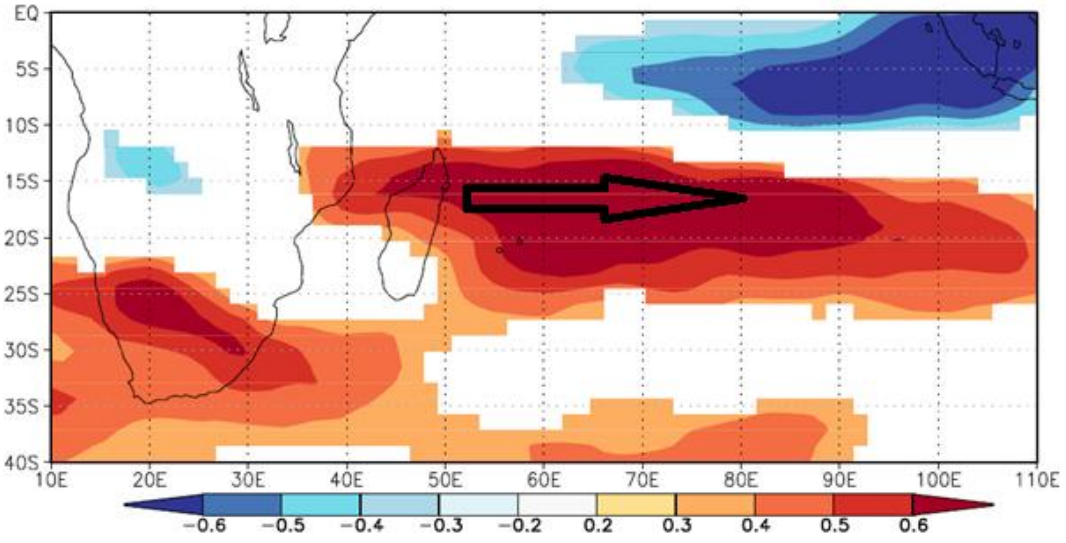

Figure 4.20: Correlation of Niño 3.4 and zonal wind at the a) surface and b) 500 hPa over the South Indian Ocean (90% significance).

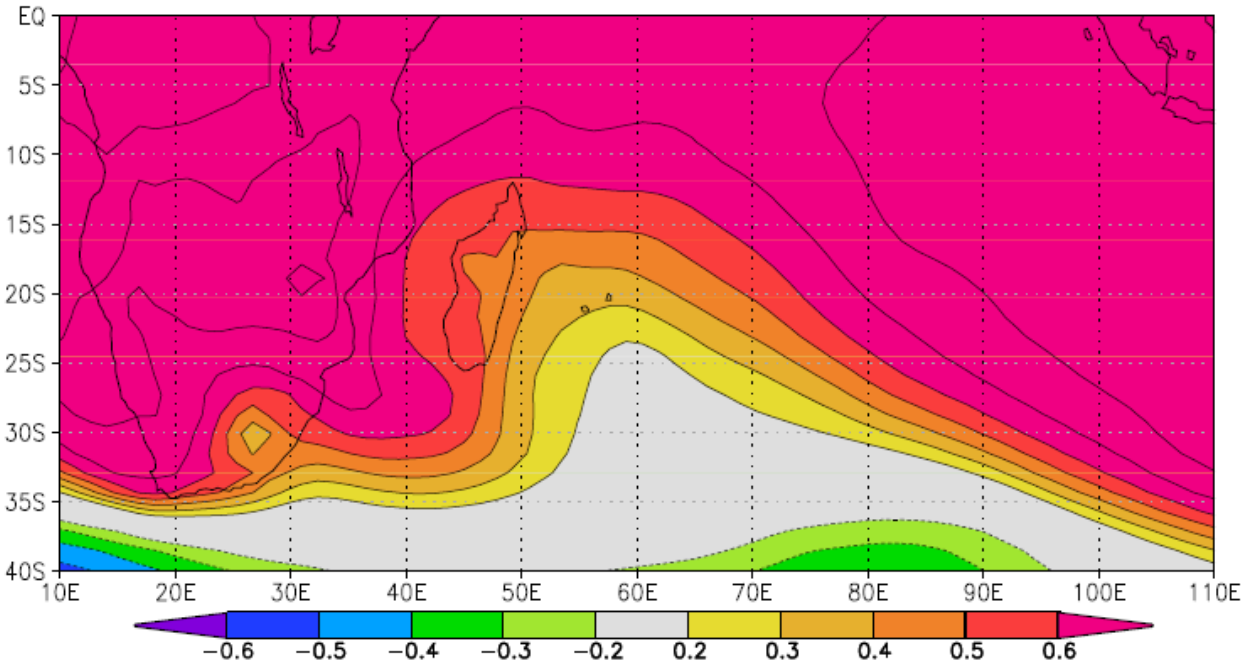

Figure 4.21: Niño.3.4 correlation with austral summer geopotential height at 850 hPa over the South Indian Ocean (1985-2014).

Table 4.3: ENSO seasons for the period 1985-2014

El Niño	La Niña
1986/87	1988/89
1987/88	1996/97
1991/92	1999/00
1994/95	2007/08
1997/98	2010/11
2004/05	
2009/10	

4.6.2 IOD

MSLP in the Mascarene High comprises of an inverse relationship with IOD variability on the northeastern part of the South Indian Ocean (Figure 4.22). However, the inverse relationship is not always present. Positive IOD phases are found to influence a weakening in the Mascarene High strength. Weakening in strength of the Mascarene High influences weaker trade winds and this results in reduced moisture flux towards the interior. This finding is in agreement with a study done by Hastenrath and Polzin (2004), which also suggested that the equatorial Indian Ocean trade winds play a vital role in the evolution of IOD.

Positive IOD events are found to be linked with a widespread below normal rainfall conditions over the southern African region (Figure 4.23). But, it is also noted that east African rainfall tends to be above normal during positive SIOD phases. This results from evaporation and convection from warm SSTs located the west of the Indian Ocean. During positive IOD, warm SSTs in the west of the Indian Ocean create a region of low pressure which regulates evaporation and convection that influences above normal rainfall over east Africa during positive IOD phases.

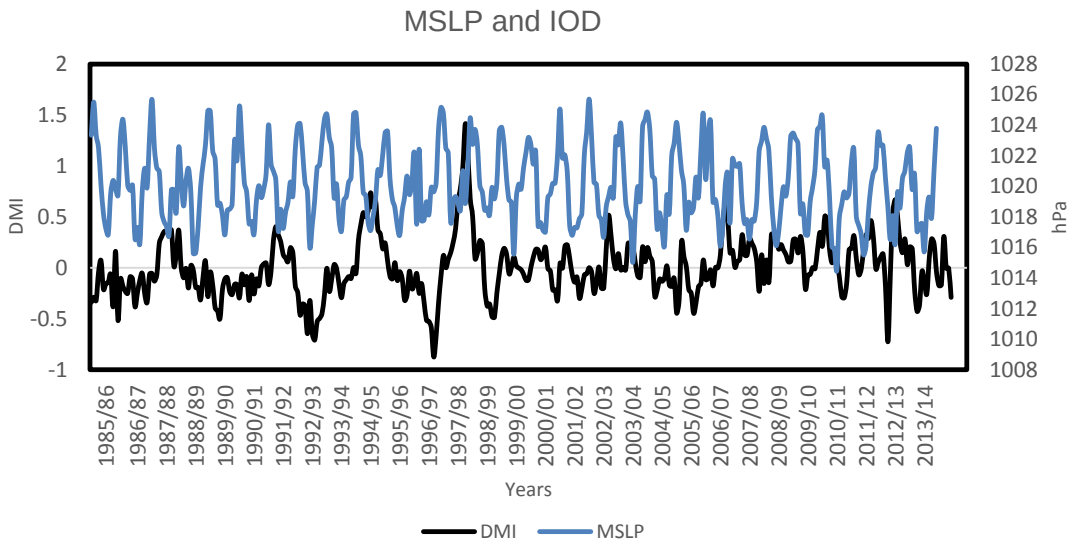

Figure 4.22: MSLP (hPa) and IOD over the South Indian Ocean (1985-2014).

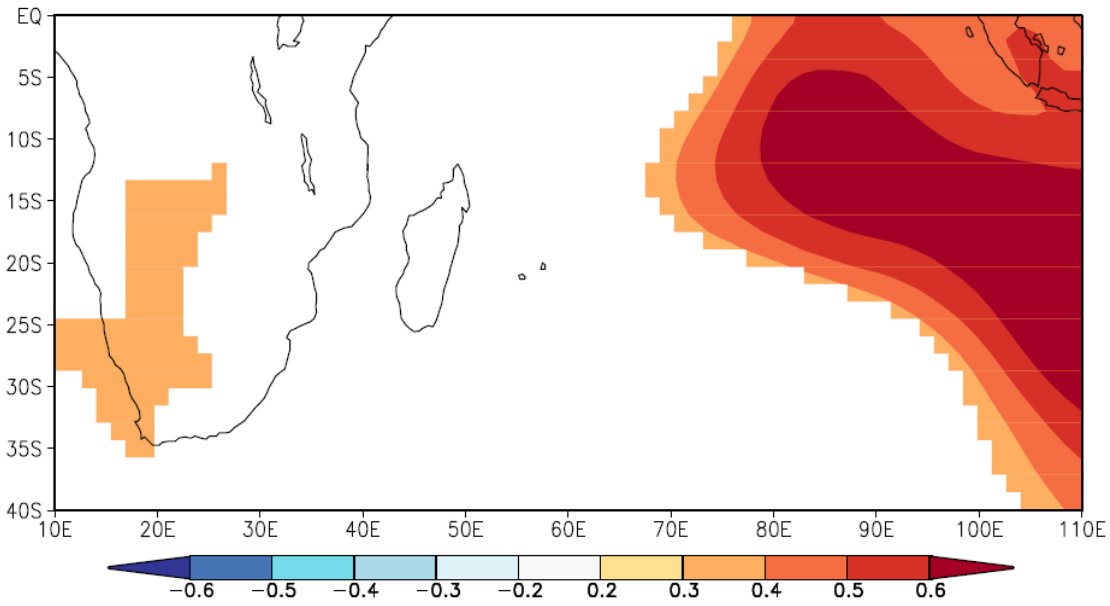

Figure 4.23: Correlation of DMI and geopotential height at 850 hPa over the South Indian Ocean (Aug-Sep).

4.6.3 SIOD

During austral summer, SIOD phases have been found to be influenced by the Mascarene high which is distributed widely over the South Indian Ocean on an interannual timescale (e.g., Venegas *et al.* 1998; Goddard and Graham, 1999 and Behera and Yamagata, 2001). The relationship between MSLP and SOID is directly proportional (Figure 4.24 and Figure 4.26). Location of the Mascarene High is also found to be influenced by the warming of the South Indian Ocean SSTs. Positive (negative) phases of the SIOD appear to have a relationship with high (low) values of South Indian Ocean MSLP. The relationship between MSLP and SIOD is largely present during austral summer. This is when the Mascarene High is found to be less intense (1020 hPa). SIOD occurrences are also found to be seasonally phase-locked to the austral summer in agreement with findings by Behera and Yamagata (2001). The relationship tends to be dominant in the southern part of the South Indian Ocean during austral summer (Figure 4.25a).

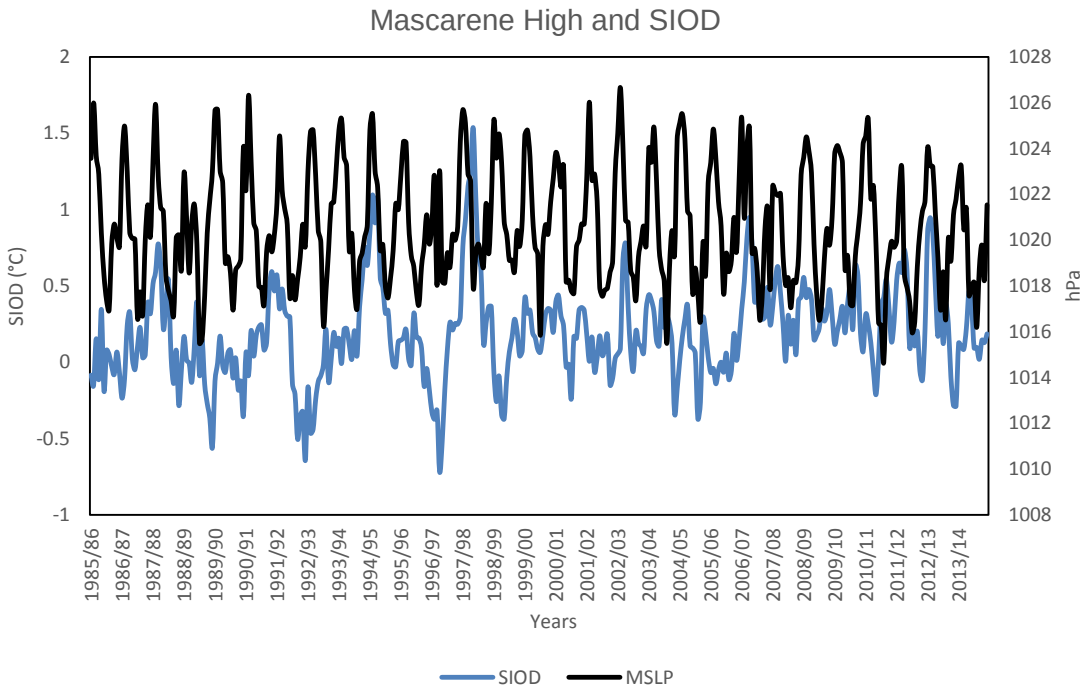

Figure 4.24: SIOD and South Indian Ocean MSLP (hPa) for the period 1985-2014.

a)

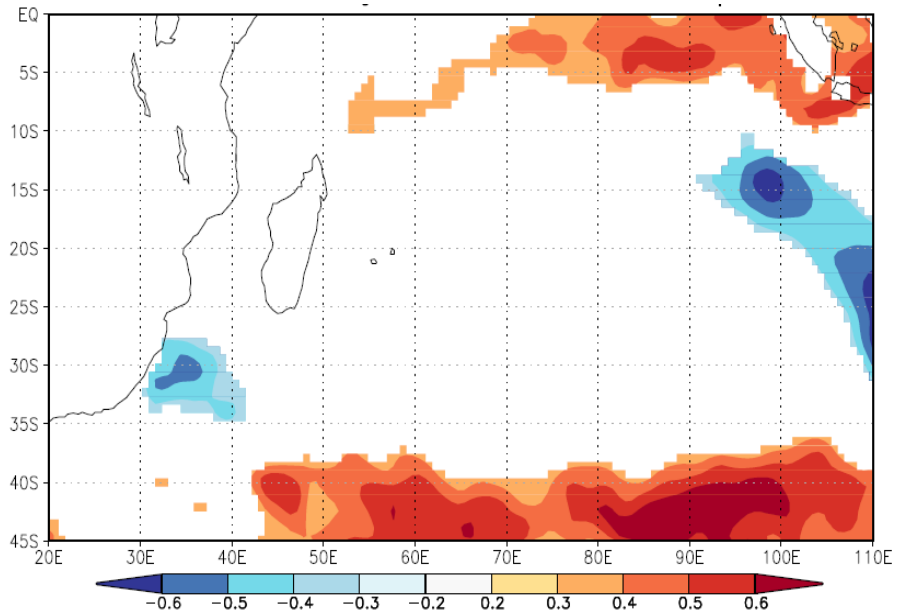

b)

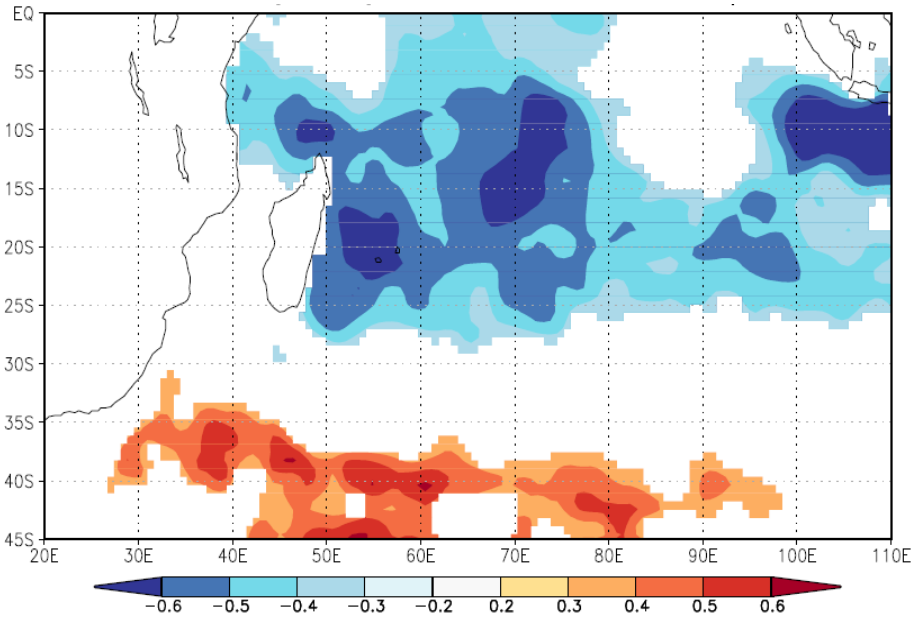

Figure 4.25: Austral a) summer and b) winter correlation of MSLP (hPa) and SSTs over the South Indian Ocean (90% significance).

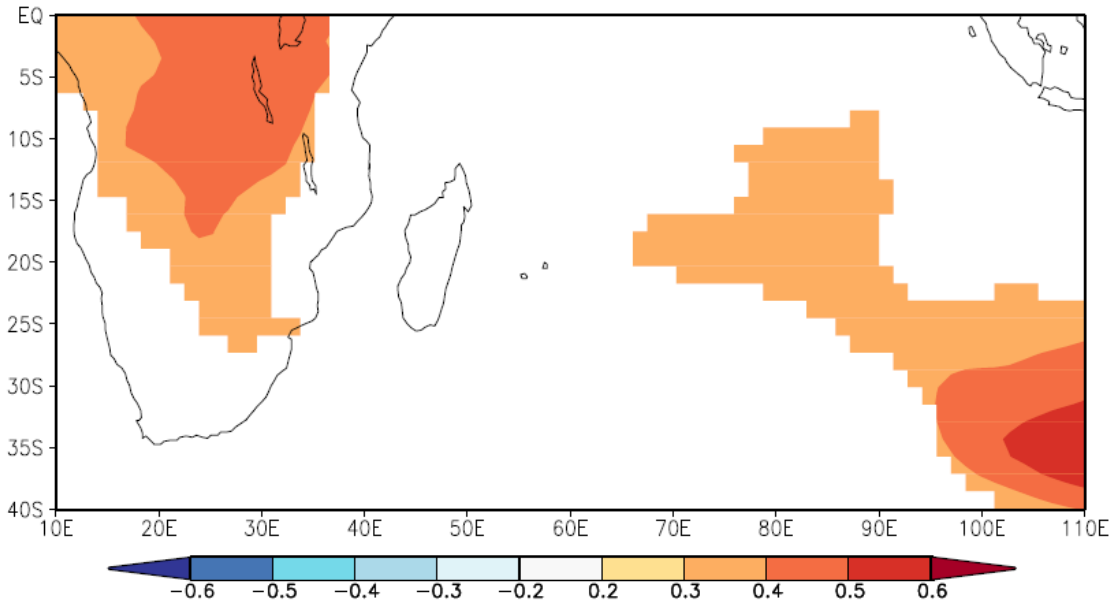

Figure 4.26: Austral summer correlation of SIOD and geopotential height at 850 hPa over the South Indian Ocean (90% significance).

4.7 Summary

In this chapter, mapping mean distribution and seasonal shifts of the Mascarene High have been presented. Ocean-atmospheric circulations related to the Mascarene High have also been investigated. Spatial distribution and temporal variability of the Mascarene High have been studied at seasonal, intraseasonal and interannual time scales. Therefore, is it important to note that fundamental findings of this chapter are:-

a) Mascarene High consists of north-south and west-east migrations.
b) Monthly location of the Mascarene High varies spatially and temporally.
c) Spatio-temporal characteristics of MSLP follow seasonal latitudinal and longitudinal variation in location.
d) The Mascarene High is intense (1023 hPa) during austral winter
e) The ITCZ and SICZ influence location of the Mascarene High.
f) South Indian Ocean warm SSTs influence the location of the Mascarene High.
g) ENSO phases have a major influence on the strengthening (weakening) of Indian Ocean trade winds.
h) IOD is found to be inversely proportional to the Mascarene High. With the SIOD directly proportional to the Mascarene High.

i) The SIOD and Mascarene High consists of a directly proportional relationship.

j) SIOD occurrences are also found to be seasonally phase-locked to the austral summer

The next chapter focuses on Mascarene high blocking and anomalous induced weather events over southern Africa.

CHAPTER 5: MASCARENE HIGH BLOCKING AND ANOMALOUS WEATHER EVENTS OVER SOUTHERN AFRICA

5.1 Introduction

In this chapter, day-to-day synoptic scale circulation of the Mascarene High blocking is examined. This is when the eastern lobe of the Mascarene High is tracked east or stagnant over the same location for more than one day and is identified by slow movement of the Mascarene High in the South Indian Ocean. The main objective of this chapter is to identify and investigate Mascarene High blocking events. Studying key ocean-atmosphere feedbacks involved during blocking can be useful for enhancing developments for future predictions. This chapter identifies cut-off lows, tropical cyclones (TCs) and tropical temperate troughs which may be blocked by the Mascarene High.

Several studies have shown that the effect of Mascarene High blocking causes anomalous day-to-day weather conditions over southern Africa (e.g. Trenberth, 1985; Sinclair, 1996 and Favre *et al.* 2012). Frequency and distribution of blocking over the South Indian Ocean is identified by mapping persistent geopotential height anomalies at 500 hPa. This is done by employing event scale analysis and composite anomaly representations of the Mascarene High for several events based on a blocking index.

5.2 Mascarene High blocking identification

The study identifies mean sea level pressure (MSLP) for Mascarene High features and also geopotential height at 850 and 500 hPa to identify blocking. The blocking index defined by Tibaldi and Molteni (1990), modified from Lejenas and Okland (1983) is employed. This is for real-time atmospheric monitoring, isolating regions of easterly flow at 500 hPa associated with high-latitude blocks. Using this method, 17 clear events of blocking over the South Indian Ocean due to the Mascarene High are identified. However, six events are selected for further analysis and discussion.

5.3 Blocking and landfalling TCs

This section investigates two TC events over the Southwest Indian Ocean (SWIO) making landfall over southeast Africa, steered by anomalously strong trade winds generated by Mascarene High blocking. TCs that are investigated were long-lived as they propagated towards the mainland

dumping heavy rainfall. TC motion is largely due to the large scale environmental flow. It is steered by advection of planetary vorticity by the geostrophic wind (Chikoore *et al.* 2015)

Event 1: TC Leon-Eline (1-29 February 2000)

TC Eline formed over the eastern Indian Ocean and was named Leon and was renamed Eline when it crossed into the SWIO. The Mascarene High is observed by daily mean geopotential height at 500 hPa to be anomalously slow (Figure 5.1). This occurrence largely influenced passage for TC Leon-Eline trajectory, steered by the anomalous strong easterly trade winds (Figure 5.3 and 5.5) generated by Mascarene High blocking (Figure 5.2). Mascarene High blocking lasted for numerous days, playing a pivotal role for steering TC Leon-Eline by generating a strong easterly wave flow directed towards southeast Africa. Despite the Pacific La Niña, cumulative rainfall over southern Africa was meagre in early summer of the 1999-2000 season, with TC Hudah later making landfall during the same season. TC Leon-Eline was one major system contributing to vast amounts of rainfall over the subcontinent. TC Leon-Eline is one of the most long-lived TC ever recorded (Reason and Keibel, 2004). Formation took place in early February 2000 and dissipated on 29 February when it made landfall over southern Africa. After formation over the South Indian Ocean, for a number of days it tracked towards southeast Africa (Figure 5.3), dumping heavy rainfall over this region (Figure 5.4). It is clear that Mascarene blocking largely contributed to steering of TC Leon-Eline towards the subcontinent. The absence of Mascarene High blocking would have resulted on TC Leon-Eline steered away from southeast Africa to the South Indian Ocean, then dissipating.

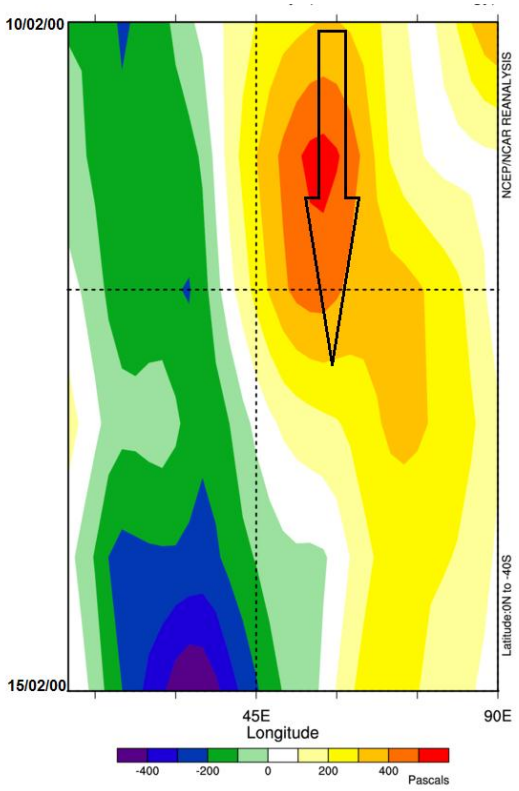

Figure 5.1: Daily composite anomaly Hovmoller for geopotential height (m) at 500 hPa over the SWIO (10-15 February 2000).

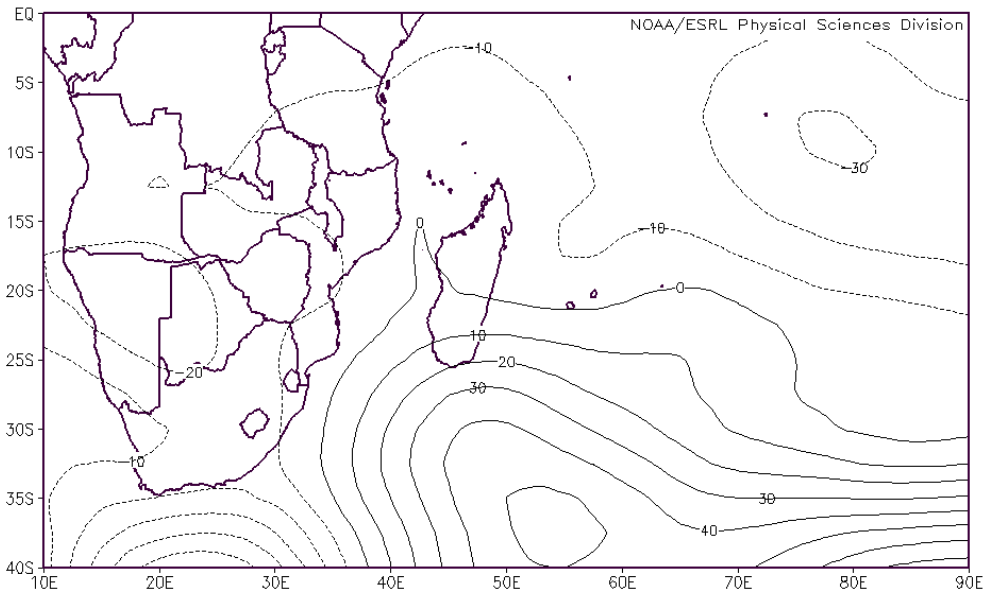

Figure 5.2: Daily composite anomaly geopotential height (m) at 500 hPa over southern Africa and SWIO (10-15 February 2000).

Figure 5.3: TC Leon-Eline track over SWIO (Source NOAA Historical Hurricane Tracks).

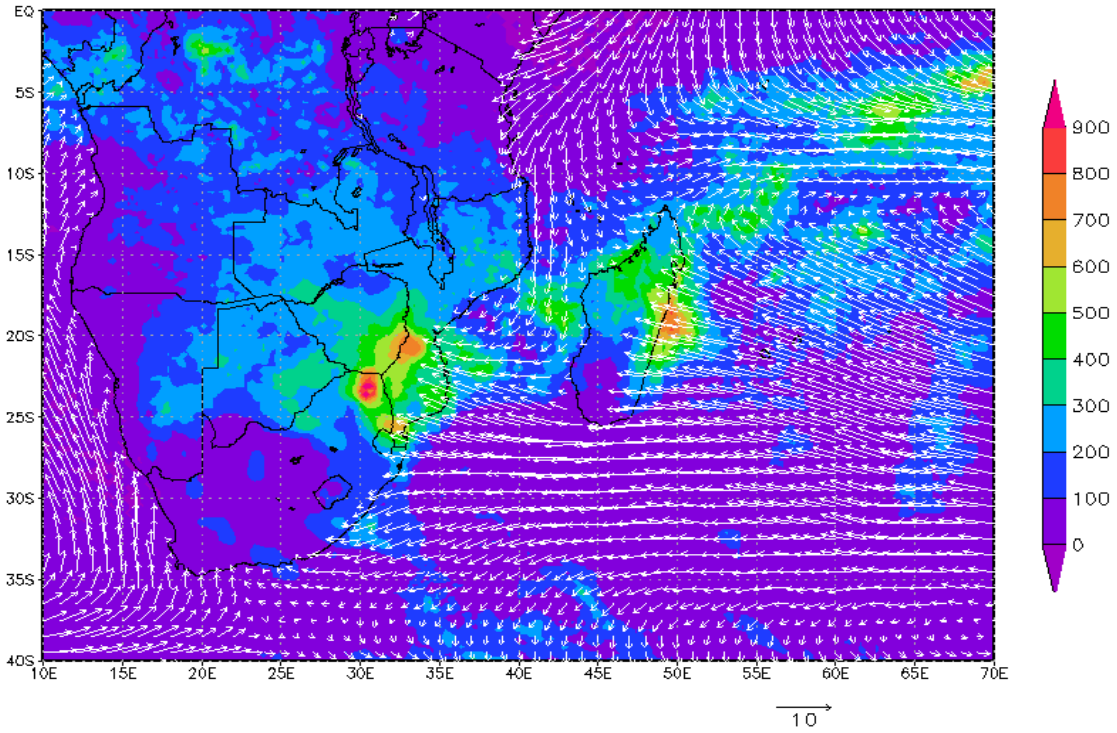

Figure 5.4: Surface wind (m/s) and rainfall (mm/month) at the surface for TC Leon-Eline track over SWIO (Source: NOAA Historical Hurricane Tracks).

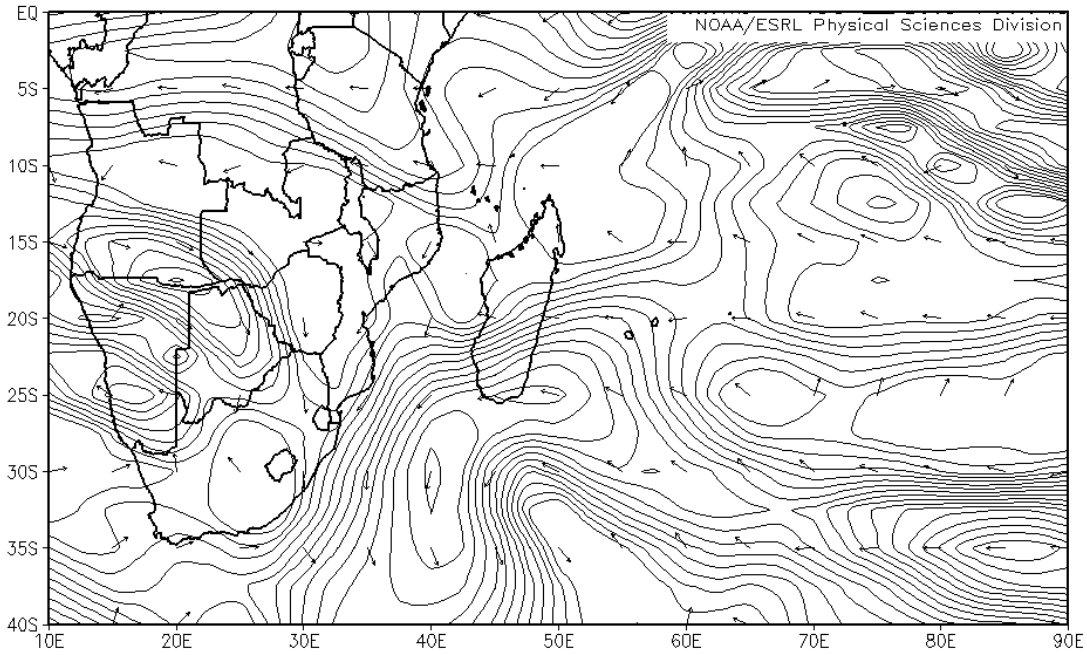

Figure 5.5: Wind anomaly (m/s) at 500 hPa over southern Africa and SWIO (10-15 February 2000).

Event 2: TC Jaya (26 March – 8 April 2007)

During the 2006-07 austral summer season, on the 26th of March, Mascarene High blocking extended well from southeast Africa to the South Indian Ocean (Figure 5.6). During this time, a tropical depression formed over the SWIO. It later developed into a TC that was steered by the extended easterly wave flow resulting from the Mascarene High blocking (Figure 5.8 and Figure 5.10). TC Jaya formed in the later austral summer on the 26th of March and lasted for a number of days, extending well to the 8th of April 2007. It then tracked towards low-lying areas over southeast Africa, dumping heavy rainfall over northeast Madagascar (Figure 5.9). However, it had no major penetration inwards southeast Africa as it retrogressed backwards until it dissipated. Even though TC Jaya had no further penetration over southeast Africa, it had been steered westward for an extended period by an anomalous slow moving Mascarene High. The Mascarene High circulation had propagated east after initial blocking. TC Jaya was significantly influenced by Mascarene High blocking (Figure 5.7) and when the Mascarene High had tracked east it had no further penetration over southeast Africa.

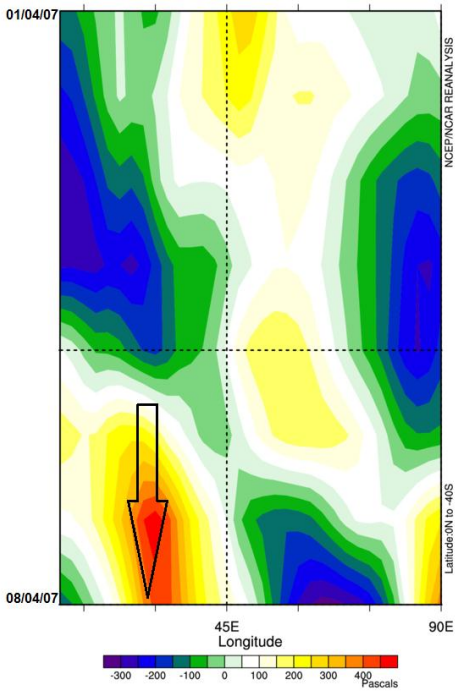

Figure 5.6: Daily composite anomaly Hovmoller for geopotential height (m) at 500 hPa over the SWIO (26 March-8 April 2007).

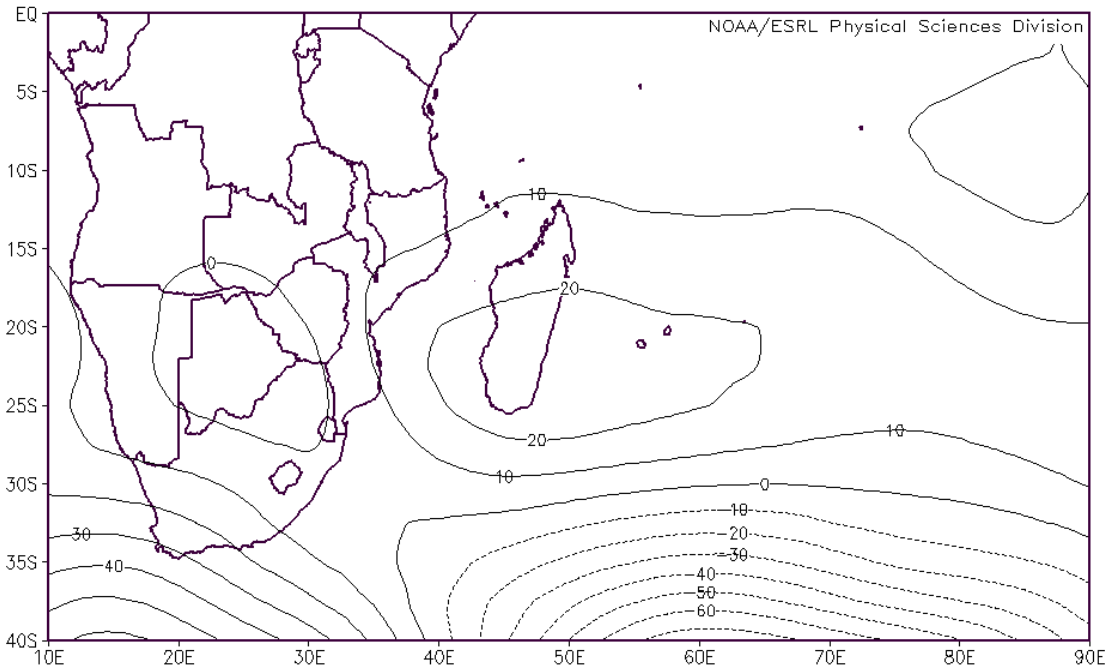

Figure 5.7: Daily composite for geopotential anomaly (m) at 500 hPa over southern Africa and SWIO (26 March-8 April 2007).

Figure 5.8: TC Jaya track over SWIO (Source NOAA Historical Hurricane Tracks).

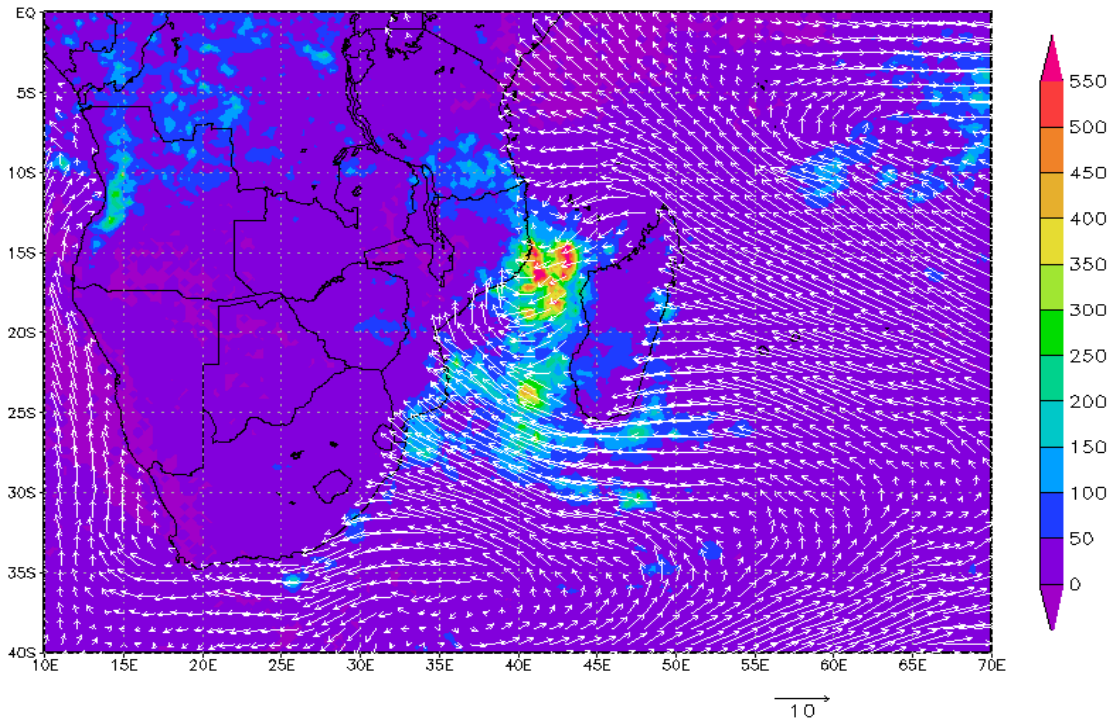

Figure 5.9: Surface wind (m/s) and rainfall (mm/month) at the surface for TC Jaya track over SWIO (26 March-8 April 2007).

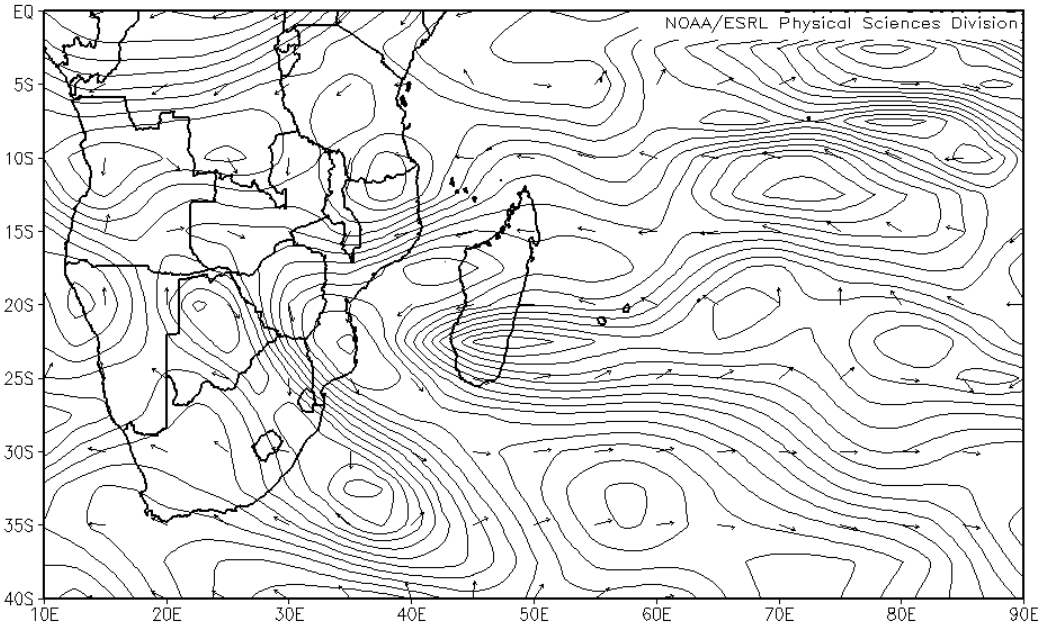

Figure 5.10: Wind anomaly (m/s) at 500 hPa over southern Africa and SWIO (26 March-8 April 2007).

5.4 Blocking and cut-off lows

Cut-off lows are identified on upper air analysis as closed contours in the geopotential heights (Singleton and Reason, 2007). An occurrence of a single cut-off low event can produce a large percentage of seasonal rainfall over a region, having amounts often in excess of the monthly mean in a single day. Enhancing knowledge on Mascarene High blocking and cut-off lows is vital for southern African climate research.

In this section, two cut-off low events associated with a blocking Mascarene High are investigated. Extreme rainfall conditions induced by the presence of these cut-off low weather systems over southern Africa are also detailed. Events in this section are identified to have spanned for a period of three days or more. The first event spanned from 31 October to 2 November 1985. The second event is from 27 to 29 September 1987.

Event 1: 31 October-2 November 1985

A quasi-stationary Mascarene High in the middle-levels (Figure 5.11 and 5.12) was present over southern Africa, for a period of three days (31 October to 2 November, 1985). Slowly propagating and persistent over the South Indian Ocean, causing blocking of west-east movement of transient weather systems along the westerly wave over southern Africa. A protracted cut-off low weather

system dumped 20 mm/day of rainfall over the southeast Africa (Figure 5.14) with vast of moisture saturation covering regions north-east of South Africa (Figure 5.14).

Parts of southeast Africa experienced relatively high amount of moisture uplift, this indicates rapid uplift of air mainly over South Africa (Figure 5.13). Surface rainfall rate shows that rainfall is comparatively high over the southern tip of southern Africa. This is precisely due to high moisture uplift, induced by presence of the low pressure aloft and low temperatures at the surface. The region experiences high rates of convection (Figure 5.15) and OLR at 200 hPa (Figure 5.15) over the north-east regions also indicates that the rate of convection is high.

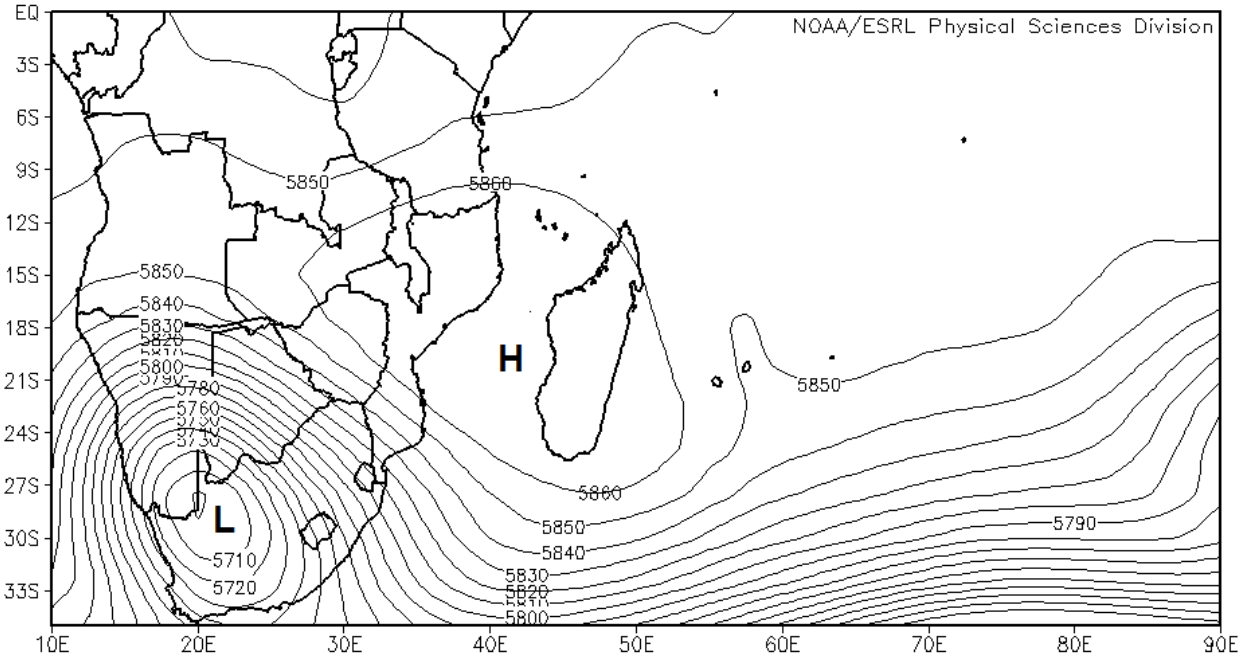

Figure 5.11: Daily mean geopotential height (m) at 500 hPa over southern Africa and SWIO (31 October-2 November 1985).

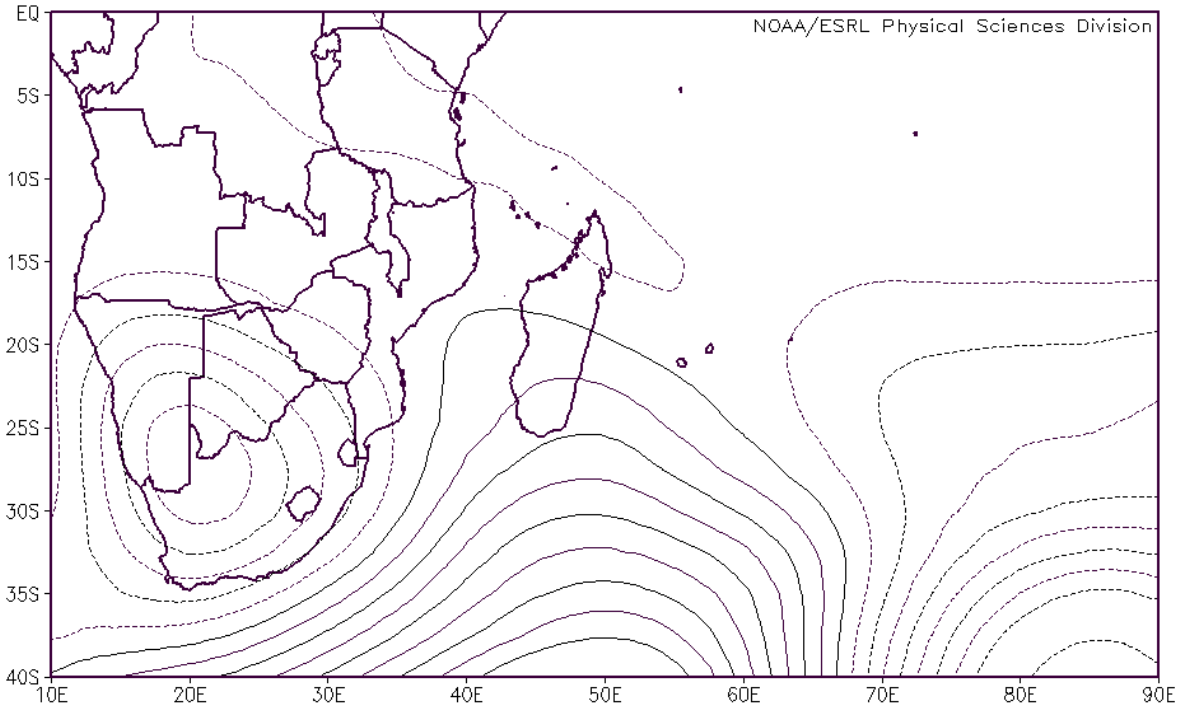

Figure 5.12: Daily composite mean geopotential height (m) anomaly at 500 hPa over southern Africa and SWIO (31 October-7 November 1985).

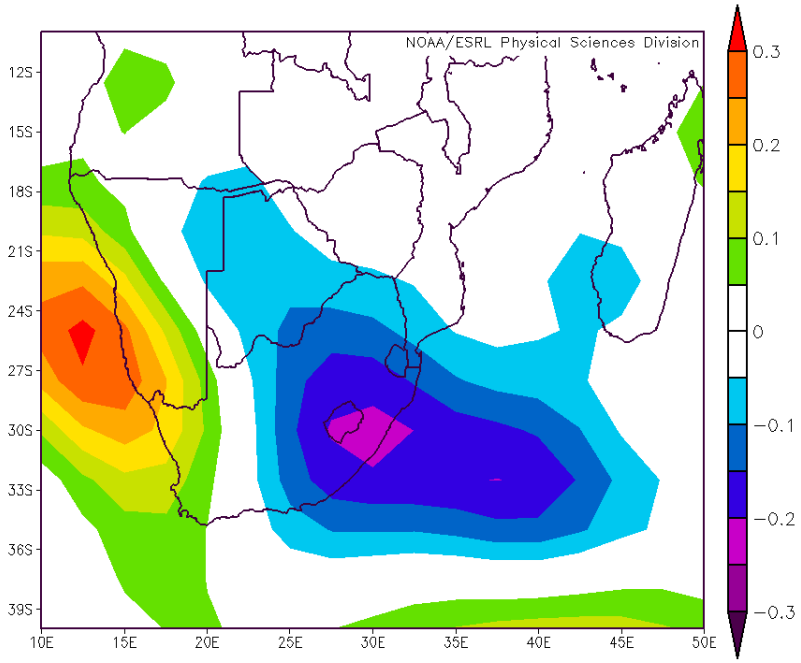

Figure 5.13: Omega anomaly at 500 hPa over southern Africa (31 October-2 November 1985).

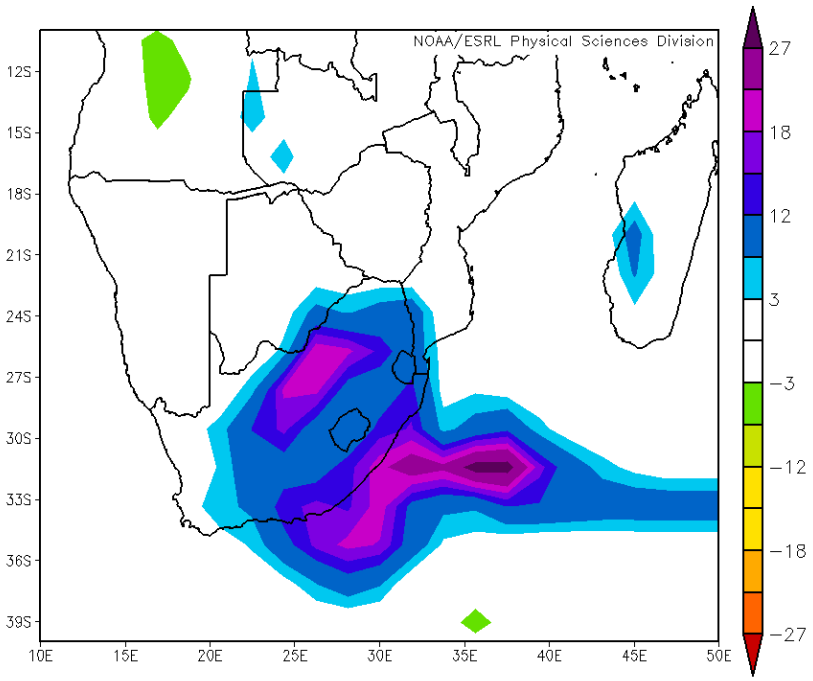

Figure 5.14: Rainfall rate (mm/day) anomaly over southern Africa (31 October-2 November 1985).

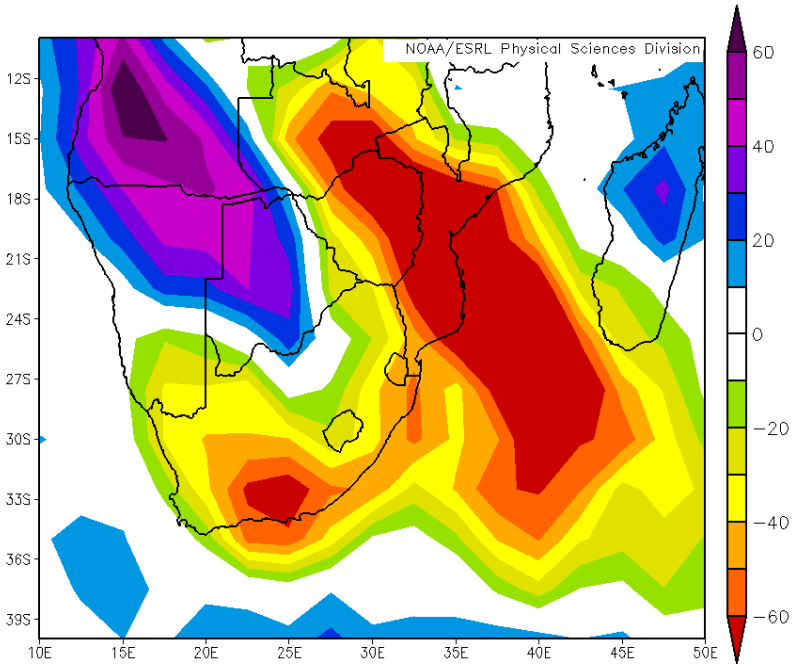

Figure 5.15: OLR (W/m^2) anomaly at 200 hPa over southern Africa (31 October-2 November 1985).

Event 2: 27-29 September 1987

On the 27th-29th September 1987, a cut-off low formed over southern Africa. The independent spinning of the cut-off low detached from the westerly wave is attributed to the persistence of the Mascarene High blocking. Blocking played a vital role in the occurrence and slow movement of the cut-off low (Figure 5.16 and 5.17). Mascarene High blocking influenced slow movement of the cut-off low and forced the weather system to persist over southern parts of South Africa. This caused the cut-off low to enhance successive blocking of the west-east movement of the westerly wave. Conditions over South Africa during this period were anomalously cold and wet (Figure 5.19). Cloud clover (Figure 5.20) and heavy rainfall is identified following the location of the cut-off low, with moisture uplift also identified being high over the subcontinent (Figure 5.18) due to the cut-off low being cold cored.

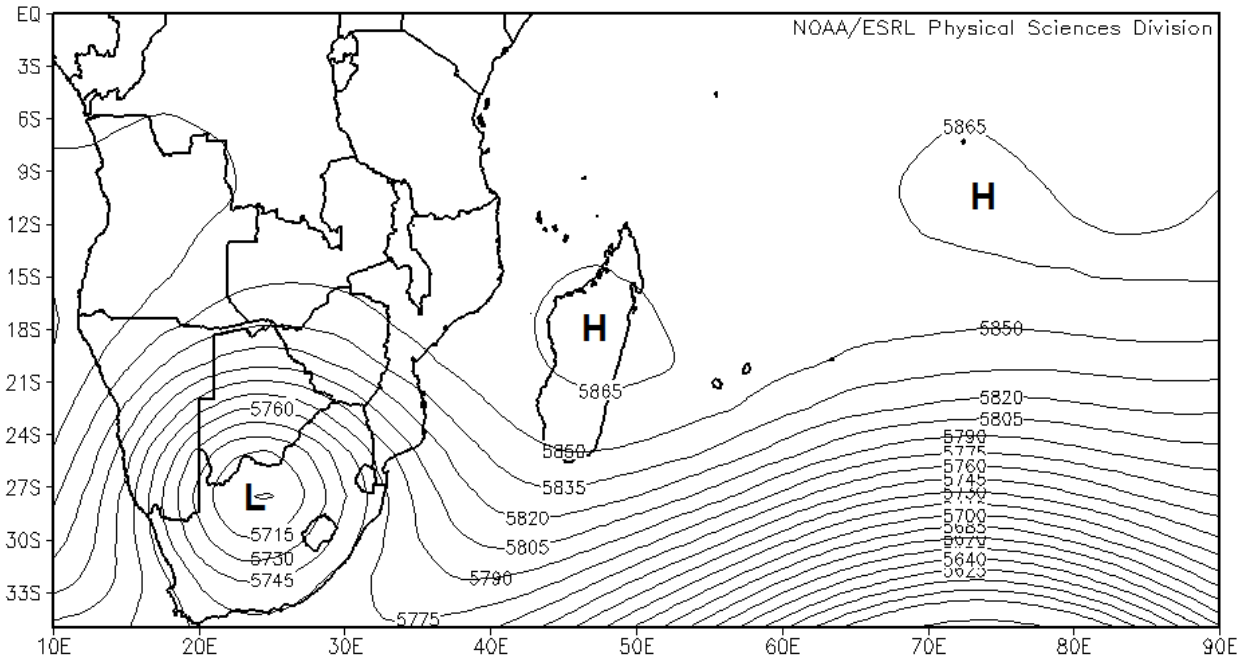

Figure 5.16: Daily mean geopotential height (m) at 500 hPa over southern Africa and SWIO (27-29 September 1987).

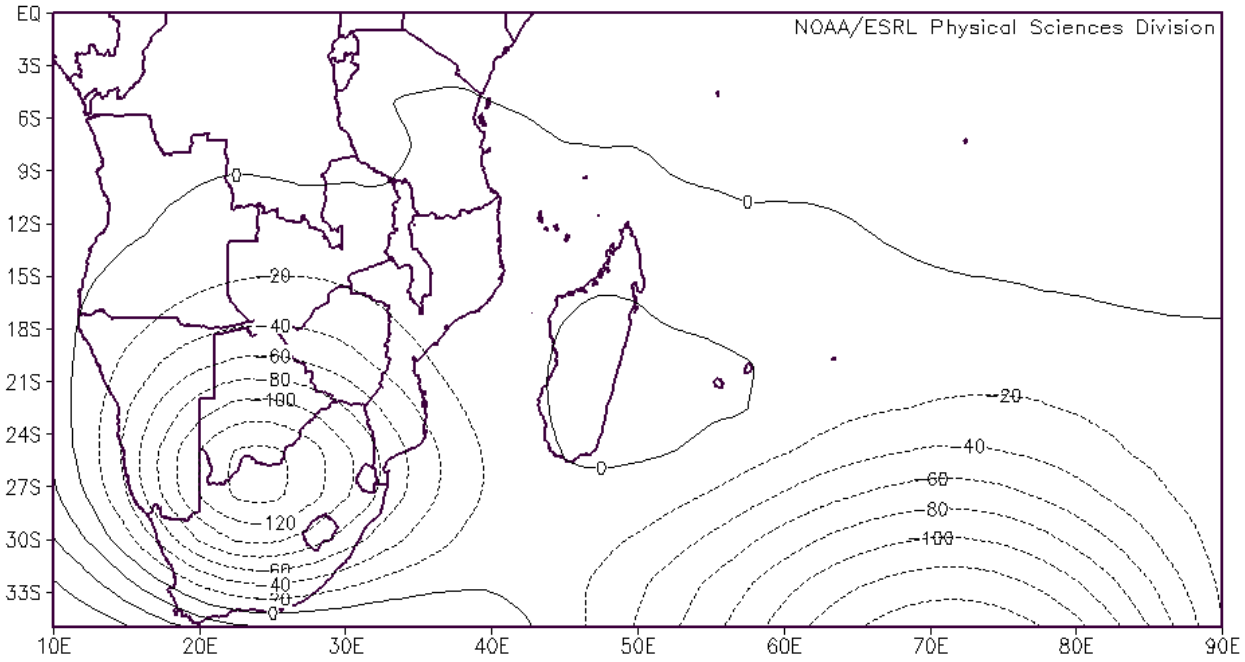

Figure 5.17: Daily composite mean geopotential height (m) anomaly at 500 hPa over southern Africa and SWIO (27-29 September 1987).

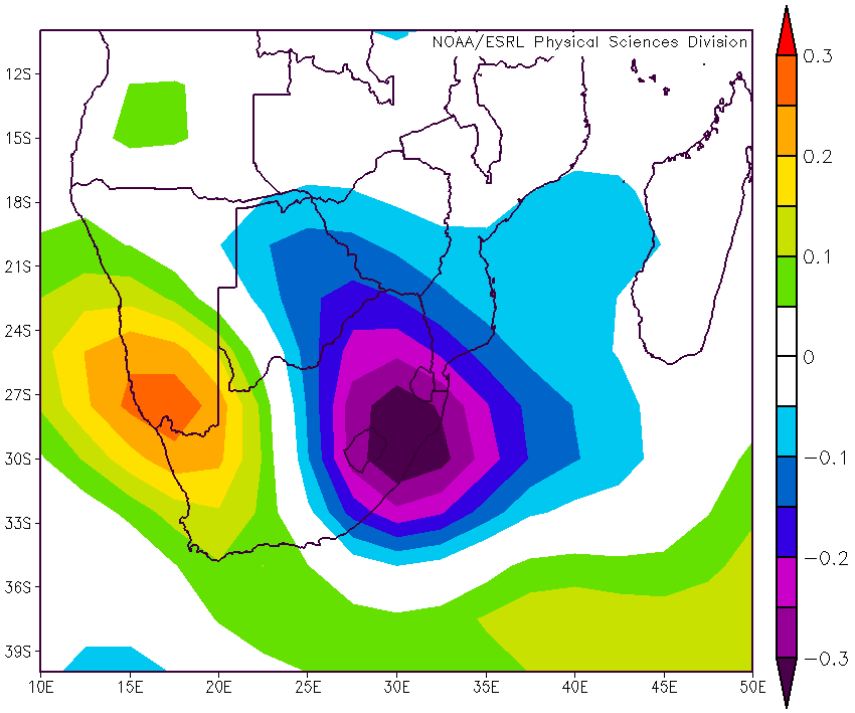

Figure 5.18: Omega anomaly at 500 hPa over southern Africa (27-29 September 1987).

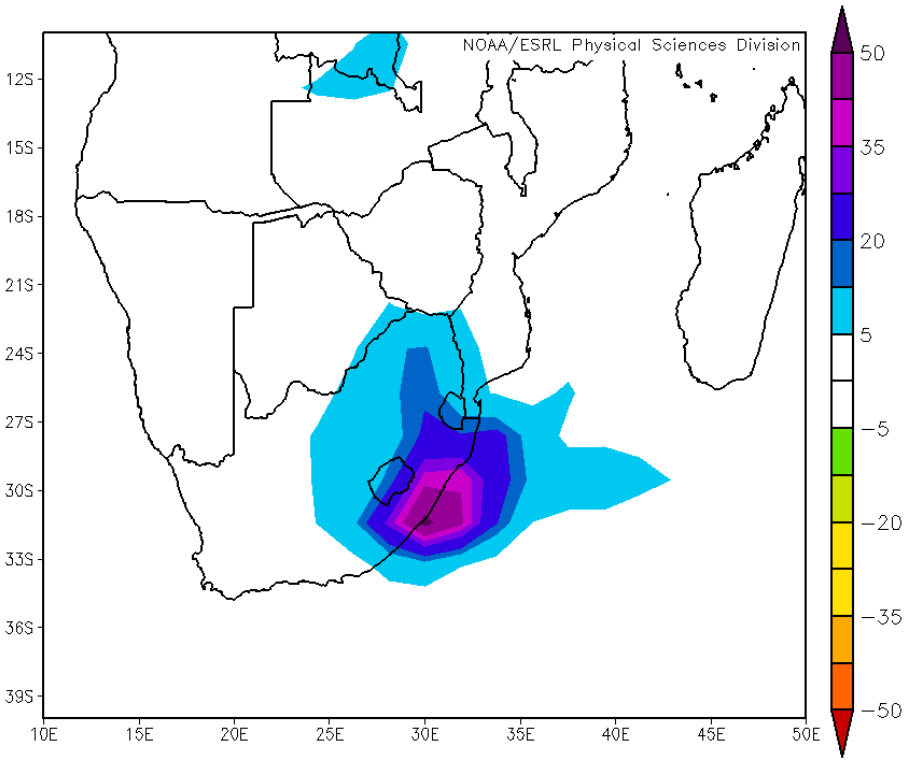

Figure 5.19: Rainfall rate (mm/day) anomaly over southern (27-29 September 1987).

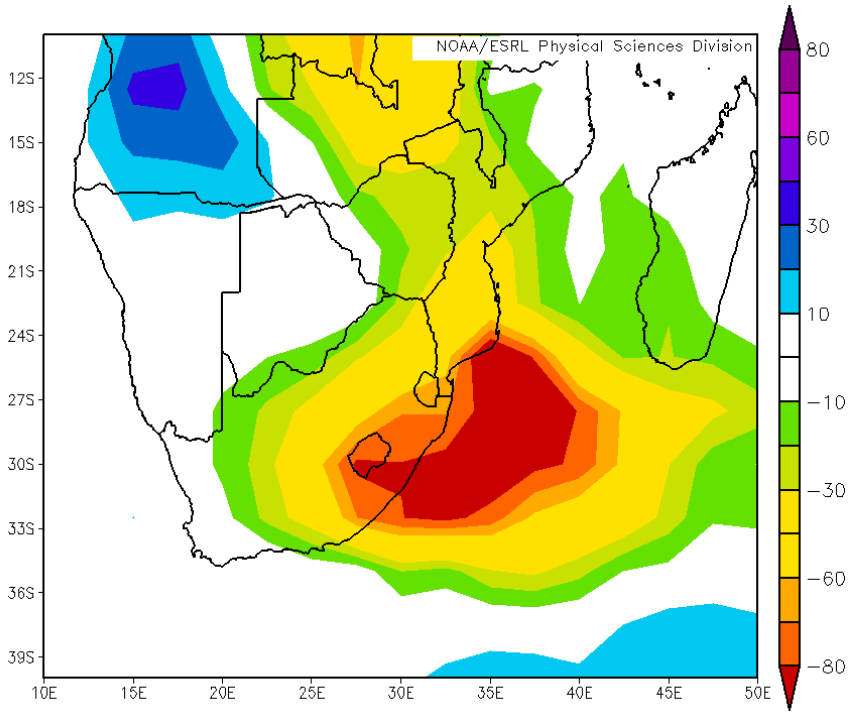

Figure 5.20: OLR (W/m^2) anomaly at 200 hPa over southern Africa (26-27 September 1987).

5.5 Blocking and slow moving cloud bands

Occurrence of cloud bands is induced by Mascarene High blocking and this influences austral summer rainfall over southern Africa (Engelbrecht *et al.* 2014). In some events, cloud bands tend to last longer than normal, causing heavy rainfall over the subcontinent (Hart *et al.* 2013). Heavy rainfall induced by cloud bands conditions occur at a day-to-day scale over southern Africa and are presented in this section. In addition, this section investigates two cloud bands events triggered by Mascarene High blocking.

Event 1: 31 December 1997-2 January 1998

Slow movement of the cloud band was largely induced by Mascarene High blocking (Figure 5.21, 5.22 and 5.23). A distinct cloud band over southern Africa was evident on December 31, 1997. This occurrence was persistent with the presence of the Angola low and northeasterlies wind circulation over Zimbabwe and Botswana. The cloud band lasted for three days, propagating slowly (west-to-east) over the subcontinent. Anomalous and substantial rainfall persisted from 31 December (Figure 5.24), with strong moisture flux and low-level convergence on 1 and 2 January. Heavy rainfall and low OLR were also evident across the range of the cloud band for the three days. Low OLR over the subcontinent shows that there was convection over the semi-arid regions. OLR anomalies at 200 hPa (Figure 5.25) also support that there was presence of above normal moisture uplift and cloud cover along the cloud band. Convection also enhanced upper-level divergence over the subcontinent and resulted in strong wind gradients on the cloud band south-western flank.

a) b)

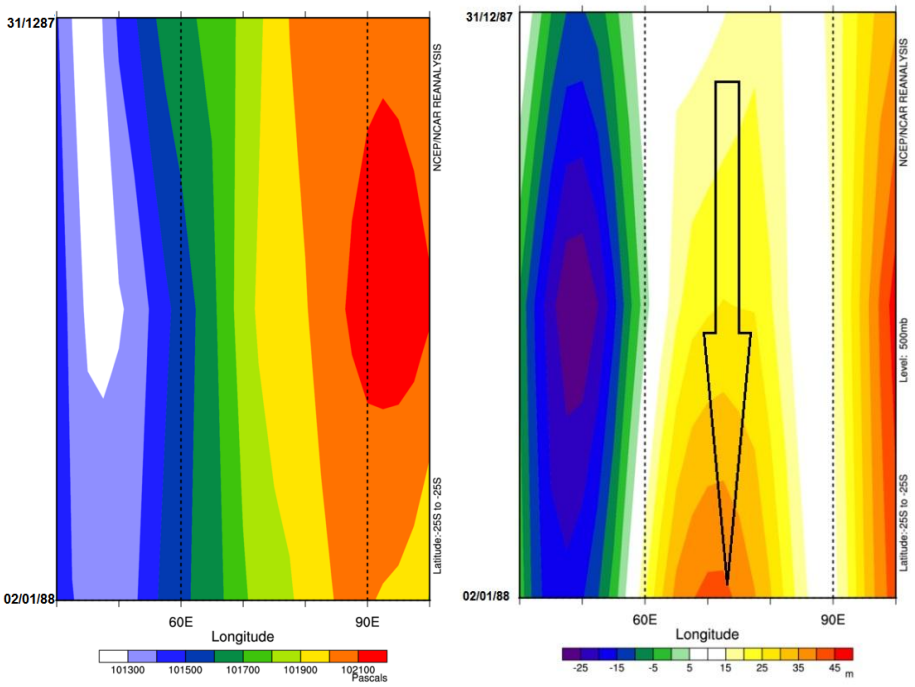

Figure 5.21: Hovmoller for a) MSLP (hPa) and b) geopotential composite (m) anomaly at 500 hPa (31 December- 2 January 1988).

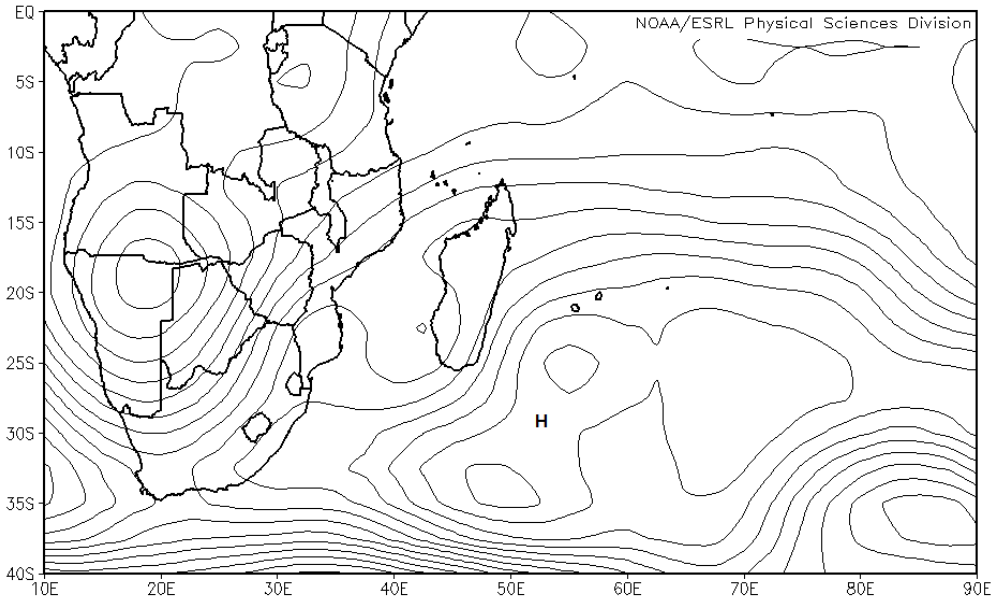

Figure 5.22: Daily composite mean geopotential height (m) at 850 hPa over southern Africa and SWIO (31 December 1997-2 January 1998).

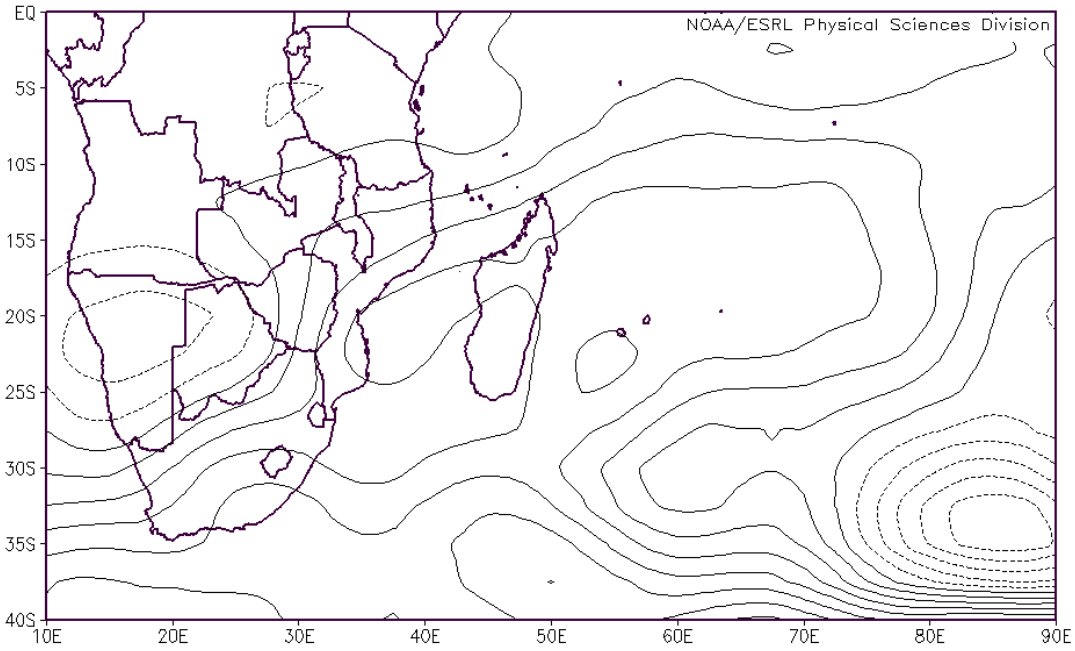

Figure 5.23: Geopotential height anomaly (m) at 850 hPa over southern Africa and SWIO (31 December- 2 January 1998).

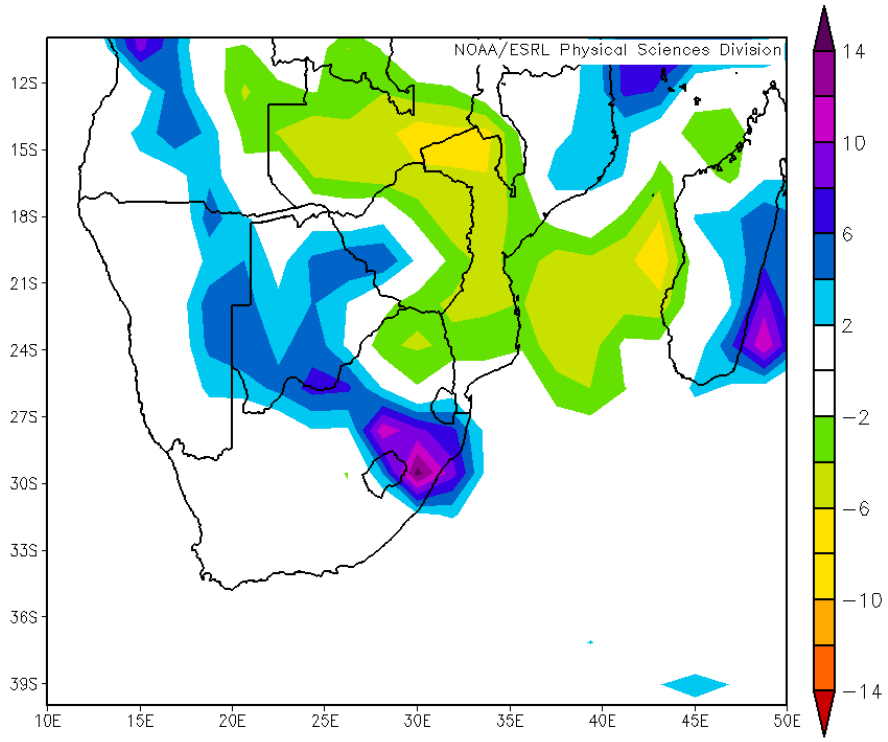

Figure 5.24: Surface rainfall rate (mm/day) anomaly over southern Africa (31 December- 2 January 1998).

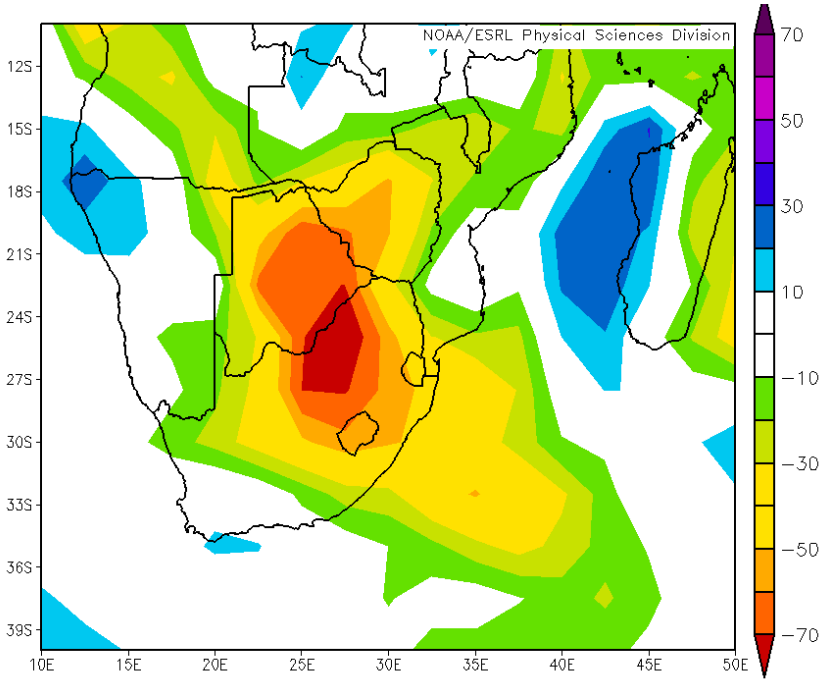

Figure 5.25: OLR (W/m^2) anomaly at 200 hPa over southern Africa (31 December- 2 January 1998).

Event 2: 5-7 January 1998

During this event, the duration of the cloud band was from 5-7 January, 1998. Mascarene High blocking triggered slow west-east propagation of the cloud band weather system over southern Africa. Low OLR, convection and heavy rainfall over Namibia, Botswana and South Africa, for 5 and 6 January, 1998 were observed. The strong Angola low (Figure 5.27) allowed for transportation of moisture flux towards the subcontinent. OLR anomalies at 200 hPa (Figure 5.30) show that there was above normal convection during the occurrence of the cloud band.

The quasi-stationary synoptic scale Mascarene High (Figure 5.26 and 5.27) situated over the warm Indian Ocean during this period allowed for moisture, primarily from the warm Indian Ocean to be transported towards southern Africa. Transportation of moisture flux was majorly influenced by the presence of the intense Angola Low. This influenced steep pressure gradients and strong wind flow towards southern Africa. South-western flank of the Angola Low consisted of strong low-level northeasterlies (Figure 5.28). There was substantial rainfall over the east of the subcontinent (Figure 5.29), where intense convection was dominant. This is also shown by the presence of low OLR over the region (Figure 5.30). Rainfall distribution over the same region for a protracted period was also influenced by the slow propagation of the blocking Mascarene High.

a) b)

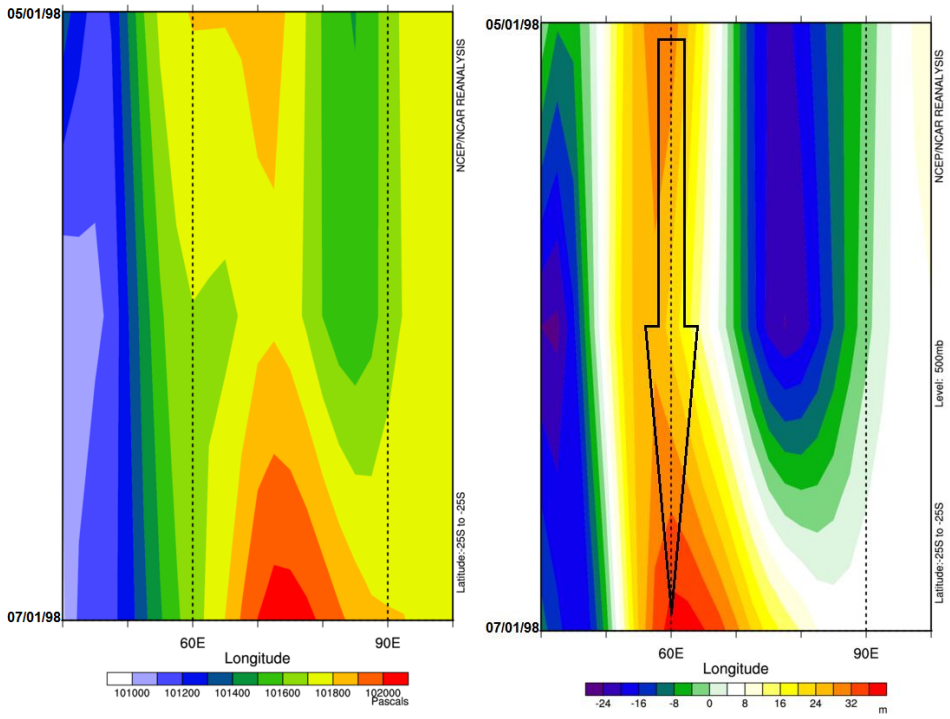

Figure 5.26: Hovmoller for a) MSLP (hPa) and b) geopotential composite anomaly (m) at 500 hPa (5-7 January 1998).

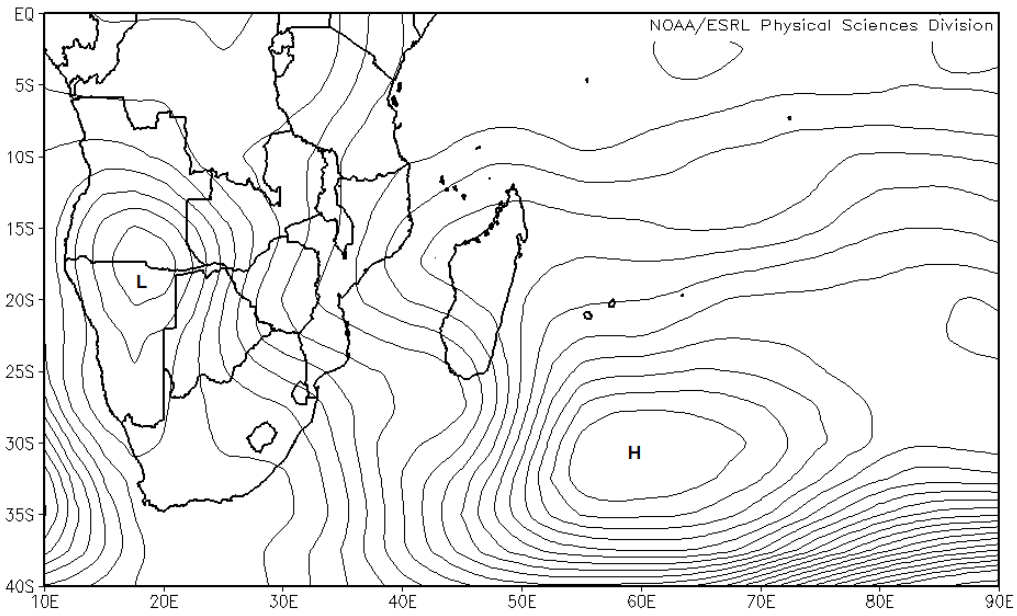

Figure 5.27: Daily mean geopotential height (m) at 850 hPa over southern Africa and SWIO (5-7 January 1998).

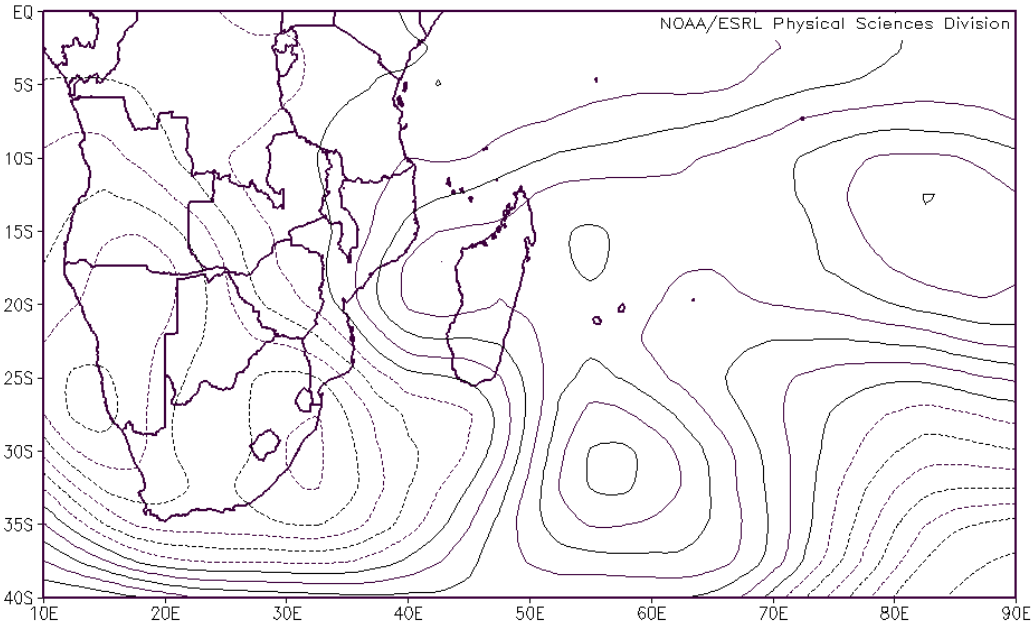

Figure 5.28: Geopotential height anomaly (m) at 850 hPa over southern Africa and SWIO (5- 7 January 1998).

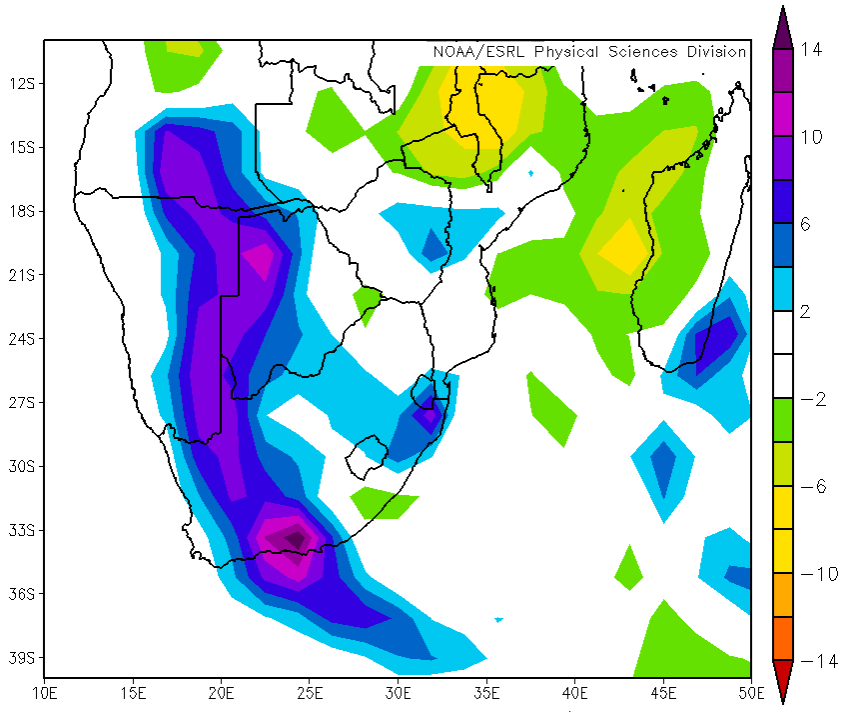

Figure 5.29: Surface rainfall rate (mm/day) anomaly over southern Africa (5-7 January 1998).

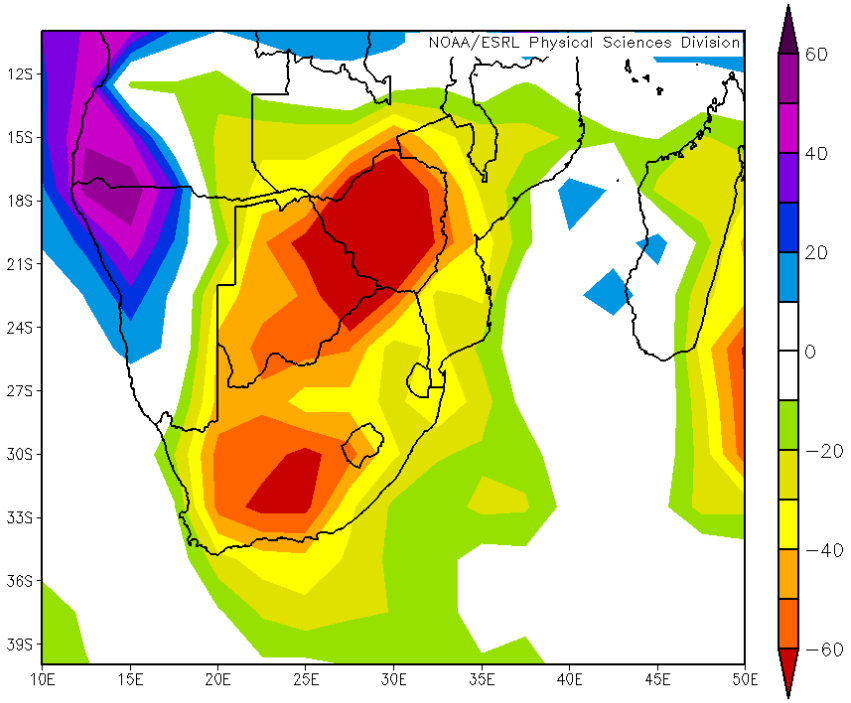

Figure 5.30: OLR (W/m^2) anomaly at 200 hPa over southern Africa (5-7 January 1998).

5.6 Summary

In this chapter, Mascarene High blocking events were investigated and the results indicate that Mascarene High blocking induces heavy rainfall conditions over southern Africa. Propagation of cut-off lows, TCs and cloud bands events appear to be largely influenced by a slow moving Mascarene High. During events of Mascarene High blocking, rainfall is found to be anomalously high over southern Africa and in some events complemented by cold conditions. TC tracks may penetrate onto the subcontinent as they are driven by easterlies, generated from the circulation of the Mascarene High. Cloud bands are found to be a major rainfall bearing system over southern Africa during austral summer, their anomalous occurrence is found to be unique and brings heavy rainfall events over southern Africa.

This chapter employed the event scale analysis technique and important findings of this chapter are:-

a) Mascarene High blocking causes slow west-east movements of weather systems, inducing heavy rainfall over southern Africa.
b) Mascarene High blocking events vary in location over the South Indian Ocean spatially and temporally and are more frequent in austral summer.

c) Trade winds during Mascarene High blocking are found to be anomalously strong, driving TCs towards southeast Africa during austral summer and during negative ENSO phases through large scale flow.
d) Mascarene High blocking is identified at 500 hPa and can last for about a period of three days or more over the South Indian Ocean.
e) Over southern Africa, cut-off lows tend to be regional and not widespread.
f) Cut-off lows also causes subsequent blocking of the westerly wave as the weather system consists of slow mid-tropospheric movements over southern Africa.
g) Absence of Mascarene High blocking can be directly linked to normal mean weather conditions over southern African.

In the next chapter, the study focuses on future changes in intensity and spatial characteristics of the Mascarene High using the Conformal-Cubic Atmospheric Model (CCAM) projections.

CHAPTER 6: FUTURE CHANGES IN INTENSITY AND SPATIAL CHARACTERISTICS OF THE MASCARENE HIGH

6.1 Introduction

In this chapter, simulations made with the Conformal-Cubic Atmospheric Model (CCAM) using Representative Concentration Pathways (RCPs) 4.5 and 8.5 scenarios for present and future climate are discussed. The focus of the chapter is on the Mascarene High pressure cell, and two 30 year periods are considered namely, 1985 to 2014 and 2070 to 2099. For both RCP4.5 and RCP8.5, six different simulations were made with sea surface forcing from six earth system models. Results are presented in terms of percentiles, and therefore not all six members are discussed individually, but the uncertainty in the simulations is presented. The main aim of this chapter is to analyse how the Mascarene high is projected to change in the future, and how it links up to other variables.

Confidence in projections made by a particular model relies on the model's ability to simulate present day climate with skill, because future climate observations are not available for a verification to be possible. The first part of this chapter discusses how the present day CCAM simulations compare to observations discussed in chapter 4, and projections of the different variables are then discussed later.

6.2 Present day simulations vs. observations

The RCP4.5 and RCP8.5 simulations are the same until the year 2000, and therefore the simulations with the same surface forcing are similar for just over half the present day period. The 10^{th}, 50^{th} and 90^{th} percentiles of the 30 year average MSLP are almost similar for all the simulations (Figure 6.1). Similarities in the simulations suggests that there is little uncertainty in the simulated structure of the Mascarene High. Agreement in CCAM projections and observations enhances consistency for using the data to project future scenarios in the study.

Mascarene High simulations from CCAM over the South Indian Ocean shows dominance for the region extending from 25-35°S and 40-110°E (Figure 6.1 and 6.2). CCAM Mascerene High simulations over the warm South Indian Ocean are comparable with observations presented in Chapter 4 (Figure 4.2, 4.3, 6.1 and 6.2). CCAM simulations for the period 1985-2014 (Figure 6.2 and 6.3), indicate a distinct mode of seasonal Mascarene High distribution, varying in seasonal dominance and intensity. During austral summer (winter), CCAM Mascarene High simulations

locate southward (northward) over the Indian Ocean. Consistent with observations, CCAM simulations also support that the Mascarene High tends to be intense (1023 hPa) during austral winter and a northward propagation is also simulated.

The wind circulation around anticyclones is counter-clockwise as already discussed in Chapter 4. The centre of the high is associated with smaller wind speeds as already seen in Figure 4.12. The RCP8.5 simulations are able to capture this feature best, with smaller winds speeds around the centre for the high and larger magnitudes away from the centre. The circulation is also clearly counter-clockwise in all the RCP8.5 simulations. The winds north of the Mascerene High are easterly as expected (Figure 6.4). In winter the northward propagation of the high is also simulated well with accompanying weaker winds around the centre, and counterclockwise motion around the high (Figure 6.5).

Positive omega values are associated with downward motion, because pressure decreases with height. Most of the Indian Ocean is associated with positive values, which further confirms that high pressure cells are associated with fair weather conditions. The northern parts of Madagascar are associated with negative values, which is indicative of systems that are associated with uplift in summer (Figure 6.6). In winter the positive omega values extend further north to also include the area north of Madagascar that was associated with negative values in summer (Figure 4.13; Figure 6.7). CCAM is able to capture these seasonal differences. In the next sections projections made with the CCAM for the far future climate are discussed.

a) b)

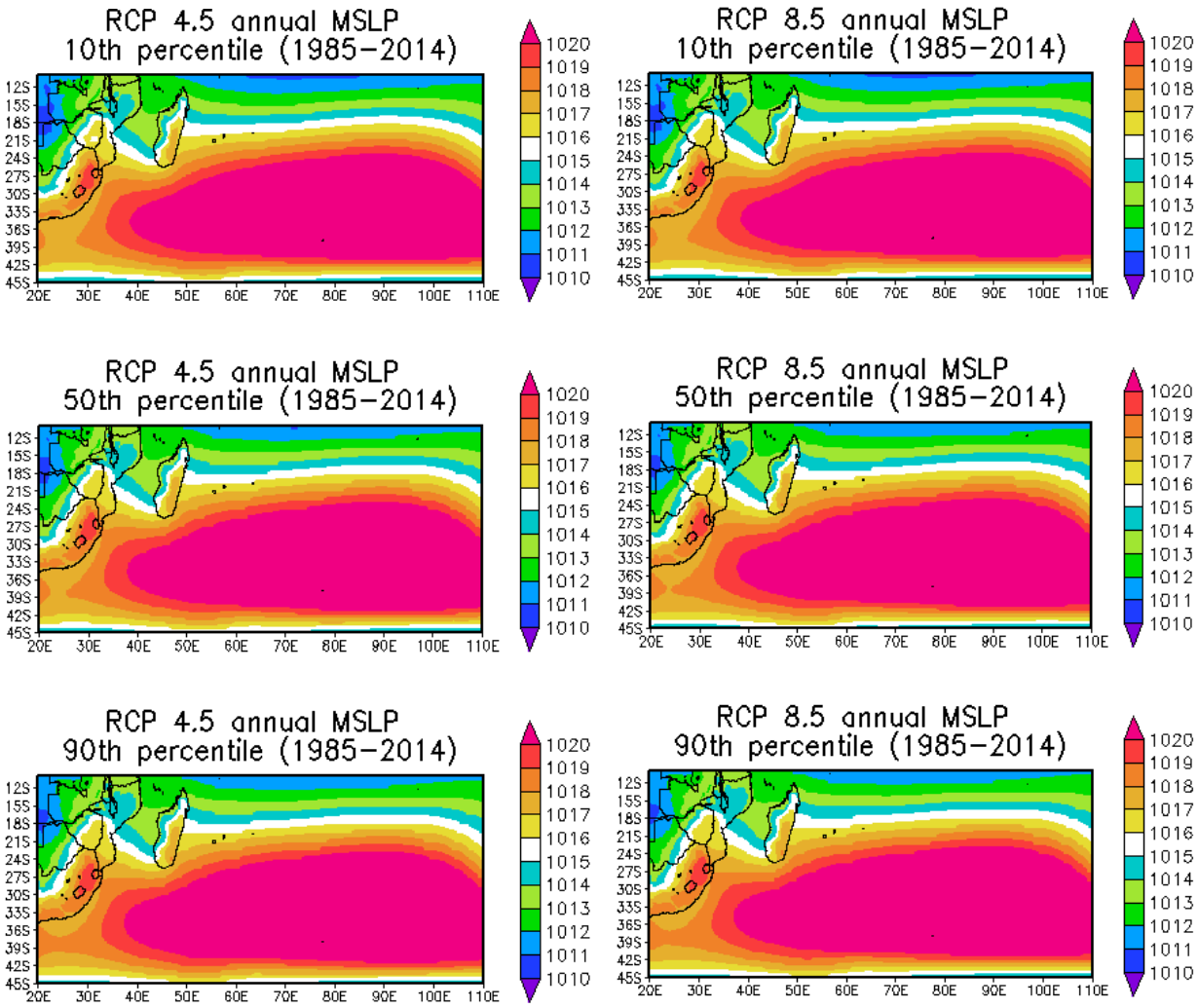

Figure 6.1: Annual RCP a) 4.5 and b) 8.5 CCAM percentiles for MSLP (hPa) over the Southwest Indian Ocean (SWIO) for the period 1985-2014.

a) b)

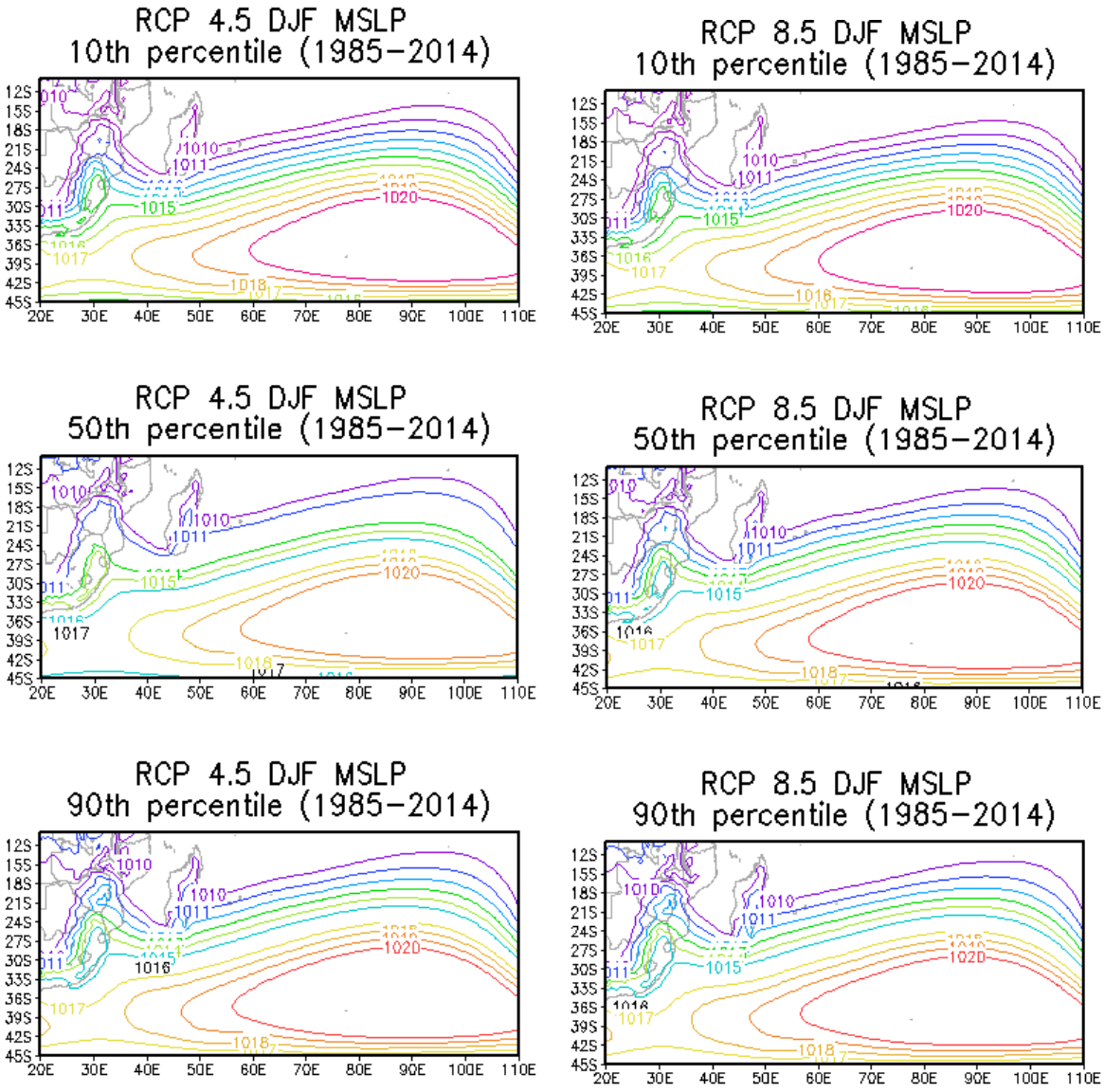

Figure 6.2: Austral summer RCP a) 4.5 and b) 8.5 CCAM percentiles for MSLP (hPa) over the SWIO for the period 1985-2014.

a) b)

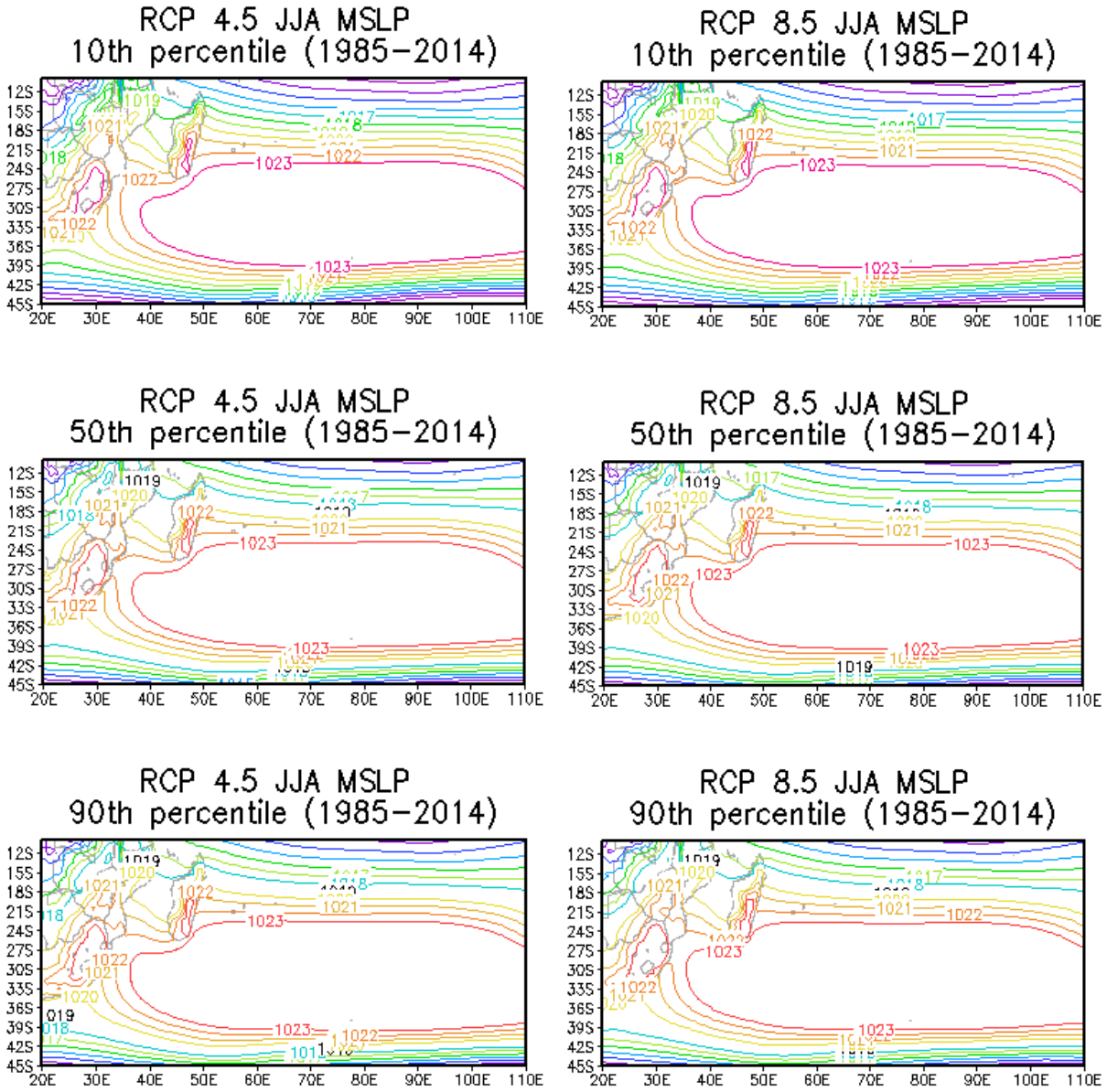

Figure 6.3: Austral winter RCP a) 4.5 and b) 8.5 CCAM percentiles for MSLP (hPa) over the SWIO for the period 1985-2014.

a) b)

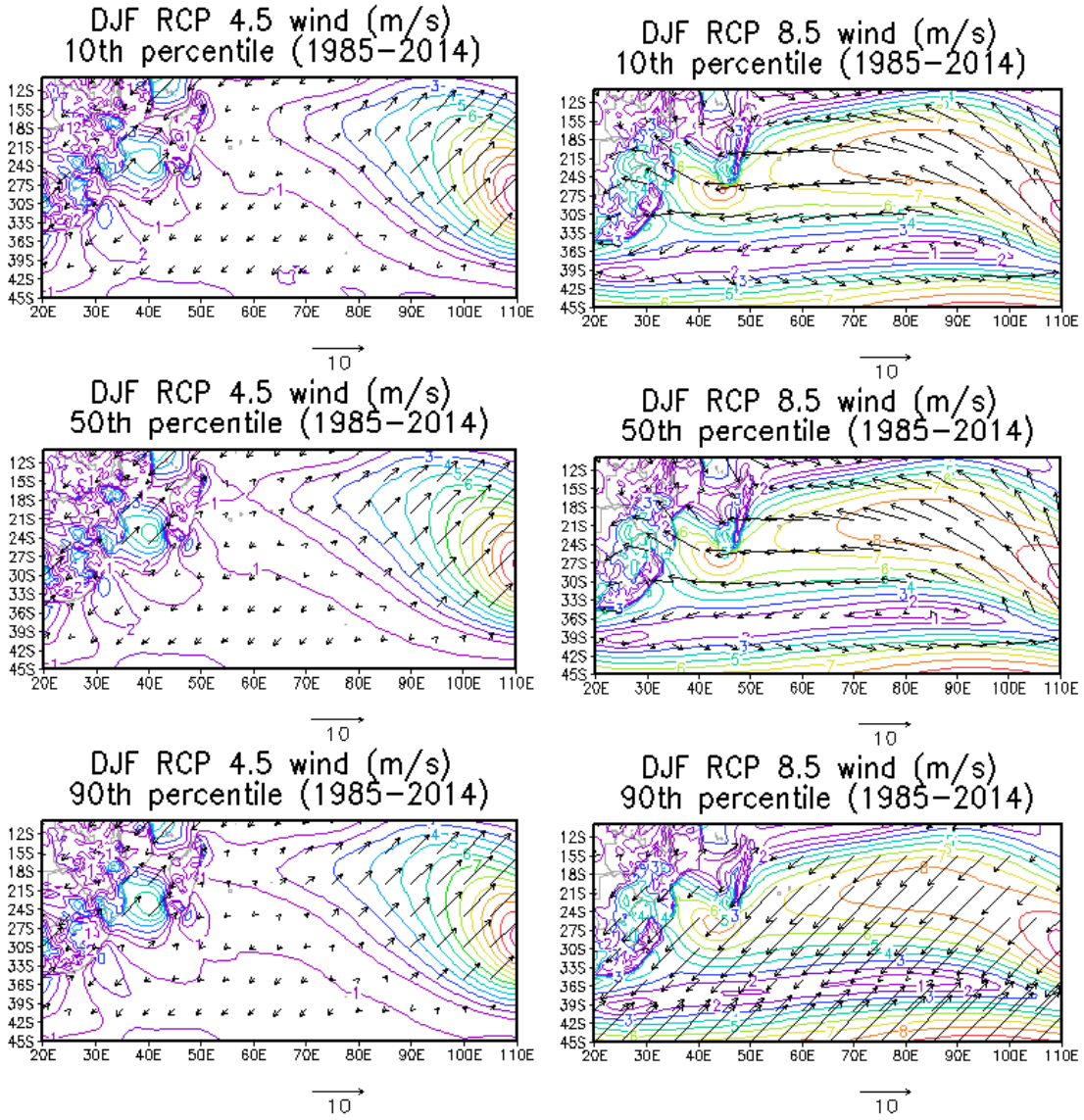

Figure 6.4: Austral winter RCP a) 4.5 and b) 8.5 CCAM percentiles for wind (m/s) over the Southwest Indian Ocean for the period 1985-2014.

a) b)

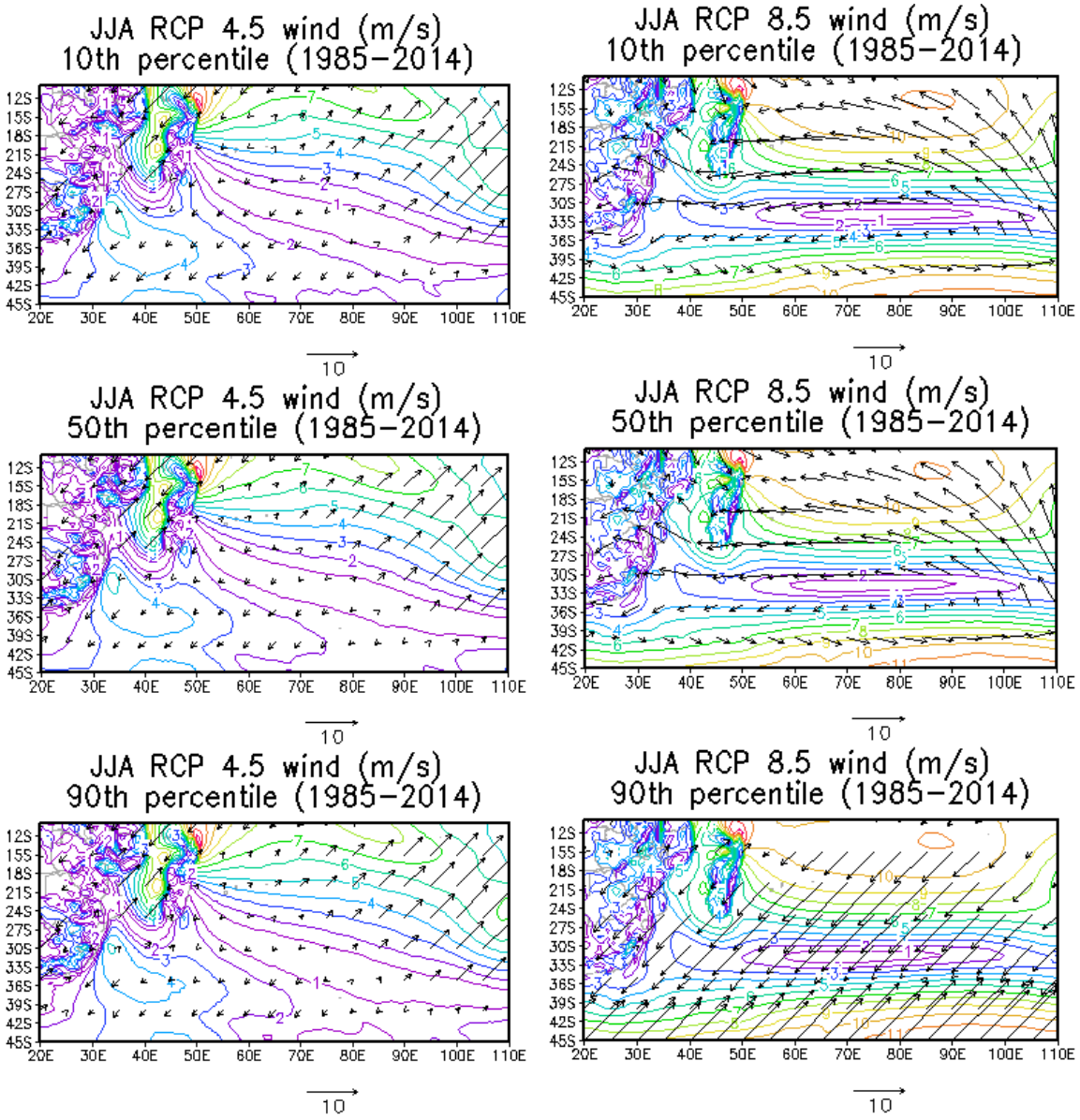

Figure 6.5: Austral winter RCP a) 4.5 and b) 8.5 CCAM percentiles for wind (m/s) over the SWIO for the period 1985-2014.

a) b)

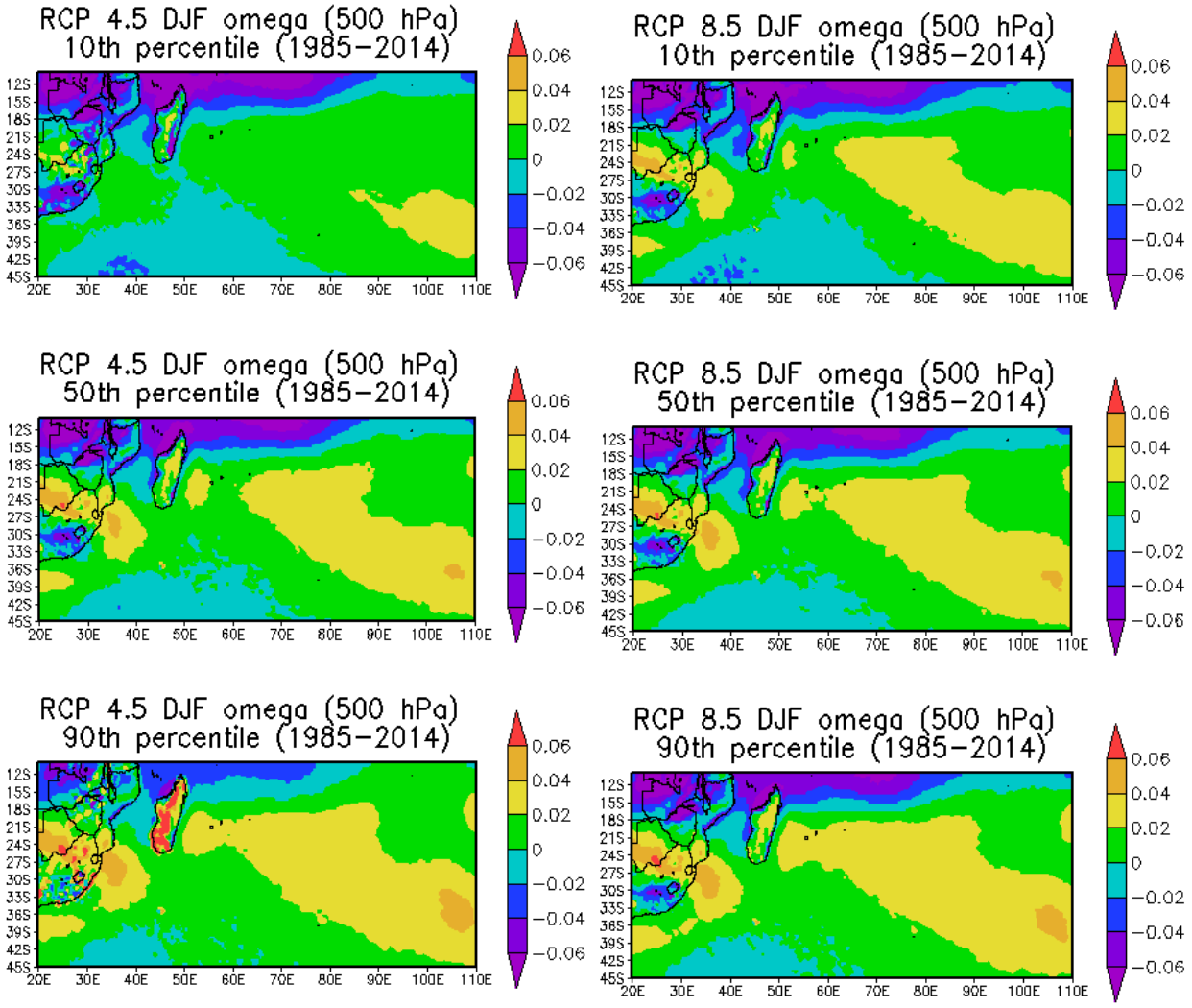

Figure 6.6: Austral summer RCP a) 4.5 and b) 8.5 CCAM percentiles for omega (500 hPa) over the SWIO for the period 1985-2014.

a) b)

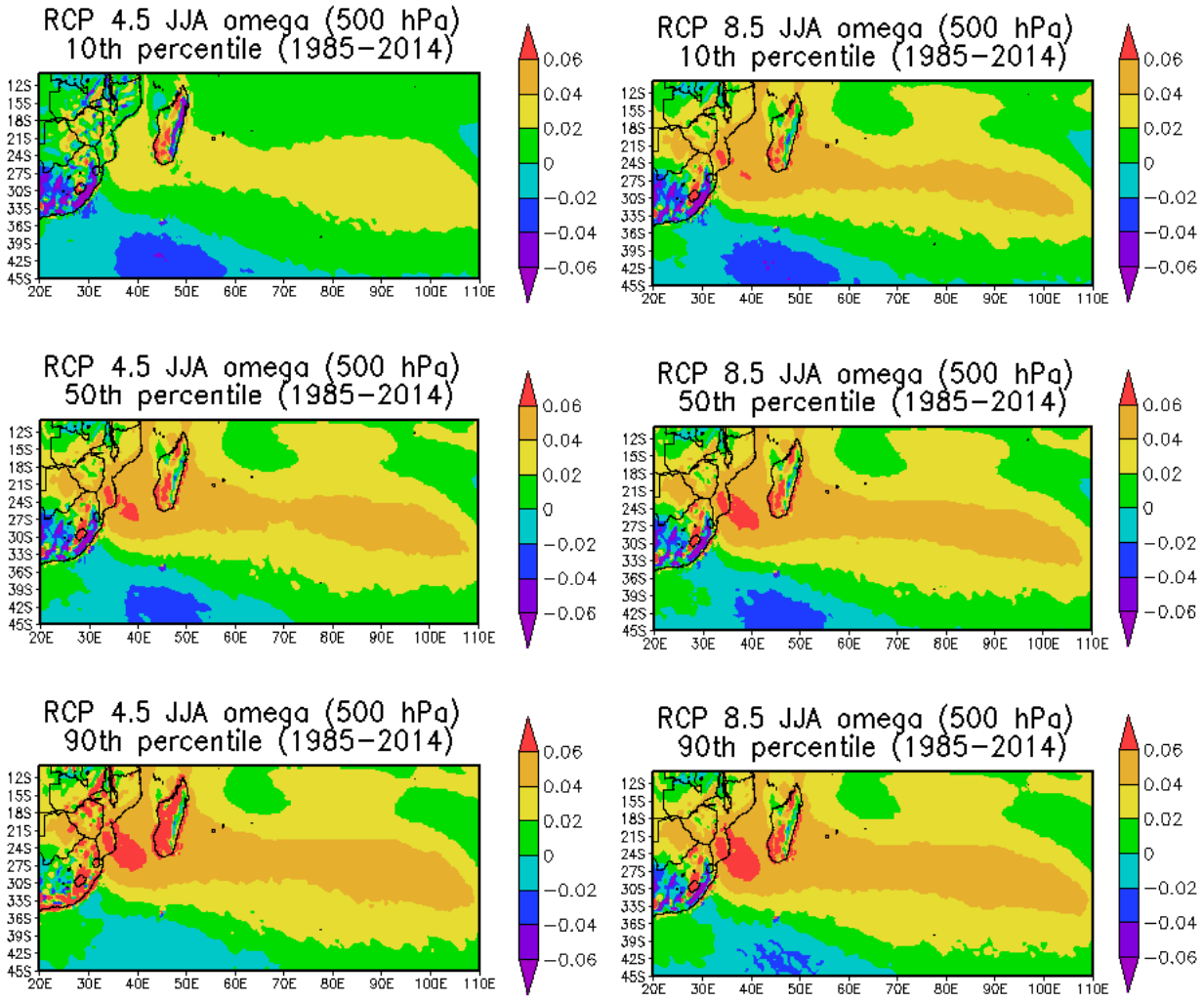

Figure 6.7: Austral winter RCP a) 4.5 and b) 8.5 CCAM percentiles for omega (500 hPa) over the SWIO for the period 1985-2014.

6.3 Climate periods differences (2070-2099 -1985-2014)

6.3.1 MSLP differences (2070-2099) – (1985-2014)

Annual projections of the MSLP show some uncertainty, with ensemble members predicting both a strengthening and a weakening of the Mascarene high. There is no clear trend when annual averages are considered (not shown). In summer the RCP4.5 scenario is predicting increases in MSLP east of Madagascar for ensemble members, however the area where the Mascarene high dominates is associated with small negative values (Figure 6.9). This result suggests the

expansion of the high pressure belt, but not necessarily the strengthening of the belt. The RCP8.5 simulations suggest larger uncertainty in the simulations than those associated with RCP4.5. Percentile 10 suggests a decrease in MSLP over most of the Indian Ocean in the future climate. The 50th and 90th percentiles show positive values north of the area dominated by the Mascarene high further suggesting an expansion of the high pressure belt. Only the 90th percentile shows positive values over the area that is dominated by the Mascarene in present day summer, which is the only suggestion of strengthening of the Mascarene high.

Austral winter projections also show high values of uncertainty for future MSLP over the South Indian Ocean (Figure 6.10). The 10th percentile is associated with negative values for both RCP4.5 and RCP8.5 which suggest neither an expansion nor a strengthening of the Mascarene high. The 50th percentile is also mostly negative, with positive values moving into the domain from the south east and south west. The 90th percentile is associated with positive values over the eastern side of the domain, as well as the south west, for both RCP4.5 and RCP8.5. Over other parts of the Indian Ocean the RCP4.5 and RCP8.5 differ. This suggests that the climate change signal in winter is less clear than the one found in summer.

CCAM projections also suggest an expansion of the Mascarene High in the future in summer, (Figure 6.9 and 6.10) but not an obvious intensification signal. Austral summer future expansions suggest an equatorward migration of tropical revolving systems, penetrating regions north of southeast Africa. This also suggests that a changing climate may influence a change in weather and climate patterns over southern Africa. These projections also suggest that the Mascarene High will have a vital role in poleward migration of cold fronts over southern Africa in the future. The Mediterranean climate experienced over the Western Cape (South Africa) may change. These future seasonal expansions are linked to a changing climate and migration in location of westerly (easterly) wave flows that influence southern African weather and climate. Li (2013) investigated that austral expansion of the Mascarene High results from increase diabatic heating over continents and cooling of the ocean. Intensification is due to an increase in greenhouse gas emissions. Mascarene High expansion and intensification have vital implications in weather and climate changes over southern Africa. The winter projections are less clear with neither expansion nor intensification being clearly seen because of a large uncertainty seen from the projections. The larger the uncertainty in the projections the less the confidence in any statements regarding the climate change signal.

a) b)

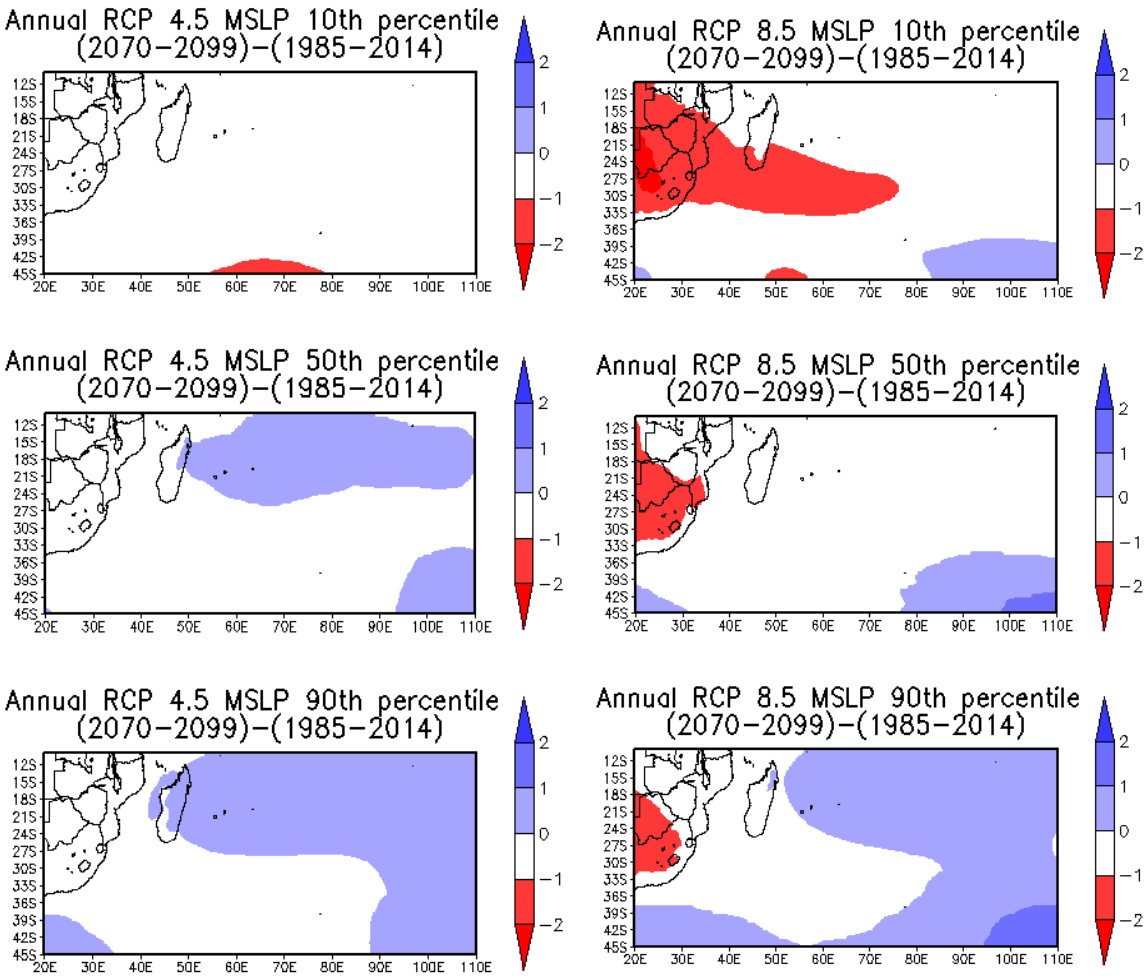

Figure 6.8: Annual RCP a) 4.5 and b) 8.5 MSLP (hPa) percentile differences (2070-2099 - 1985-2014) over the SWIO and southern Africa.

a) b)

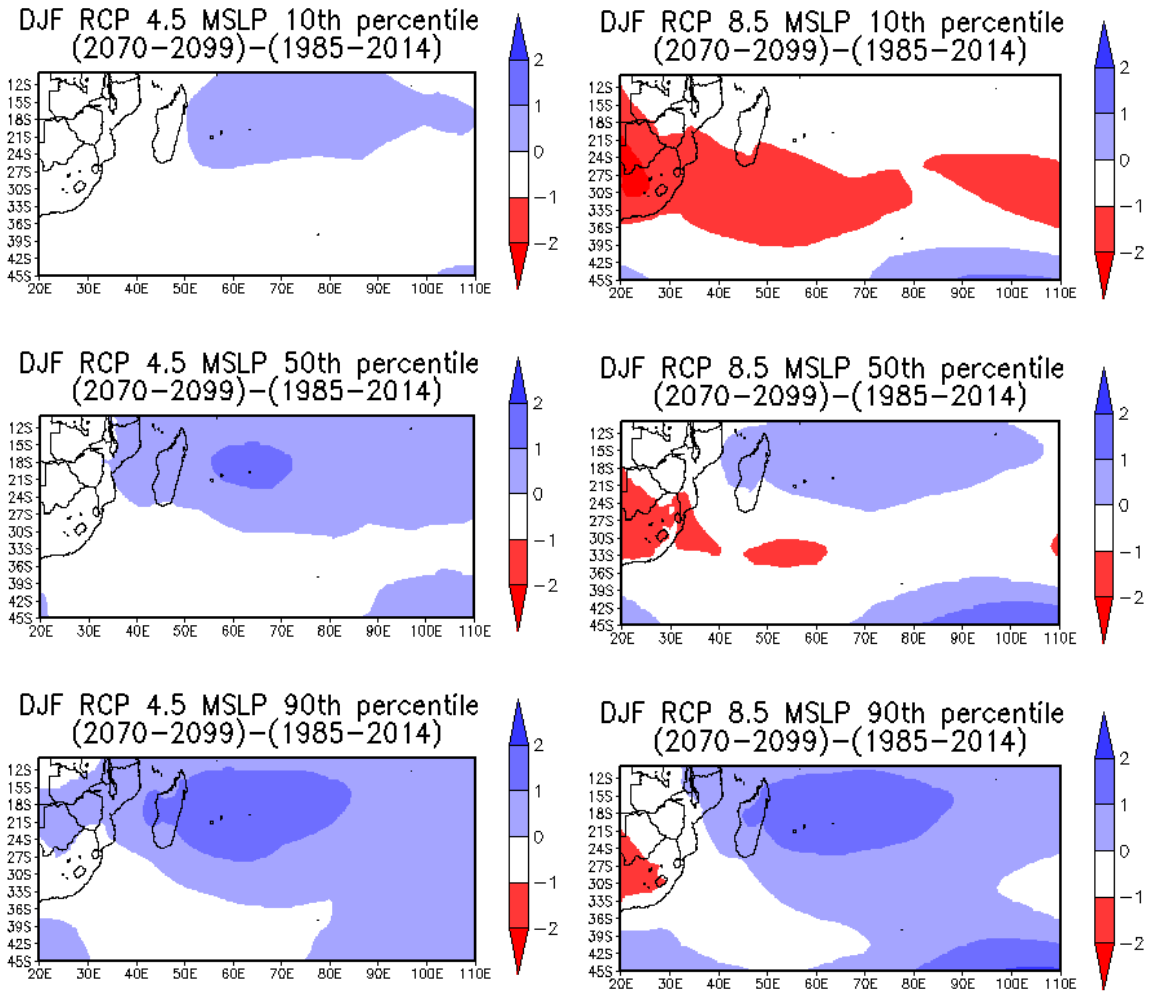

Figure 6.9: Austral summer RCP a) 4.5 and b) 8.5 MSLP (hPa) percentile differences (2070-2099 - 1985-2014) over the SWIO and southern Africa.

a) b)

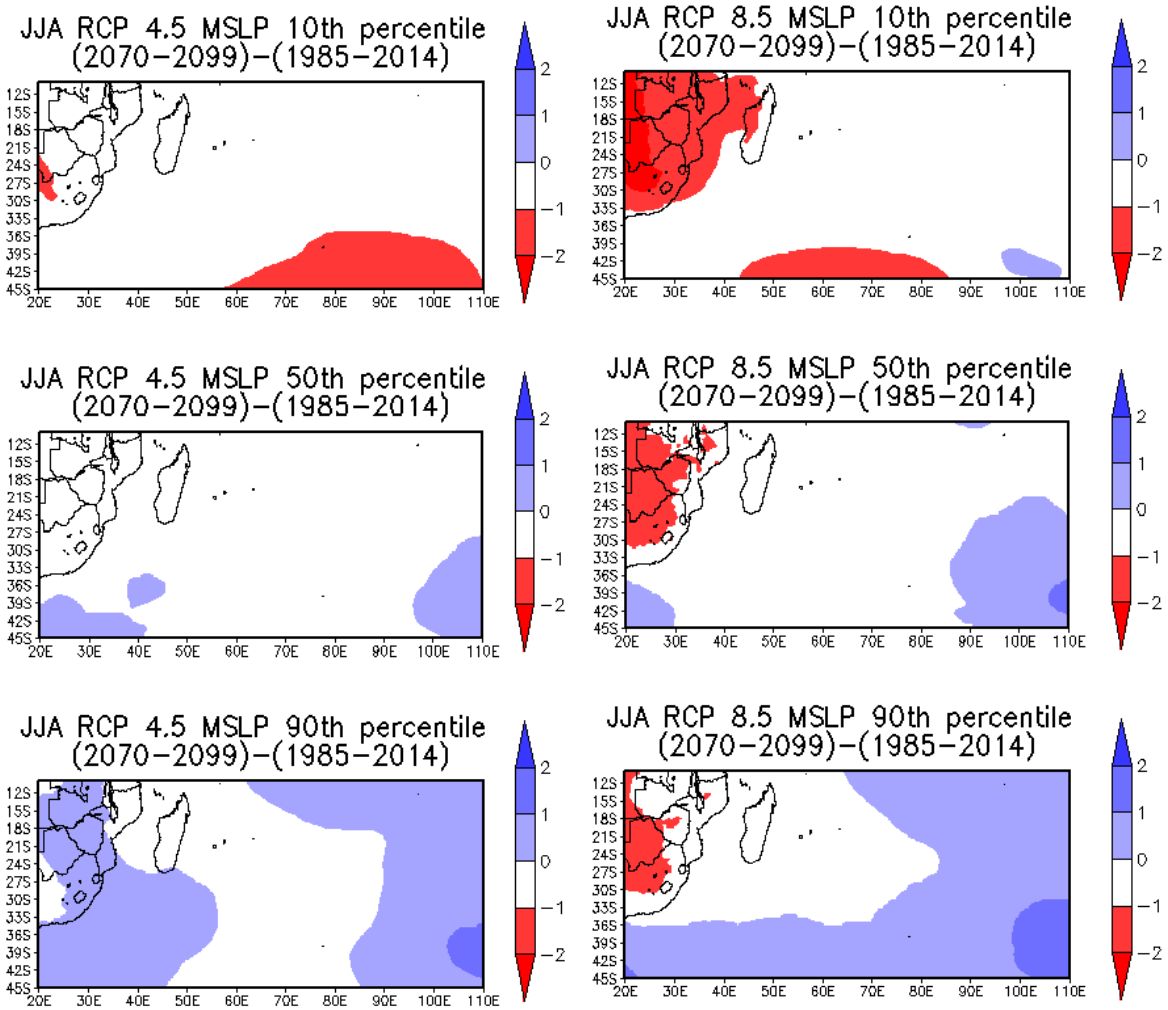

Figure 6.10: Austral winter RCP a) 4.5 and b) 8.5 MSLP (hPa) percentile differences (2070-2099 - 1985-2014) over the SWIO and southern Africa.

6.3.2 Wind differences (2070-2099) – (1985-2014)

The wind plots shows the zonal wind in future climate minus the zonal wind in present climate, as well as the meridional present day climate wind subtracted from the future climate. Negative values in the zonal difference which will be indicated by easterly motion imply that present day zonal winds are larger, while northerly winds suggest that future climate meridional winds are larger (Figure 6.11). Over the area dominated by the Mascarene high in summer, the winds seem to be easterly. This result suggests that present day zonal winds are stronger. The area north of southeast Africa is associated with positive zonal and meridional winds, which suggests stronger winds in future climate. The wind projections in summer, are replicated during austral winter (Figure 6.12). The strengthening of easterly trade winds is linked to the future projected strengthening and expansion of the Mascarene High, however our results are not conclusive on this.

a) b)

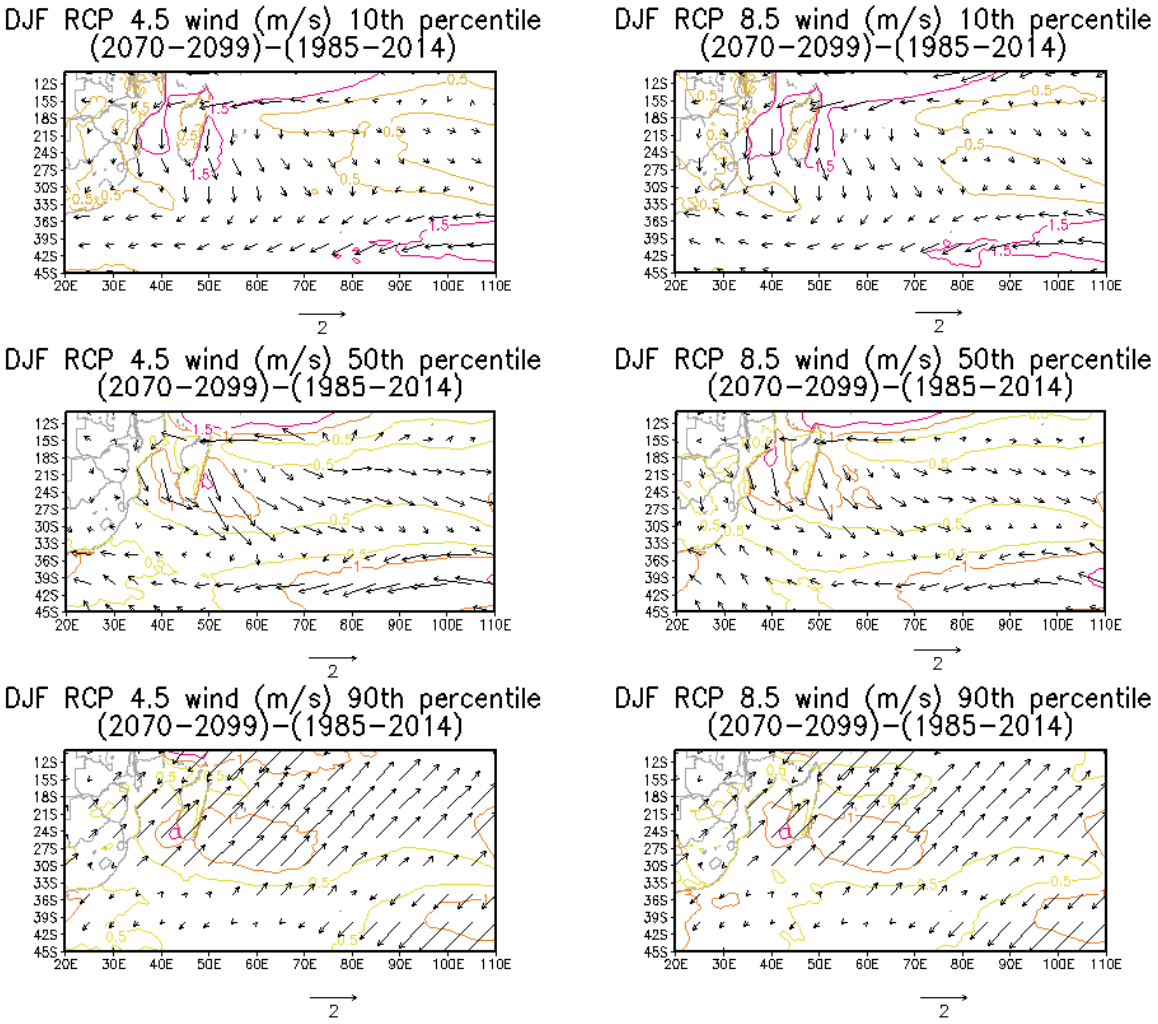

Figure 6.11: Austral summer RCP a) 4.5 and b) 8.5 wind percentile differences (2070-2099 - 1985-2014) over the SWIO and southern Africa.

a) b)

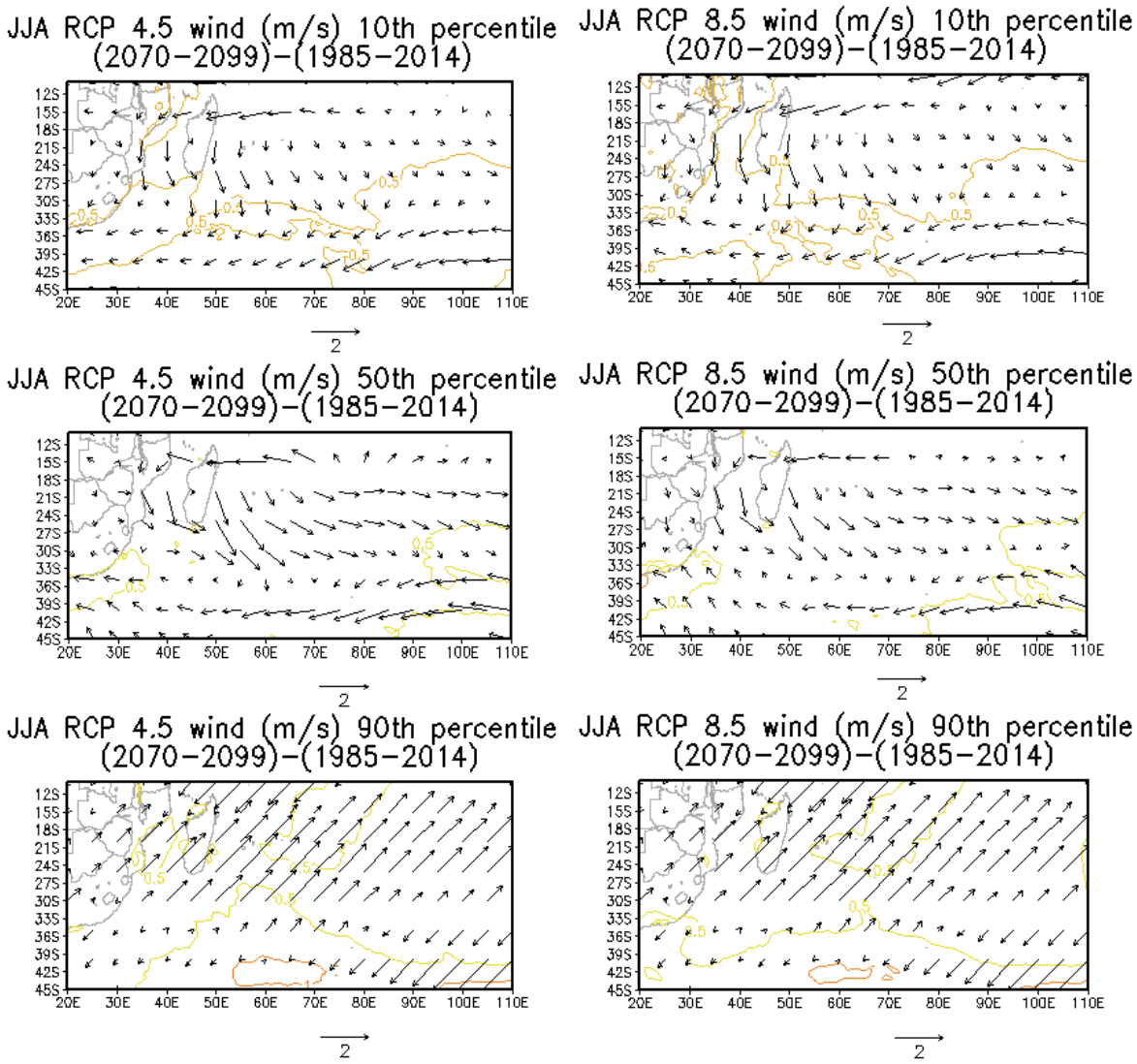

Figure 6.12: Austral winter RCP a) 4.5 and b) 8.5 wind percentile differences (2070-2099 - 1985-2014) over the SWIO and southern Africa.

6.3.3 Omega differences (2070-2099) – (1985-2014)

Positive values of omega are associated with descending motion. Positive differences support the expansion and strengthening of the Mascerene high pressure cell. The CCAM projections are not conclusive as far as the expansion and strengthening are concerned (Figure 4.13 and 14). The northern parts of Madagascar are associated with positive differences which suggest less uplift compared to present day climate. Over other parts of the Indian Ocean the projections are less conclusive about whether the future omega is larger or smaller compared to the present day values. The austral winter projection looks slightly more positive than the summer ones, which in this case will suggest some level of the strengthening of the Mascerene high.

a) b)

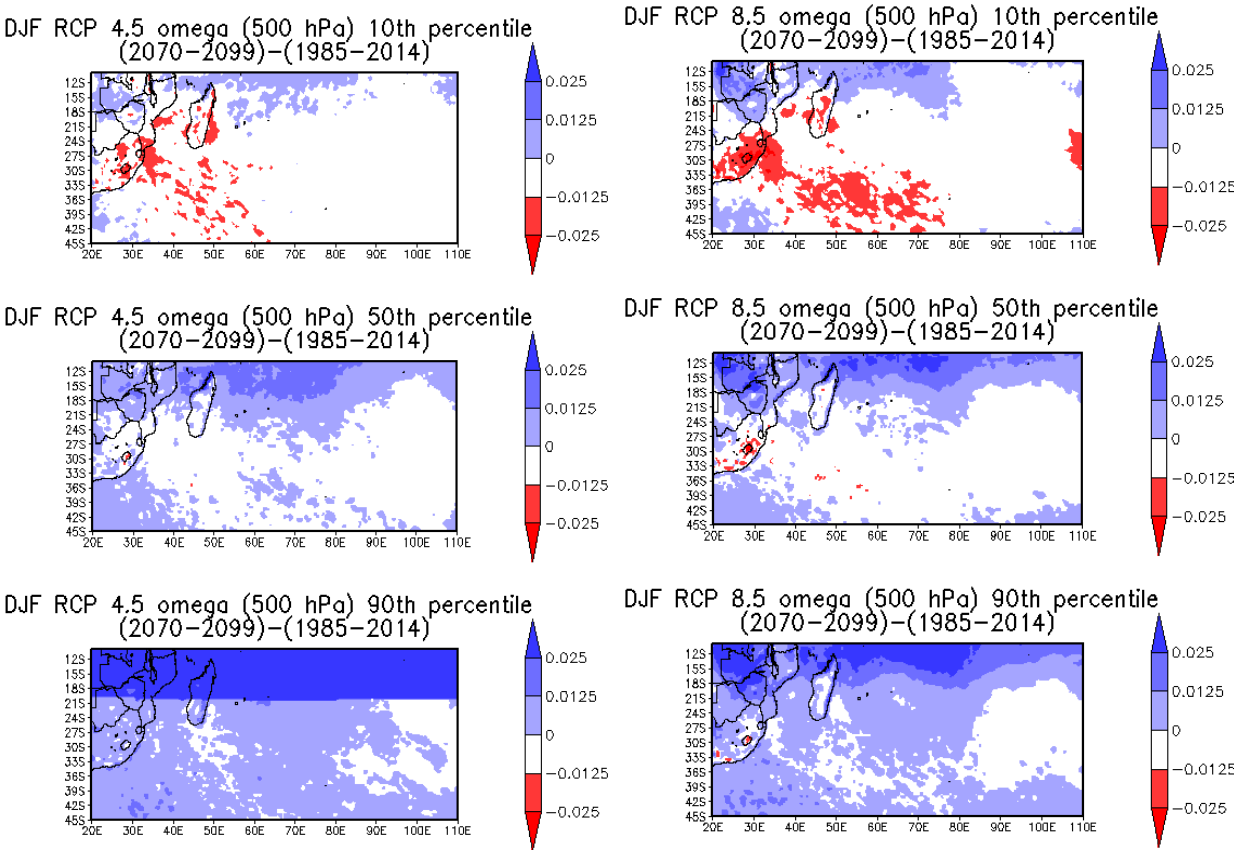

Figure 6.13: Austral summer RCP a) 4.5 and b) 8.5 omega (500 hPa) percentile differences (2070-2099 - 1985-2014) over the SWIO and southern Africa.

a) b)

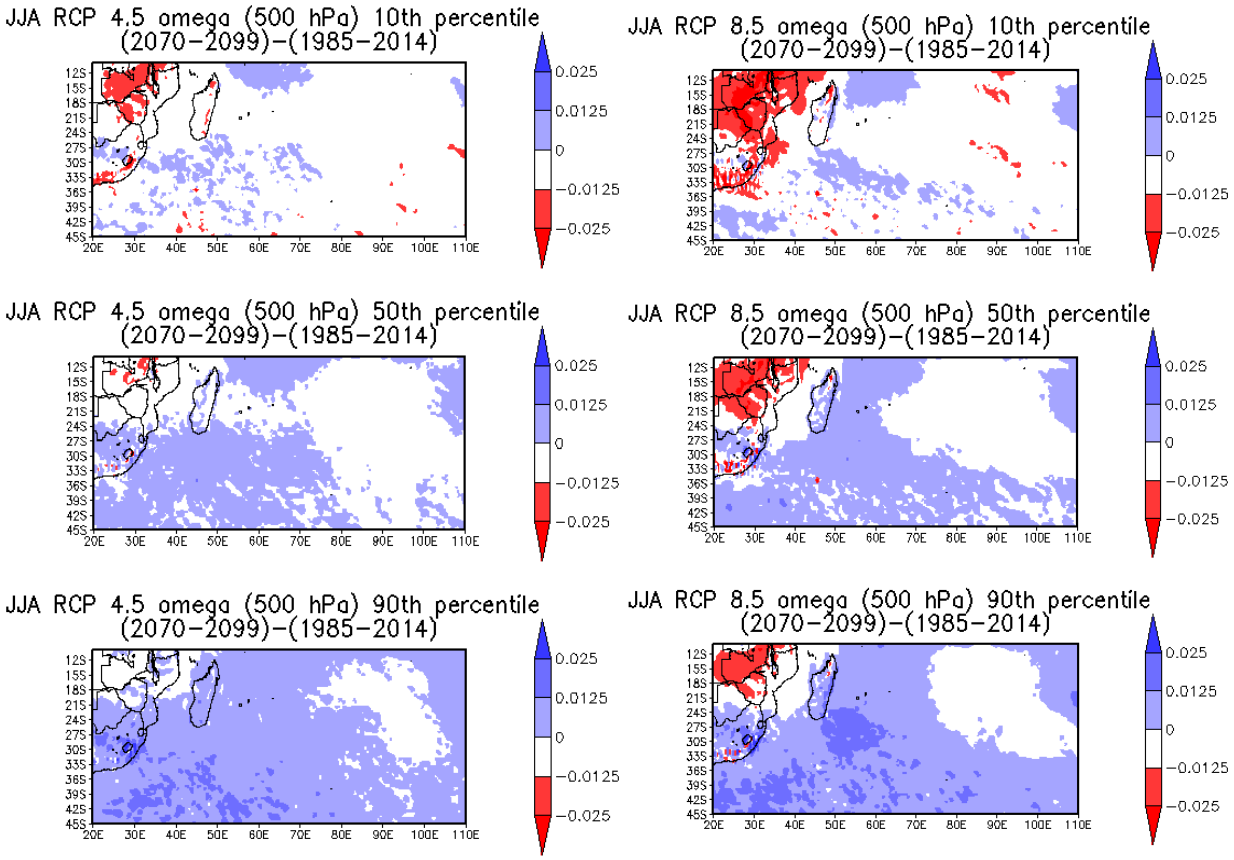

Figure 6.14: Austral winter RCP a) 4.5 and b) 8.5 omega (500 hPa) percentile differences (2070-2099 - 1985-2014) over the SWIO and southern Africa.

6.3.4 Rainfall differences (2070-2099) – (1985-2014)

RCP 4.5 seems to show a projected increase of about 25% rainfall over southeast Africa (Figure 6.15a and b). Seasonal RCP 8.5 indicates a future uncertainty is for projected rainfall over the subcontinent (Figure 6.16a and b). Projections for this uncertainty may be linked to the migration of weather systems resulting from a future expansion of the Mascerene High.

a) b)

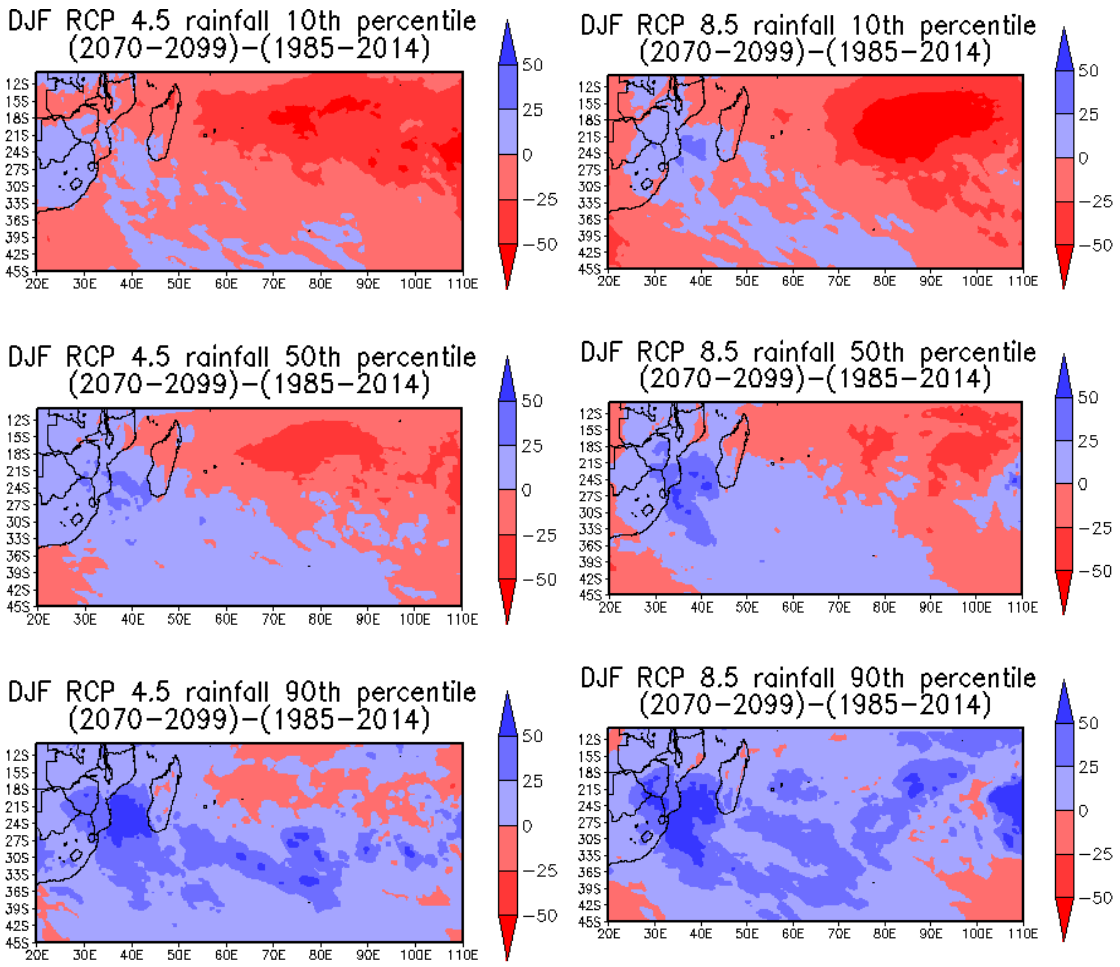

Figure 6.15: Austral summer RCP a) 4.5 and b) 8.5 rainfall percentile differences (2070-2099 - 1985-2014) over the SWIO and southern Africa.

a) b)

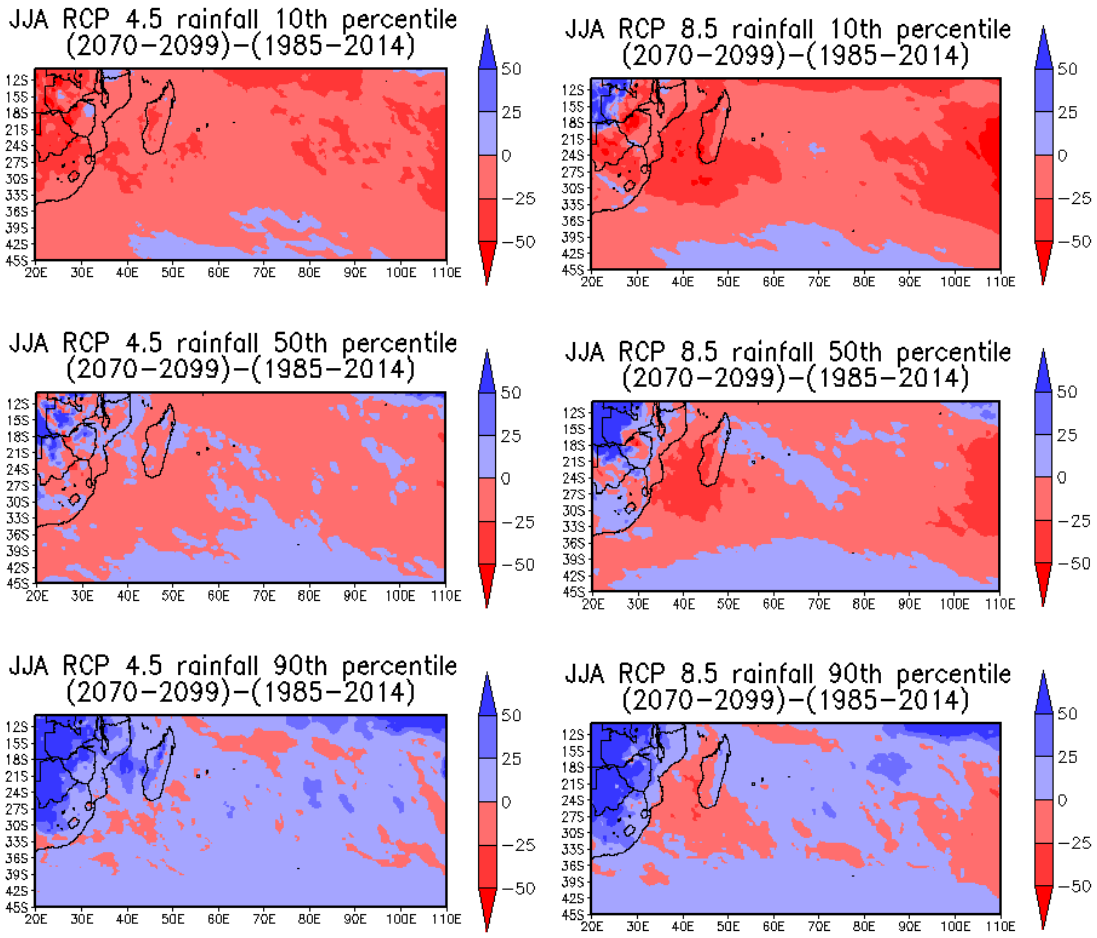

Figure 6.16: Austral winter RCP a) 4.5 and b) 8.5 rainfall percentile differences (2070-2099 - 1985-2014) over the SWIO and southern Africa.

6.3.5 Rainfall and MSLP differences (2070-2099) – (1985-2014)

RCP 4.5 seems to show uncertainty for austral winter rainfall and MSLP future projections (Figure 6.17 and 6.18). Austral summer projections indicating future decrease in rainfall over southern Africa (Figure 6.18a and 6.18a). Austral winter projections show uncertainty for the relationship between rainfall and MSLP (Figure 6.17 and 6.18). This uncertainty is also visible for RCP 8.5 for both seasonal projections, with austral summer 90th percentile (Figure 6.17b) indicating an increase in wetness over north of Madagascar in the future. On average, the projections seem to indicate that there will be decrease in rainfall patterns over southern Africa with an expansion and intensification of the Mascarene High.

a) b)

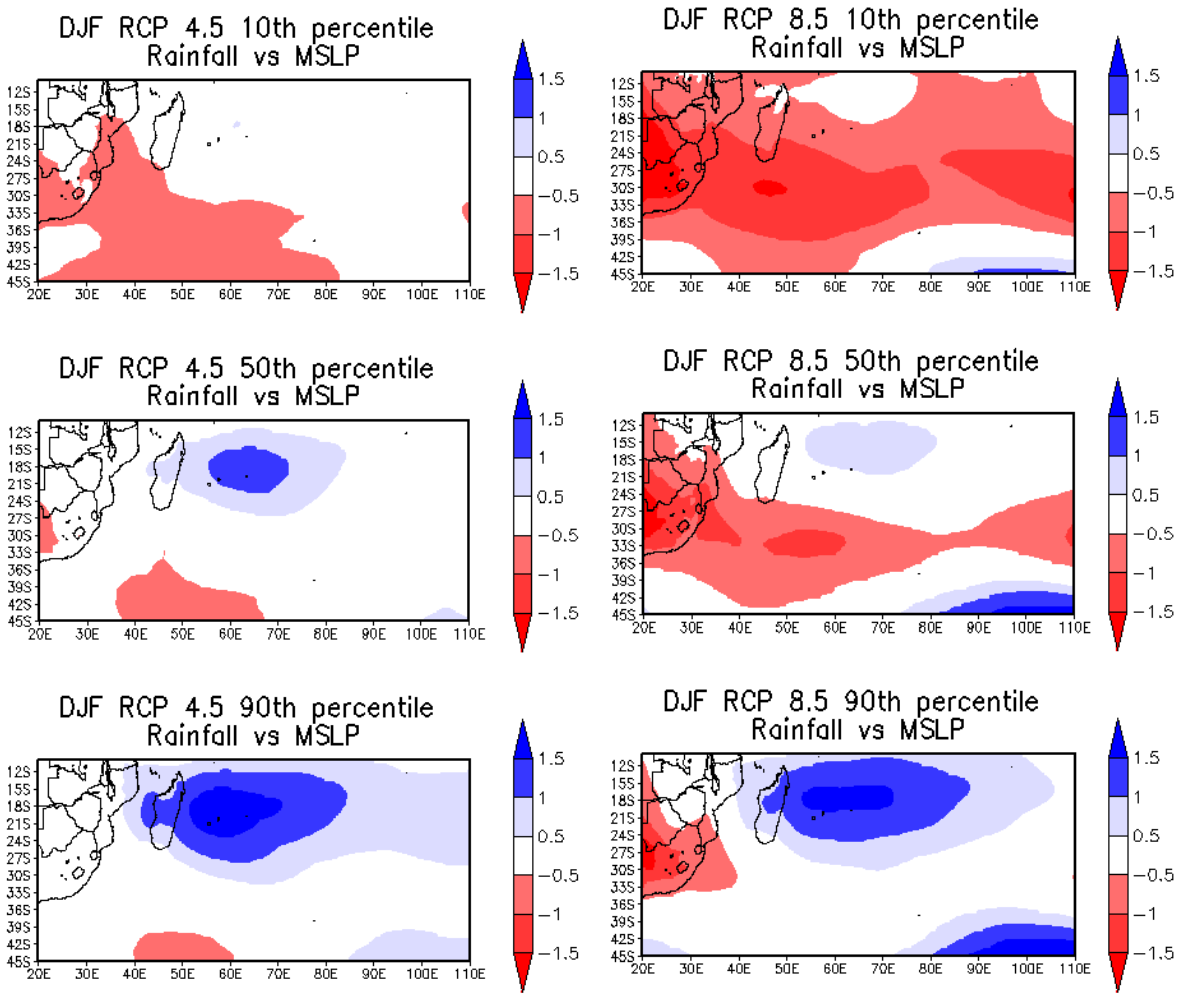

Figure 6.17: Austral summer RCP a) 4.5 and b) 8.5 rainfall vs. MSLP (hPa) percentile differences (2070-2099 - 1985-2014) over the SWIO and southern Africa.

a) b)

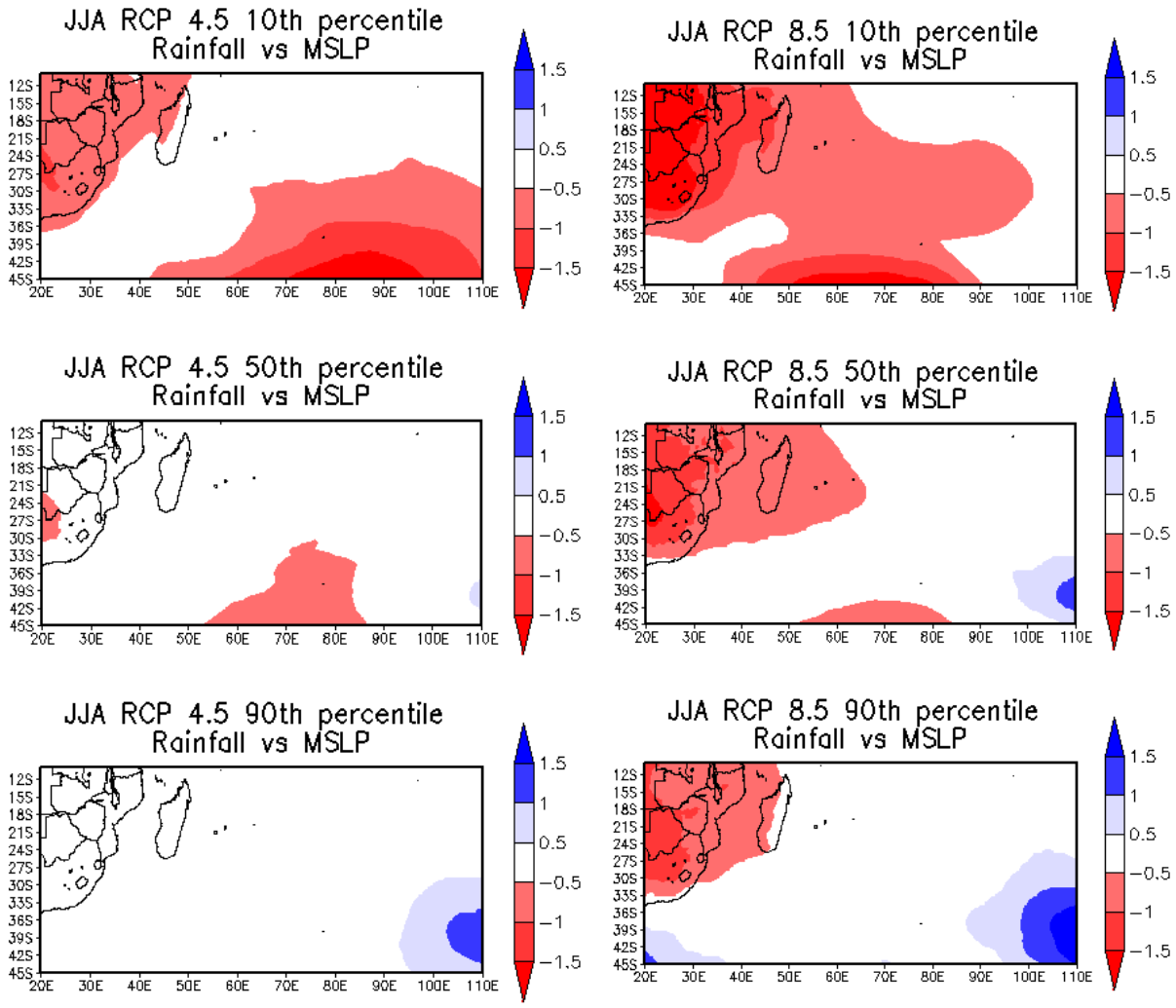

Figure 6.18: Austral winter RCP a) 4.5 and b) 8.5 rainfall vs. MSLP (hPa) percentile differences (2070-2099 - 1985-2014) over the SWIO and southern Africa.

6.3.6 Omega (500 hPa) and MSLP differences (2070-2099) – (1985-2014)

Omega (500 hPa) and MSLP projections consist of a significant relationship, whereby regions of high pressure are associate with subsidence over the South Indian Ocean. This relationship seems to be stronger (weaker) for austral summer (winter) (Figure 6.19 and 6.20). However, RCP 8.5 projections for austral summer seem to indicate that this relationship will migrate eastward in the future and this might be linked to a future expansion of the Mascarene High (Figure 6.19b).

a) b)

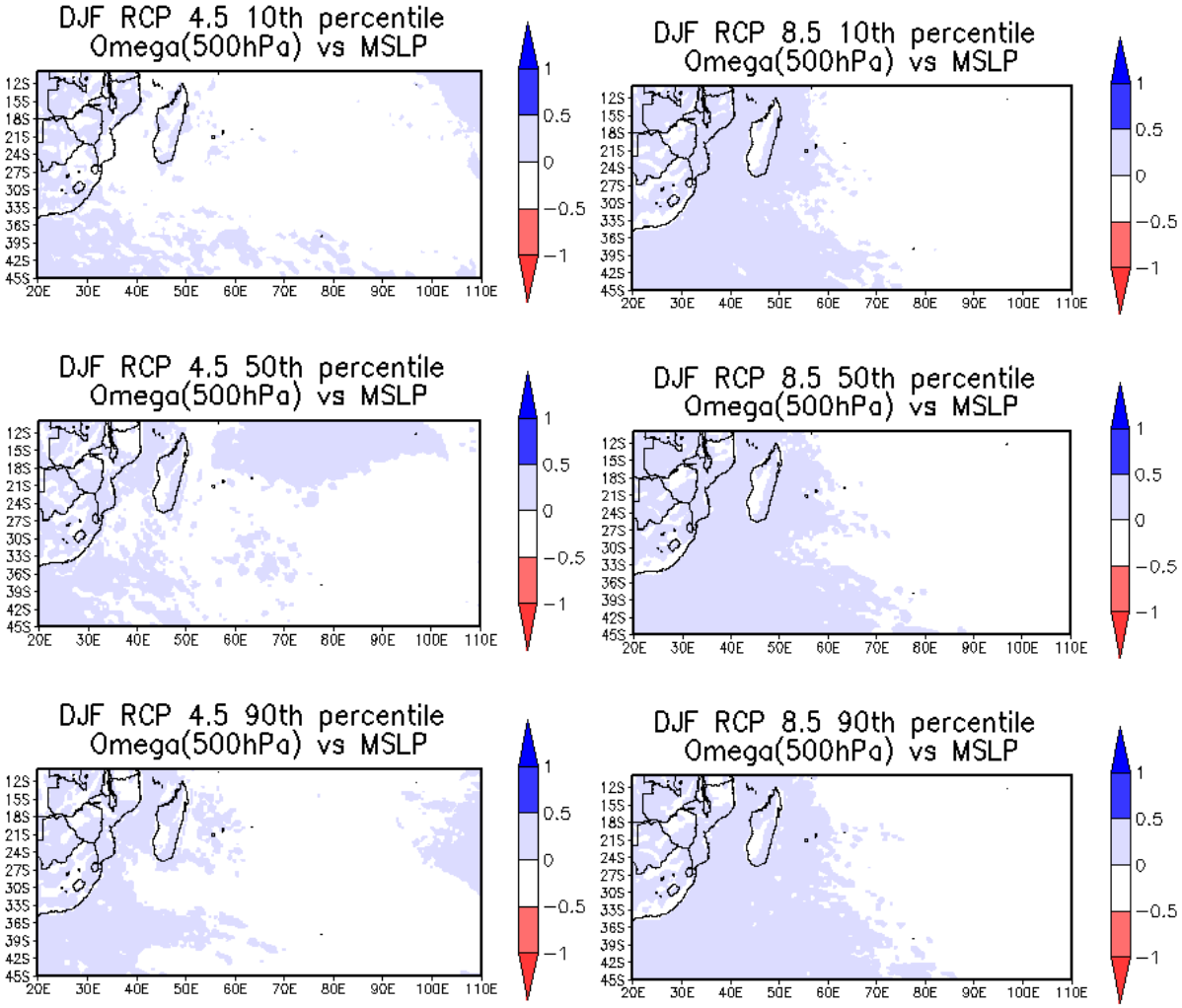

Figure 6.19: Austral summer RCP a) 4.5 and b) 8.5 omega (500 hPa) vs. MSLP (hPa) percentile differences (2070-2099 - 1985-2014) over the SWIO and southern Africa.

a) b)

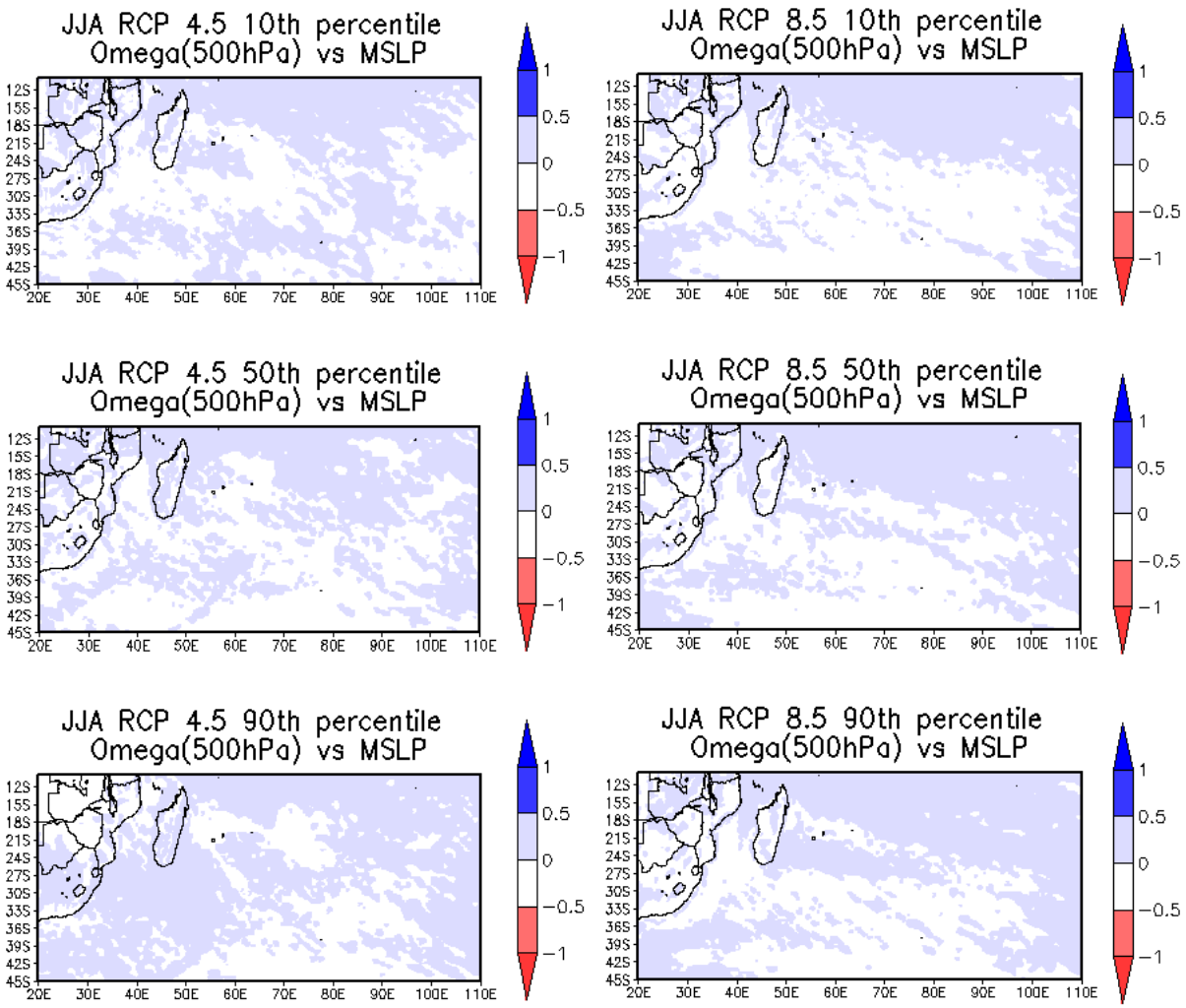

Figure 6.20: Austral winter RCP a) 4.5 and b) 8.5 omega (500 hPa) vs. MSLP (hPa) percentile differences (2070-2099 - 1985-2014) over the SWIO and southern Africa.

6.3.7 Geopotential height (500 hPa) and MSLP differences (2070-2099) – (1985-2014)

The future relationship for geopotential height (500 hPa) and MSLP during austral summer is projected to be strong over the South Indian Ocean in the future for RCP 4.5 (Figure 6.21a). RCP 4.5 austral winter conditions indicate a future decrease when the Mascarene High has been observed to be intense (Figure 6.21b). RCP 8.5 future projection appears to indicate that relationship between geopotential (500 hPa) and MSLP is expected to be strong over vast regions of the South Indian Ocean (Figure 6.21b and 6.22b). These future projections can be linked to changes due to intensification and expansion of the Mascerene High.

a) b)

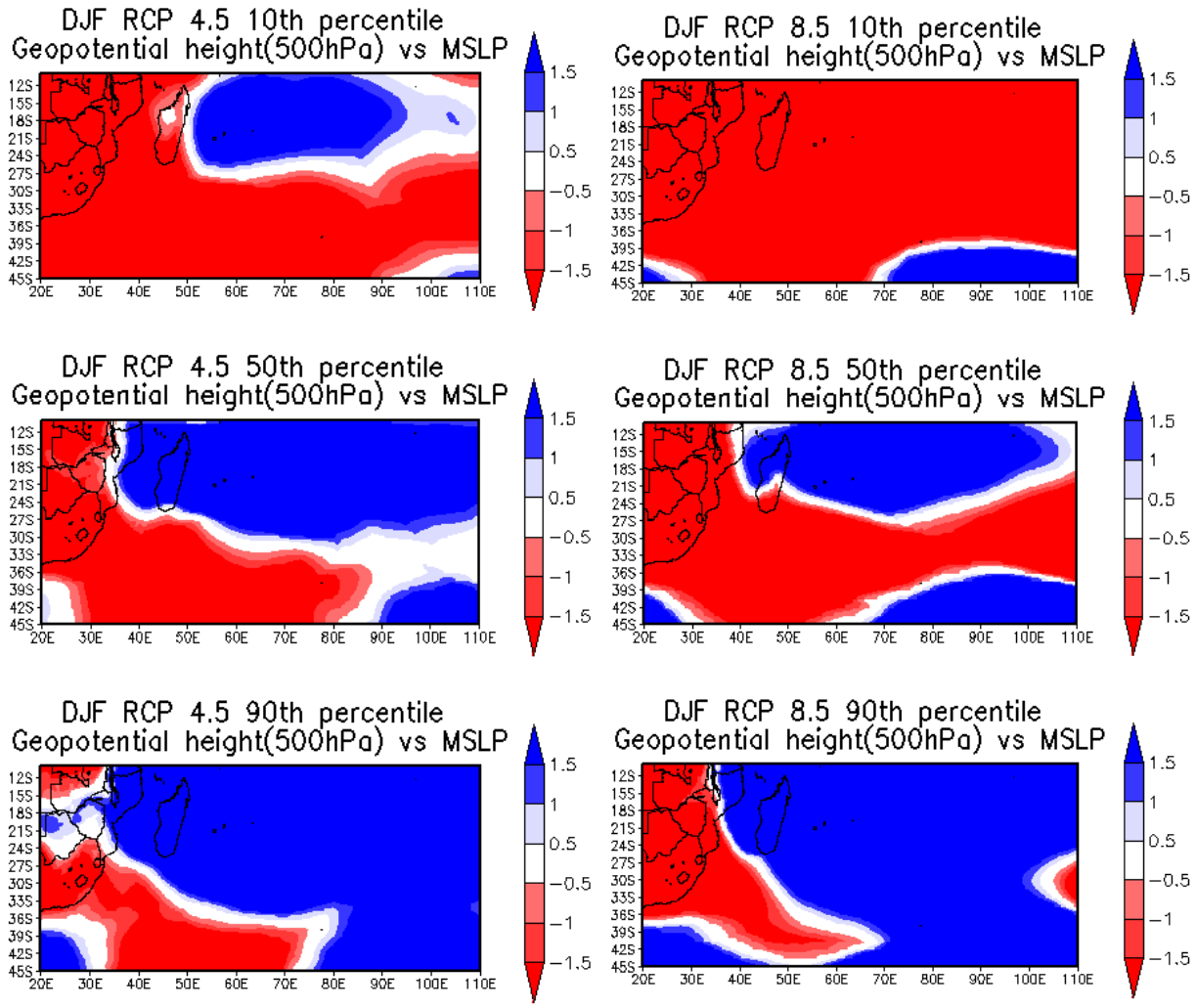

Figure 6.21: Austral summer RCP a) 4.5 and b) 8.5 geopotential height (500 hPa) vs. MSLP (hPa) percentile differences (2070-2099 - 1985-2014) over the SWIO and southern Africa.

a) b)

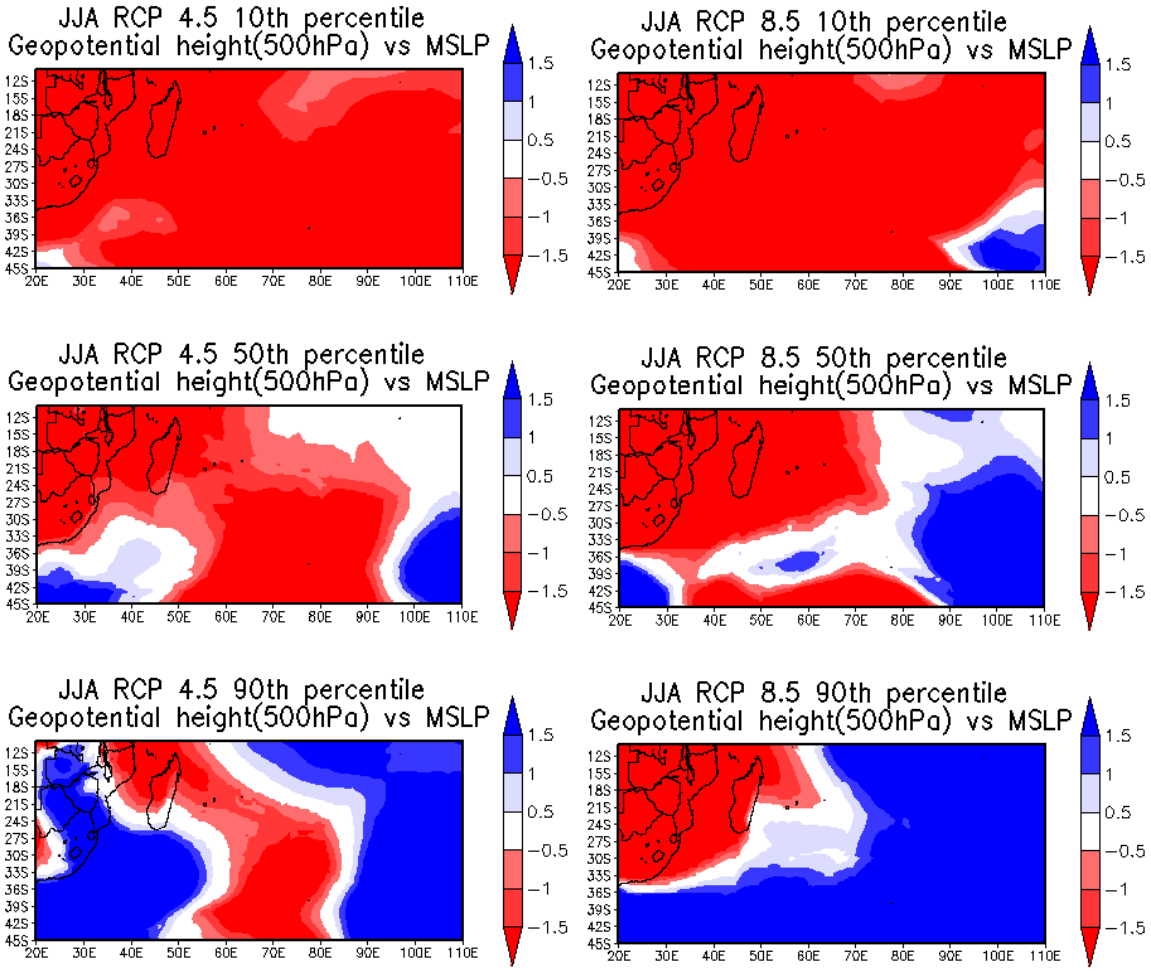

Figure 6.22: Austral winter RCP a) 4.5 and b) 8.5 geopotential height (500 hPa) vs. MSLP (hPa) percentile differences (2070-2099 - 1985-2014) over the SWIO and southern Africa.

6.3.8 Temperature (°C) differences (2070-2099) – (1985-2014)

Most of the climate change studies focus on projected changes in precipitation and temperature. In most of these studies, the precipitation projections are found to be less robust as compared to those of temperature. Projections of the Mascarene high have been found to be less robust, and as a result the temperature projections are also discussed to determine if there are robust projections of any variables in the simulations. The future projections of surface temperature are positive for both RCP4.5 and RCP8.5 and for all the ensemble members. The increase in temperature associated with the low mitigation scenario are as expected associated with higher values of temperature.

a) b)

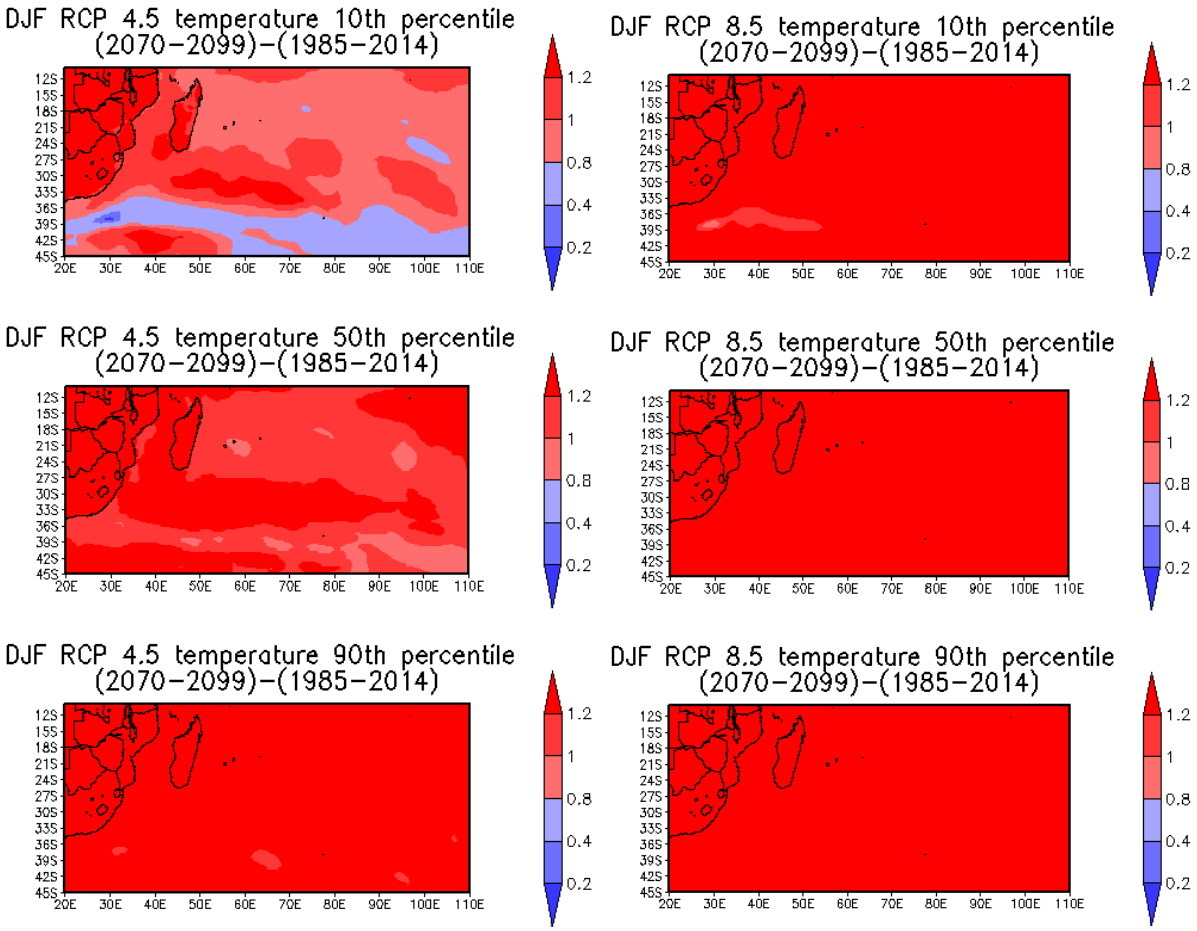

Figure 6.23: Austral summer RCP a) 4.5 and b) 8.5 temperature (°C) percentile differences (2070-2099 - 1985-2014) over the SWIO and southern Africa.

a) b)

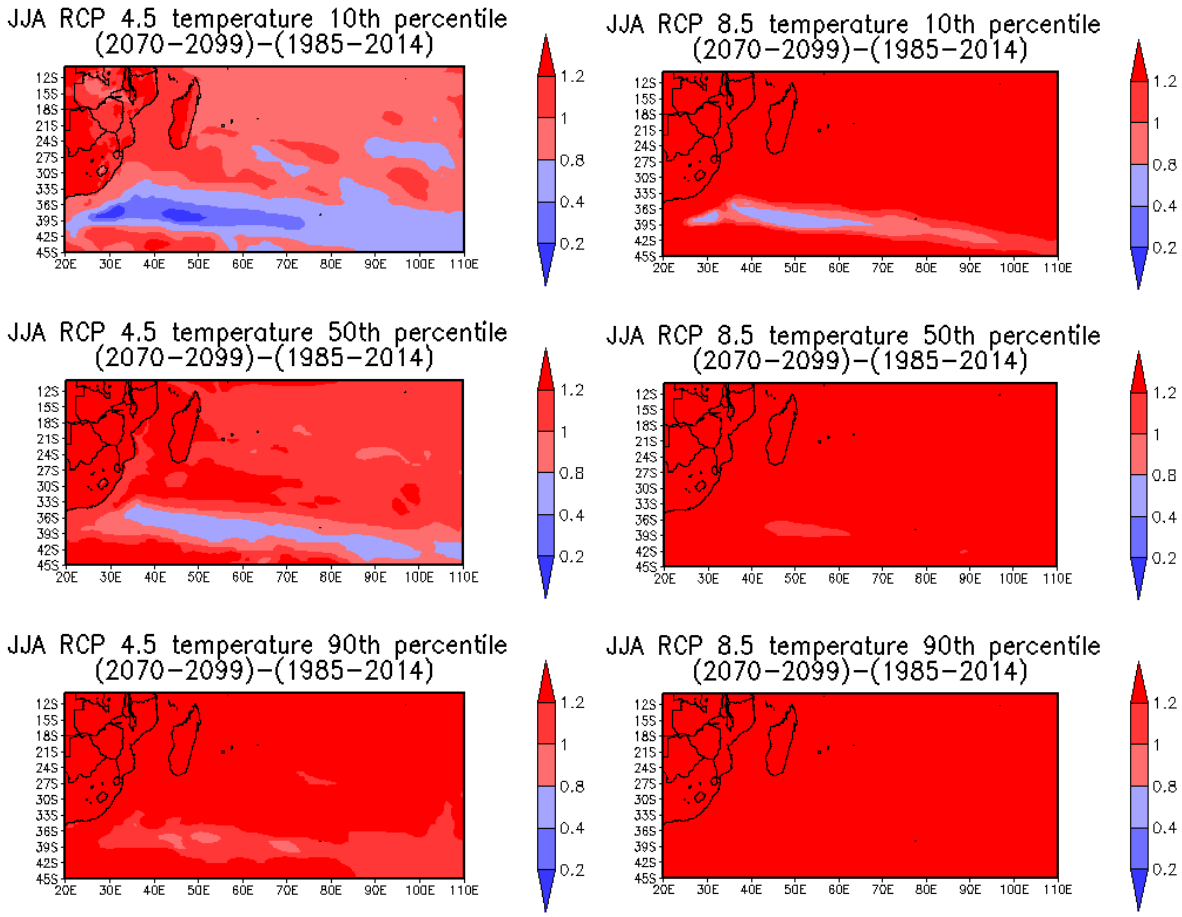

Figure 6.24: Austral winter RCP a) 4.5 and b) 8.5 temperature (°C) percentile differences (2070-2099 - 1985-2014) over the SWIO and southern Africa.

6.4 Summary

In this chapter, future projections in intensity and expansion of the Mascarene High, and other ocean-atmospheric variables have been extensively studied. The projected Mascarene High has been presented as a modulating factor for weather and changes in climate patterns over the South Indian Ocean and southern Africa. Strengthening and intensification of the Mascarene High is primarily influence for changes in weather and climate patterns over the subcontinent. Such strengthening will influence strengthening of easterly trade winds and indicates important future characteristics of the Mascarene High in modulating weather and climate on a regional scale.

This chapter employed CCAM projections and important findings are:-

a) A projected future expansion and intensification of the Mascarene High.

b) Easterly trade winds are projected to intensify.
c) A significant decrease in future rainfall patterns over southern Africa.
d) The expansion of the Mascarene High suggests that TCs tracks and landfalls over southeast Africa may be displaced equatorward.
e) Future Mascarene High intensification may influence poleward migration of cold fronts.
f) Southern regions over Madagascar are projected to have future increase in rainfall.
g) Regions equatorward southeast Africa (15-21°S) may expect an increase in future TCs landfall.
h) A changing climate is projected to influence changes in weather patterns over southern Africa.

The next chapter presents a synthesis of major findings and conclusions of the study. This is done by revisiting each objective in terms of its outcomes, culminating with recommendations and ideas for future research.

CHAPTER 7: DISCUSSION AND CONCLUSIONS

7.1 Introduction

The study focused on the Mascarene High pressure cell over the South Indian Ocean and how it influences weather and climate over southern Africa. Southern Africa is largely semi-arid and receives most of its rainfall during austral summer, with the Mascarene High having a vital role in the mean (anomalous) regional weather and climate patterns. In some cases, the subcontinent is also vulnerable to anomalous weather and climate phenomena, such as floods and droughts.

The study has examined Mascarene High characteristics, sensitivity of the ocean-atmospheric response over southern Africa and future projections (2071-2100) of climate at multidecadal time-scales using the Conformal-Cubic Atmospheric Model (CCAM). Spatio-temporal variability and climatology of the Mascarene High in the South Indian Ocean for the present-day climate (1985-2014) at intraseasonal, seasonal, interannual time-scales was also presented.

This chapter provides a discussion and synthesis of key major findings of this work, mainly from chapter 4-6. Recommendations and implications for future research related to the Mascarene High pressure cell are also offered.

7.2 Discussion and synthesis of key findings

7.2.1 Present climate of the Mascarene High

The Mascarene High centre migrates north-south (28-37°S) and west-east (60-87°E) locations over the South Indian Ocean. Major influence for displacements is due to migration of the Inter-tropical Convergence Zone (ITCZ), South Indian Convergence Zone (SICZ) and Indian Ocean warm sea surface temperatures (SSTs) fluctuations. Such seasonal migrations play a major role in moisture transport and rainfall variability over southern Africa. During austral summer, Mascarene High pressure cell location largely influences transport of moisture flux towards the subcontinent. Mean location of the Mascarene High has been defined as the region from 25-35°S and 40-110°E. This region was used for identification, analysis of migration, movement and Mascarene High blocking.

7.2.2 Interannual variability and ocean-atmosphere interactions

The Mascarene High was found to be intense (>1023 hPa) during austral winter, when it has migrated equatorward. Warm Indian Ocean SSTs, strongly influence Mascarene High location as the Mascarene High tends to locate over warm SSTs. El Niño Southern Oscillation (ENSO) phases were also found to have major influences on circulation and direction of Indian Ocean trade winds. The occurrence of El Niño in the equatorial Pacific Ocean largely influences anomalous west-east flow of trade winds, transporting moisture away from the subcontinent and this induces drought occurrences over southern Africa (Tyson and Preston-Whyte, 2000). The Indian Ocean Dipole (IOD) was also found to be inversely proportional to the Mascarene High (Figure 4.22). Subtropical Indian Ocean Dipole (SIOD) phases are directly proportional to the Mascarene High (Figure 4.24). These findings emphasize the important role of ocean-atmosphere interactions.

7.2.3 Blocking and anomalous weather over southern Africa

The study investigated event scale anomalous conditions over southern Africa during Mascarene High blocking. Mascarene High blocking events cause slow west-east movements of the westerly wave weather systems, inducing anomalous weather over southern Africa (Molekwa, 2013). Spatial characteristics of Mascarene High blocking was found to consist of spatio-temporal variation. This implies that each Mascarene High blocking event has unique characteristics. The study also found that Mascarene High blocking events can last for a period of three or more days. Mascarene High blocking events investigated resulted to heavy rainfall over parts of southern Africa and this occurrence proved to be frequent during austral summer. This occurrence influences tropical cyclone (TC) tracks during La Niña, mid-tropospheric cut-off lows and elongated cloud bands joining to a cold front. These anomalous occurrences over southern Africa all result from the quasi-stationary west-east movement of Mascarene High blocking.

Mascarene High blocking triggers a stagnation in the propagation of the westerly wave. This can enhance the formation of a cut-off low (Molekwa, 2013), which spins independently from the westerly wave causing additional blocking over southern Africa. A fully developed cut-off low circulates independently causing additional blocking from Mascarene High blocking. Cut-off low blocking is another form of quasi-stationary west-east tracking, causing unsettled weather over the subcontinent for an extended period in the process. It is very important to outline that Mascarene High blocking plays a major role on inducing anomalous rainfall over southern Africa. Lastly, there is vast significance in studying the causes of Mascarene High blocking in the future.

7.2.4 Mascarene High future projections

In this study, CCAM RCP 4.5 and 8.5 projections using 6 ensemble members are comparable to observational trends and patterns (Engelbrecht *et al.* 2009) for Mascarene High influencing weather and climate over southern Africa. Mascarene High projections show a future expansion and intensification of the weather system for the period 2070-2099. This also indicates future changes in weather and climate patterns over southern Africa. The projected Mascarene High expansion will play a vital role in equatorward migration of landfalling TCs and poleward migration of cold fronts in the future. Future easterly trade winds from the easterly wave have also been projected to increase in magnitude. These assimilated changes may cause a further inland penetration of landfalling tropical revolving systems over southern Africa.

7.3 Conclusions

While some results are in agreement with findings of earlier studies, the findings in this study strengthen earlier studies with some new approaches to attain the results. The future findings may bring some more new knowledge on the Mascarene High pressure cell.

A clear distinction is that this study presented future projections of the Mascarene High and weather variability over southern Africa. It is also apparent that climate change may have evolving influences on future Mascarene High mean circulations as discussed by Engelbrecht *et al.* (2009). The projected changes suggest that it may play a major role in driving temperature and rainfall changes over southern Africa. These projected changes indicate how southern Africa communities may need to adapt and strategize for future changes in weather and climate over this region. The study motivates for a consideration of other climate variation occurrences besides ENSO, IOD and SIOD that influence the Mascarene High and weather variability over southern Africa.

7.4 Implications and future work

The ability of southern African countries to adapt to climate stresses tends to be hindered by widespread poverty, political instability and civil war. These are major issues, as a number of climate change models project that some regions will experience an increase in temperature and a general decrease in rainfall amounts. This indicates that there will be an increase in climate and weather related challenges in the future. A better consideration of physical processes that influence temperature and rainfall variability, changes and trends over southern Africa such as the Mascarene High may prove to be very useful in adapting to projected future climate changes.

This may also improve the reliability of forecasting anomalous events caused by Mascarene High blocking, which could lead to positive implications for quality of life, economic well-being and growth over southern Africa.

The study gave a detailed mean monthly and seasonal location of the Mascarene High and this was presented by mapping and analysing ocean-atmospheric interactions that influence the distribution, development and movement of the Mascarene High. At an event scale the study analysed the influence of the Mascarene High blocking over southern Africa and how this contributed to anomalous weather events. While seasonal patterns of the Mascarene High have been studied, the causes of Mascarene High blocking are still not conclusive and requires further research. The study also employed CCAM to illustrate future projections of the Mascarene High in a changing climate.

At regional scales, future projections for weather and climate were mainly based on dynamic model applications which use laws of physics applied to the earth system with a set of complex partial differential equations. Future global climate change projections were based on climate general circulation models (CGCMs) that simulate coupled ocean, atmosphere and land-surface processes. Dynamic regional climate models (RCMs) were also applied to obtain such detailed projections of the climate in southern Africa. They were applied at very high-resolution for regions of interest. This reasoning and understanding allowed for future projections using CCAM.

The ocean-atmosphere interactions in relations to the Mascarene High have been investigated and discussed in chapter 4. Influences of the Southern Annular Mode (SAM) and Quasi-Biennial Oscillation (QBO) still need to be investigated further in understanding in relation to the Mascarene High. The Mascarene High is an important weather system for southern Africa weather and climatology patterns. Lastly, the following research questions may be considered for future work:

- To what extent are blocking events over the SWIO predictable?
- What role does the Southern Annual Mode (SAM) and Quasi-Biennial Oscillation (QBO) play on the intensity and expansion of the Mascarene High?
- How will the expansion and intensification of the Mascarene High influence the SIOD?

REFERENCES

Anderson, R.C. and Keefer, D.R. 1975. Observation of the Temperature and Pressure Changes during the 30 June 1973 Solar Eclipse. *J. Atmos. Sci.,* 32, 228-231.

Arkin, P.A. and Meisner, B.N. 1987. The relationship between large scale convective rainfall and cold cloud over the Western Hemisphere during 1982-1984. *Mon. Wea. Rev., 115*, 51-74.

Ash, K.D. and Matyas, C.J. 2012. The influences of ENSO and the subtropical Indian Ocean. *Int. J. Climatol.*, 32, 41-56.

Bell, G.D. and Bosart, L.F. 1989. A 15-Year Climatology of Northern Hemisphere 500 mb Closed Cyclone and Anticyclone Centres. *Mon. Wea. Rev., 117*, 2142-2163.

Behera, S.K. and Salvekar P. S. and Yamagata, T. 2000. Simulation of interannual SST variability in the tropical Indian Ocean, *J. Climate.,* 13, 3487-3499.

Behera, S.K. and Yamagata, T. 2001. Subtropical SST dipole events in the southern Indian Ocean. *Geo. Research. Let.,* 28, 327-330.

Bengtsson, L. and Shukla, J. 1988: Integration of space and in situ observations to study global climate change. *Bull. Am. Meteorol. Soc.,* 69, 1130–1143.

Bjerknes, J. 1969. Atmospheric teleconnections from the equatorial pacfiic 1. *Mon. Wea. Rev.,* 97, 163-172.

Bollen, J, Van de Sompel, H., Hagberg A. and Chute, R. 2009. A Principal Component Analysis of 39 Scientific Impact Measures. PLoS ONE., 4, e6022. doi:10.1371/journal.pone.0006022

Chang-Seng, D. S. and Jury, M.R. 2010. Tropical Cyclones of the Southwest Indian Ocean. Part 2: structure and impacts at the event scale. *Meteor. Atmos. Phys.*, 106, 163-178.

Chikoore, H., Vermeulen J, H. and Jury, M.R. 2015. Tropical Cyclones in the Mozambique Channel: January-March 2012. *Nat Hazards.,* DOI 10.1007/s11069-015-16-91-0.

Chu, P.S. 2004. ENSO and tropical cyclone activity. Hurricanes and Typhoons: Past, Present, and Future. Murnane RJ, Liu K-B. (eds). Columbia University Press: New York. 11, 297-322.

Cook, K.H. 1998. On the response of the Southern Hemisphere to ENSO. Proc. 23rd Climate Diagnostics and Prediction Workshop, Miami, FL, *Bull. Am. Meteorol. Soc.,* 37, 323–326.

Cook, K.H. 2000. The South Indian convergence zone and interannual rainfall variability over southern Africa. *J. Climate.,* 13, 3789–3804,.

Davis, C.A. 2010. Simulations of SubTropical Cyclones in a Baroclinic Channel Model. *J. Atmos. Sci., 67*: 2871-2891.

Davis, R.E., Hayden, B. P., Gay, D. A., Phillips, W. L. and Jones, G.V. 1997. The North Atlantic Subtropical Anticyclone. *J. Climate.,*10, 728-744.

Diab, R., Preston-Whyte, R. and Washington, R. 1991. Distribution of rainfall by synoptic type over Natal, South Africa. *Int. J. Climatol.*,11, 877–888.

Engelbrecht, F. A., McGregor, J.L. and Engelbrecht, C.J. 2009. Dynamics of the Conformal-Cubic Atmospheric Model projected climate-change signal over southern Africa. *Int. J. Climatol.,* 29, 1013–1033.

Engelbrecht, F. A., Landman, W.A., Engelbrecht, C.J., Landman, S., Bopape, M.M., Roux, B., McGregor, J.L. and Thatcher, M. 2011: Multi-scale climate modelling over southern Africa using a variable-resolution global model. *Water SA.,* 37, 647–658.

Elliott, R. D. and Smith, T.B. 1949. A study of the effects of large blocking anticyclones on the general circulation in the Northern Hemisphere westerlies. *J. Appl. Meteorol.,* 6, 67-85.

Finley, J. and Raphael, M. 2007. The relationship between El Niño and the duration and frequency of the Santa Ana winds of Southern California. *Prof. Geogr.,* 59, 184–192.

Frederiksen, J. and Frederiksen, C. 1993b. Southern Hemisphere storm tracks, blocking and low. *J. Atmos. Sci.,* 50: 3148-3168.

Goddard, L. and Graham, N.E. 1999. Importance of the Indian Ocean for simulating rainfall anomalies over eastern and southern Africa. *J. Geophys. Res.,* 104, doi: 10.1029/1999JD900326. ISSN: 0148-0227.

Gong, D.Y. and Ho, C.H. 2002. The Siberian High and climate change over middle to high latitude Asia, *Theor. Appl. Climatol.*, 12, 72, 1-9.

Gray, W.M. and Sheaffer, J.D. 1991. El Niño and QBO influences on tropical cyclone activity. Teleconnections linking worldwide climate anomalies. Glantz MH, Katz RW, Nicholls N. (eds). 535. Cambridge University Press: Cambridge, UK.

Greenhut, G. K. 1977. A new criterion for locating the subtropical high in West Africa. *J. Appl. Meteorol.,*16, 727-734.

Halpert, M. S. and Ropelewski, C.F. 1992. Surface temperature patterns associated with the Southern Oscillation. *J. Climate.*, 5, 577–593.

Harangozo, S. and Harrison, M. 1983. On the use of synoptic data indicating the presence of cloud bands over southern Africa. *S. Afr. J. Sci.,*79, 413.

Hart, N.C., Reason, C.J. and Fauchereau, N. 2013. Cloud bands over southern Africa: seasonality, contribution to rainfall variability and modulation by the MJO. *Clim Dyn.,* DOI 10.1007/s00382-012-1589-4.

Hastenrath, S. and Polzin, D. 2004. Dynamics of the surface wind field over the equatorial Indian Ocean. *Q. J. Roy. Meteorol. Soc.,* 130, 503– 517.

Hastings, D.A. and Paula, K.D. 1999. Global Land One-kilometer Base Elevation (GLOBE) Digital Elevation Model, Documentation, Key to Geophysical Records Documentation (KGRD) 34. National Oceanic and Atmospheric Administration, National Geophysical Data Centre, 1: 1-38.

Hayes, M.J., Svoboda, M.D., Wilhite, D.A. and Vanyarkho, O.V. 1999. Monitoring the 1996 drought using the Standardized Precipitation Index. *Bull. Am. Meteorol. Soc.,* 80, 429–438.

Hoskins, B.J. 1996. On the existence and strength of the summer subtropical. *Bull. Am. Meteorol. Soc.,*77: 1287-1292.

Huang, S. and Tang, M. 1987. On the structure of the summer monsoon regime of East Asia. *J. Meteo. Res.,* 13, 1–14.

Huang, S. and Tang, M. 1989. Medium-range oscillation and teleconnections of the atmospheric circulation systems over the Northwest Pacific and South Indian Ocean. *J. Meteo. Res.,* 3, 571–581.

Huang, B. and Shukla, J. 2006. Interannual SST variability in the subtropical and extratropical southern ocean. *COLA Tech Rep.,* 223, 20pp.

Huffman, G.J., Adler, R.F., Bolvin, D.T. and Gu, G. 2009. Improving the Global Precipitation Record: GPCP Version 2.1. *Geophys. Res. Lett.,* 36, L17808, doi: 10.1029/2009GL040000.

Hurrel, J.W. and Trenberth, K.E. 1992. An evaluation of monthly mean MSU andECMWF Global atmospheric temperatures for monitoring climate. *J. Climate.,* 5, 1424-1440.

Jury, M.R. and Mpeta, E.J. 2005. The annual cycle of African climate and its variability. *Water SA.* 30, ISSN 0378-4738.

Katzfey, J., Chattopadhyay, M., McGregor, J. L., Nguyen, K. and Thatcher, M. 2011. The added value of dynamical downscaling. *Int. Congress on Modelling and Simulation.*, 18, 2747-2753.

Kalnay, E. 1996. The NCEP/NCAR 40-Year Reanalysis Project. *Bull. Am. Meteorol. Soc.,* 77, 437-471.

Kanamitsu, M., Ebisuzaki, W., Woollen, J., Yang, S.K., Hnilo, J.J., Fiorino, M. and Potter, G.L. 2002. NCEP-DOE AMIP-II Reanalysis (R-2). *Bull. Am. Meteorol. Soc.,* 83, 1631-1643.

Kruger, A.C. 1999. The influence of the decadal-scale variability of summer rainfall on the impact of El Niño and La Niña events in south Africa. *Int. J. Climatol.*, 19, 59-68.

Landsea, C.W. 2000. El Niño-Southern Oscillation and the seasonal predictability of tropical cyclones. El Niño: Impacts of multiscale variability on natural ecosystems and society. Diaz HF, Markgraf V, Eds., 11, 149–181.

Li, W., Li, L., Ting, M., Deng, Y., Kushnir, Y., Liu, Y. and Zhang, P. 2013. Intensification of the Southern Hemisphere summertime subtropical anticyclones in a warming climate. *Geophys. Res. Lett.*, 40, 5959-5964.

Li, L., Li, W. and Kushnir, Y. 2011. Variation of the North Atlantic subtropical high western ridge. *Clim. Dynam.*, DOI 10.1007/s00382-011-1214-y.

Lin, B.D. 1983. Behavior of Stationary Waves and the Summer Monsoon. *J. Atmos. Sci.,* 40, 1163-1177.

Lindzen, R.S. and Hou, A.Y. 1988. Hadley circulations for zonally averaged heating centred off the equator. *J. Atmos. Sci.,* 45, 16–2427.

Liu, Y. and Wu, G. 2004. Progress in the study on the formation of the summertime subtropical anticyclone. *Adv. Atmos. Sci.,* 21, 322–342.

Malherbe, J., Engelbrecht, F.A. and Landman, W.A. 2011. Tropical sysytems from the southwest Indian Ocean making landfall over the Limpopo River Basin, southern Africa: a histrorical perspective. *Int. J. Climatol.,* 31, DOI: 10.1002/joc.2320.

Mason, S.J. 1995. Sea-surface temperature-South African rainfall associations, 1910-1989. *Int. J. Climatol.*, 15, 119-135.

Manatsa, D. and Behera, S.K. 2014. On the major shifts in the IOD during the last century, the role of the Mascarene High displacements. *Int. J. Climatol.*, 34, 2033-2046.

Manatsa, D., Morioka, Y., Behera S. K., Matarira, C.H., and Yamagata, T. 2014. Impact of Mascarene High variability on the East African 'short rains'. *Clim Dyn*., 42, 1259–1274. DOI 10.1007/s00382-013-1848-z.

Misiyaka, T. and Nakamura, H. 2010. Stucture and mechanisms of the Southern Hemisphere summertime subtropical anticyclones. *J. Climate.,* 23, 2115-2130.

Molekwa, S. 2013. Cut-off lows over South Africa and their contribution to the total rainfall of the Eastern Cape Province. *Masters dissertation, University of Pretoria*, 94pp.

Morioka, Y., T. Tozuka, and T. Yamagata, 2013: How is the Indian Ocean subtropical dipole excited? *Clim Dyn.,* doi:10.1007/s00382-012-1584-9.

Morioka, Y., Takaya, K., Behera, S.K. and Masumoto, Y. 2015: Local SST impacts on the summertime Mascarene high variability. *J. Climate.,* 28, 678–694, doi:10.1175/JCLI-D-14-00133.1.

Mulenga, H.M. 1998. Southern African anomalies, summer rainfall and the Angola Low. *PhD thesis*, *University of Cape Town*, 231pp.

Nicholson, S.E. and Entekhabi, D 1987: Rainfall variability in equatorial and southern Africa: Relationships with sea surface temperatures along the southwestern coast of Africa. *J. Climate Appl. Meteor.*, 26, 561–578.

Ohishi, S., Sugimoto, S., Hanawa, K. 2015. Zonal movement of the Mascarene High in austral summer. *Clim Dyn.,* 45,1739–1745. doi:10.1007/s00382-014-2427-7.

Palmen, E. 1948. On the formation and structure of tropical hurricanes. *J. Geophys. Res.,* 3, 26-38.

Palmer, E. 1949. Origin and structure of high-level cyclones south of the maximum westerlies. *Tellus.,* 1, 22-31.

Quan, X., Hoerling, M. P., Diaz, H. F. and Xue, T. 2014. How fast are the tropics expanding? *J. Climate.,* 27, 1999-2013.

Rayner, N.A., Parker, D. E., Horton, E. B., Folland, C. K., Alexander, L. V., and Rowell, D.P. 2003. Global analyses of sea surface temperature, sea ice, and night marine air temperature since the late nineteenth century. *J. Geophys. Res., 108*, doi:10.1029/2002JD002670.

Reason, C.J.C. 2001. Subtropical Indian Ocean SST dipole events and southern African rainfall. *Geophys. Res. Lett.*, 28, 11, 2225-2227.

Reason, C.J.C. and Keibel, A 2004. Tropical cyclone Eline and its unusual penentration and impacts over the southern African mainland. *J. Climatol.*, 19, 789–805.

Reason, C.J.C.. 2007. Tropical cyclone Dera, the unusual 2000/01 tropical cyclone season in the southwest Indian Ocean and associated rainfall anomalies over southern Africa. *Meteor. Atmos. Phys.*, 97, 181–188.

Richter, I. and Mechoso, C.R. 2008. What determines the position and intensity of the South Atlantic Anticyclone in. *J. Climate.,* 21, 214-229.

Rocha, A. and Simmonds, I. 1997: Interannual variability of south-eastern African summer rainfall. Part II: Modelling the impact of sea-surface temperatures on rainfall and circulation. *Int. J. Climatol.*, 17, 267-290.

Rodwell, M. J. and Hoskins, B.J. 1996. Monsoons and the dynamics of deserts. *Q. J. Roy. Meteorol. Soc.,* 122, 1385-1404.

Rodwell, M. J. and Hoskins, B.J. 2001. Subtropical anticyclones and summer monsoons. *J. Climate.,* 14, 3192-3211.

Rogers, J.C. and Rohli, R. 1991. Florida citrus freezes and polar anticyclones in the Great Plains. *J. Climate.,* 4, 1103-1113.

Rohli, R. 1995. The effect of winter anticyclone tracks on surface weather conditions in New Orleans, Louisiana. *National Weather Digest,* 19, 2-8.

Sanders, R. A. 1953. Blocking Anticyclones over the eastern north Atlantic Ocean and western Europe. *Mon. Wea. Rev.,* 11, 67-73.

Seager, R., Murtugudde, R., Naik, N., Clement, A., Gordon, N., and Miller, J. 2003. Air-Sea Interaction and the seasonal cycle of the subtropical anticyclones. *J. Climate.,* 16, 1948-1966.

Shea, D. 2015. Empirical Orthogonal Function (EOF) Analysis and Rotated EOF Analysis. *https://climatedataguide.ucar.edu/climate-data-tools-and-analysis/empirical-orthogonal-function-eof-analysis-and-rotated-eof-analysis*. accessed on 3/19/2015.

Simmons, A. J. and Hoskins, B.J. 1978. The life cycles of some nonlinear baroclinic waves. *J. Atmos. Sci.,* 35, 414–432.

Sinclair, M.R. 1996. A climatology of subtropical anticyclones and blocking for the Southern Hemisphere. *Mon. Wea. Rev.,* 124, 245-263.

Singleton, A.T. and Reason, C.J.C. 2007a. A numerical model study of an intense cut-off low pressure system over South Africa. *Mon. Wea. Rev.,* 135, 1128-1150.

Smith, A. 1985. Studies of the effects of cold fronts during rainy season weather in Zimbabwe. *Weather.,* 40, 198–203.

Sovara, M.V. 2014. Influence of the Indian Ocean Subtropical Dipole on the Agulhas Current. MSc thesis, University of Cape Town*.,* 84pp.

Sreenivasan, B. and Davidson, P. 2008. On the formation of cyclones and anticyclones in a rotating fluid. *AIP.,* DOI: 10.1063/1.2966400.

Sun, D., Zhou, T., and Xue, F. 2014. Mascarene High, Australian High, and Antarctic Oscillation Simulated by FGOALS-s2. In *Flexible Global Ocean-Atmosphere-Land System Model*., 21, 153-160.

Suzuki, R., Behera, S.K., Lizuka, S. and Yamagata, T. 2004. Indian Ocean subtropical dipole simulated using a coupled general circulation model. *J. Geophys. Res*., 109, C09001.

Taljaard, J.J. 1967. Development, distribution and movement of cyclones and anticyclones in the Southern Hemisphere during the IGY. *J. App. Meteor.,* 6, 974-987.

Taljaard, J.J. 1985. Cut-off lows in the South African region. *SA Weather Bureau., Technical Paper no 14*.

Thorncroft, C.D. and Hoskins, B. 1990. Frontal cyclogenesis. *J. Atmos. Sci.,* 47, 2317–2336.

Ting, M., 1994. Maintenance of northern summer stationary waves in a GCM. *J. Atmos. Sci.,* 51, 3268–3308.

Todd, M. and Washington, R. 1999. Circulation anomalies associated with tropical-temperate troughs in southern Africa and the southwest Indian Ocean. *Clim. Dyn.,* 15, 937-951.

Tonkin, H., Holland, G. J., Holbrook, N. and Henderson-Sellers, A. 2000. An evaluation of themodynamic estimates of climatological maximum potential tropical cyclone intensity. *Mon. Wea. Rev.,* 128, 746–762.

Tyson, P. D., Garstang, M., Swap, R., Kallberg, P. and Edwards, M. 1996. An Air Transport climatology for subtropical southern Africa. *J. Climatol.,* 16, 265-291.

Tyson, P.D. and Preston-Whyte, R.A. 2000. The Weather and Climate of southern Africa. *Oxford University Press*, Cape Town, 396pp.

Ummenhofer, C.C., Gupta, A.S., Taschetto, A.S. and England, M.H. 2009a. Modulation of Australian rainfall by meridional gradients Indian Ocean sea surface temperature. *J Climate*., 22, 5597–5610.

Ummenhofer, C.C., Gupta, A.S., England M.H. and Reason, C.J.C. 2009b. Contributions of Indian Ocean Sea surface temperatures to enhanced East African rainfall. *J. Climate*., 22, 993–1013.

Venegas, S.A., Mysak, L.A. and Straub, D.N. 1998. An interdecadal climate cycle in the South Atlantic and its links to the ocean basins. *J. Geophys. Res*., 723-736.

Vitart, F., Anderson, J. L., and Stockdale, T. 2003. Seasonal forecasting of tropical cyclone landfall over Mozambique. *J. Climate*., 16, 3932-3945.

Washington, R. and Todd, M. 1999. Tropical–temperate links in southern African and Southwest Indian Ocean Satellite-derived daily rainfall. *Int. J. Climatol.,* 19, 1601–1616.

White, G.H. 1982. An observational study of the Northern Hemisphere extratropics summertime general circulation. *J. Atmos. Sci.,* 39, 24–40.

Whittaker, L. M. and Horn, L.H. 1983. Northern Hemisphere extra-tropical cyclone activity for four mid-season months. *J. Climatol.,* 4, 297-310.

Wu, G. and Liu, Y. 2003. Summertime quadruplet heating pattern in the subtropics and the associated atmospheric circulation. *Geophys. Res. Lett., 30*, 10.1029/2002GL016209.

Xue, F., Jiang D., Lang X. and Wang, H. 2003. Influence of the Mascarene High and Australian high on the summer monsoon in East Asia: ensemble simulation. *Adv Atmos Sci*., 20, 799–809.